NATIONAL TECHNICAL UNIVERSITY OF ATHENS
School of Civil Engineering
Department of Structural Engineering
Institute of Steel Structure

DESIGN OF BUILDINGS WITH INNOVATIVE ANTI-SEISMIC SYSTEMS FUSEIS

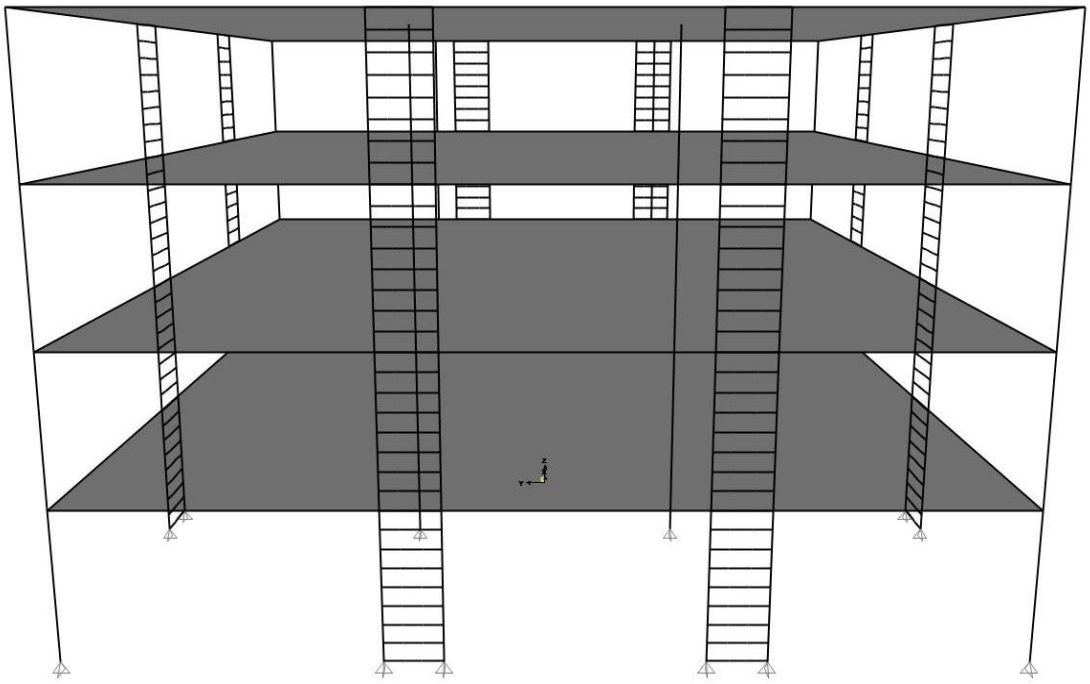

MASTER THESIS

Panagiotis A. Tsarpalis

Supervisor: prof. Ioannis Vayas

Athens, October 2017

ISS MT 2017/17

ΕΘΝΙΚΟ ΜΕΤΣΟΒΙΟ ΠΟΛΥΤΕΧΝΕΙΟ
Σχολή Πολιτικών Μηχανικών
Τομέας Δομοστατικής
Εργαστήριο Μεταλλικών Κατασκευών

ΣΧΕΔΙΑΣΜΟΣ ΚΤΙΡΙΩΝ ΜΕ ΚΑΙΝΟΤΟΜΑ ΑΝΤΙΣΕΙΣΜΙΚΑ ΣΥΣΤΗΜΑΤΑ FUSEIS

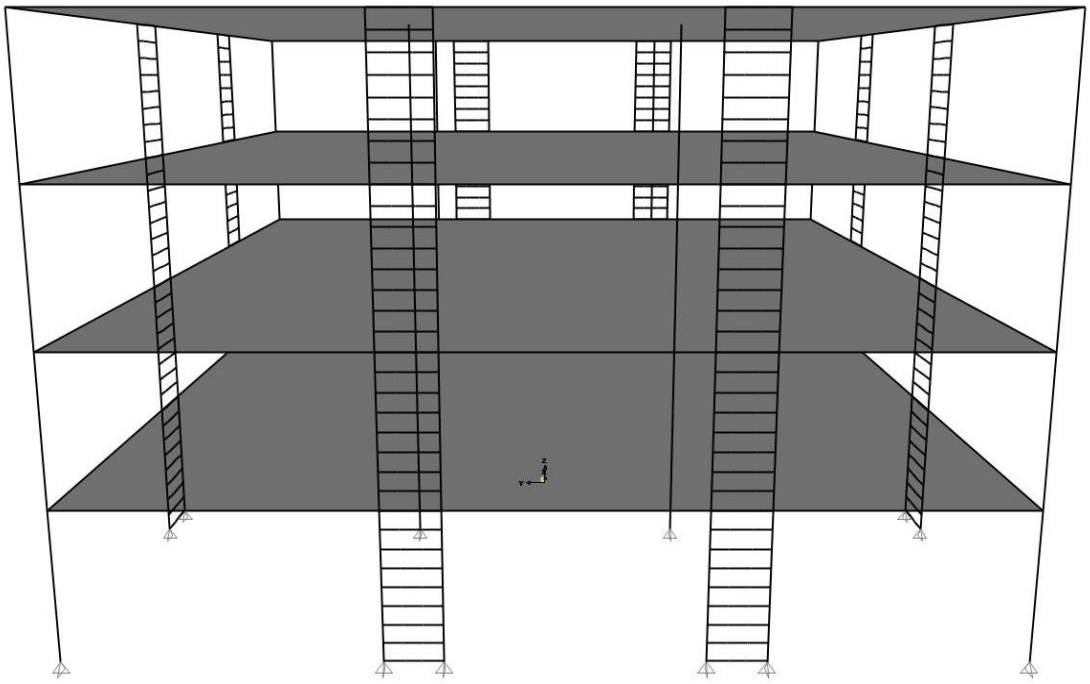

ΜΕΤΑΠΤΥΧΙΑΚΗ ΕΡΓΑΣΙΑ

Παναγιώτης Α. Τσαρπαλής

Επιβλέπων: καθ. Ιωάννης Βάγιας

Αθήνα, Οκτώβριος 2017

ΕΜΚ ΜΕ 2017/17

DESIGN OF BUILDINGS WITH INNOVATIVE ANTI-SEISMIC SYSTEMS FUSEIS

MASTER THESIS

Panagiotis A. Tsarpalis

Supervisor: Ioannis Vayas

Τσαρπαλής Π. Α. (2017).
Σχεδιασμός κτιρίων με καινοτόμα αντισεισμικά συστήματα FUSEIS
Μεταπτυχιακή Εργασία ΕΜΚ ΜΕ 2017/17
Εργαστήριο Μεταλλικών Κατασκευών, Εθνικό Μετσόβιο Πολυτεχνείο, Αθήνα.

Tsarpalis P. A. (2017).
Design of buildings with innovative anti-seismic systems FUSEIS
Master Thesis ISS MT 2017/17
Institute of Steel Structures, National Technical University of Athens, Greece

Στα αδέρφια μου Δημήτρη και Ηλία,
μαζί με τις ευχές μου για συνεχή ανέλιξη
και επίτευξη των στόχων τους

Contents

Abstract III

Περίληψη V

Ευχαριστίες VII

1 Introduction 1
1.1 General 1
1.2 Innovative seismic resistant systems 2
1.3 FUSEIS beam/pin link system 3
1.3.1 Description of FUSEIS beam link system 3
1.3.2 Description of FUSEIS pin link system 4
1.3.3 Vierendeel beam 5

2 Design Rules 7
2.1 Design for linear elastic analysis 7
2.2 Design for non-linear static analysis (Pushover) 14

3 Seismic design of two-storey steel building 19
3.1 General 19
3.2 Geometry and assumptions 19
3.3 Simulation, analysis and design 20
3.4 Seismic design 24
3.4.1 Limitation of inter-storey drift 24
3.4.2 Magnitude of 2nd order effects 25
3.4.3 Dissipative elements verifications 25
3.4.4 Non-dissipative elements verifications 27
3.5 Non-linear static analysis (Pushover) 28
3.5.1 Evaluation of the non-linear behaviour of the building 28
3.5.2 Evaluation of the behaviour factor q 31
3.6 Comparison between the two systems 32

4 Seismic design of four-storey steel building 35
4.1 General 35
4.2 Geometry and assumptions 35
4.3 Simulation, analysis and design 37
4.4 Seismic design 43
4.4.1 Limitation of inter-storey drift 43
4.4.2 Magnitude of 2nd order effects 44
4.4.3 Dissipative elements verifications 44
4.4.4 Non-dissipative elements verifications 47
4.5 Non-linear static analysis (Pushover) 48
4.5.1 Evaluation of the non-linear behaviour of the building 48
4.5.2 Evaluation of the behaviour factor q 53
4.6 Comparison between the two systems 53

5 Non-linear Dynamic Analyses (Time History) 55
5.1 General 55
5.2 Design for non-linear dynamic analysis 55
5.3 Non-linear dynamic analysis on 3D building frame 56
5.4 Residual roof drifts 57

5.5 Low cycle fatigue 61

6 References 63

Annex A. Structural detailing of 2-storey building 65

Annex B. Structural detailing of 4-storey building 71

NATIONAL TECHNICAL UNIVERSITY OF ATHENS
FACULTY OF CIVIL ENGINEERING
INSTITUTE OF STEEL STRUCTURES

MASTER THESIS
ISS MT 2017/17

Design of buildings with innovative anti-seismic systems FUSEIS

Tsarpalis P. A. (supervised by Vayas I.)

Abstract

The object of this master thesis is the design of composite buildings incorporating the FUSEIS beam and pin link system. These innovative seismic resistant systems are consisted of two strong columns rigidly connected by multiple links. The seismic energy dissipation is performed through plastification of small fuses, while leaving the rest of the structure undamaged. The links of beam system connecting the columns are consisted of a beam with reduced beam section in the ends, while the links of the pin system are consisted of the two receptacle beams and one pin in the middle. The dissipative elements of the FUSEIS beam and pin link system, are the reduced beam section and the weakened part of the pin respectively, both parts of the links that connect the system columns.

In the first chapter, an introduction about anti-seismic systems is made and then, a brief description of the FUSEIS systems that were used in the frame of this thesis.

In the second chapter, the design procedures for the practical application of the FUSEIS systems on a building and for the verification of the collapse mechanism and the plastic hinge distribution are presented, as described in the Design Guides [3], [5].

In the third chapter, two case studies are presented where the FUSEIS link systems are applied on a 2-storey composite building. The detailed design of the building under vertical and lateral loads is presented. The collapse mechanism is verified through non-linear static analysis (Pushover) and finally a comparison of the two systems is made.

In the fourth chapter, two case studies are presented where the FUSEIS pin link system is applied in two different configurations. The first case study is a 4-storey composite building incorporating the classic FUSEIS pin link system. In the second case study, an alternative configuration is studied, where the receptacle beams are removed. After the design of the building under vertical and seismic loads and the verification of the collapse mechanism, a comparison of the two alternative configurations is made and a conclusion on whether the receptacle beams are a crucial element of the system.

In the fifth chapter some results are presented from non-linear time history analyses, carried out on the building described in Chapter 4. In total ten accelerograms were used for the estimation of the dynamic response of the structure under real seismic loads. The updated model used in the analyses is described, where hysteretic behaviour was inserted

through non-linear links. Residual deformations are presented for all ten seismic records and the FUSEIS system is characterized on whether or not can work as a self-centring system, leaving the structure with practically zero deformation after a strong seismic event. Final, the Palmgren – Miner criterion is used for the check of the pins under low-cycle fatigue.

ΕΘΝΙΚΟ ΜΕΤΣΟΒΙΟ ΠΟΛΥΤΕΧΝΕΙΟ
ΣΧΟΛΗ ΠΟΛΙΤΙΚΩΝ ΜΗΧΑΝΙΚΩΝ
ΕΡΓΑΣΤΗΡΙΟ ΜΕΤΑΛΛΙΚΩΝ ΚΑΤΑΣΚΕΥΩΝ

ΜΕΤΑΠΤΥΧΙΑΚΗ ΕΡΓΑΣΙΑ
ΕΜΚ ΜΕ 2017/17

Σχεδιασμός κτιρίων με καινοτόμα αντισεισμικά συστήματα FUSEIS

Τσαρπαλής Π. Α. (Επιβλέπων: Βάγιας Ι.)

Περίληψη

Σκοπός της παρούσας μεταπτυχιακής εργασίας είναι ο σχεδιασμός μεταλλικών κτιρίων με καινοτόμα αντισεισμικά συστήματα δοκών σύζευξης και πείρων σύζευξης FUSEIS (FUSEIS beam/pin link systems). Τα καινοτόμα αυτά συστήματα αποτελούνται από δύο υποστυλώματα τα οποία συνδέονται μεταξύ τους με πολλαπλούς συνδέσμους. Η απορρόφηση της σεισμικής ενέργειας γίνεται μέσω πλαστικοποίησης μικρών, εύκολα αντικαταστάσιμων στοιχείων, ενώ τα υπόλοιπα δομικά μέλη παραμένουν ελαστικά. Ένας σύνδεσμος του συστήματος δοκών σύζευξης FUSEIS, αποτελείται από ένα μεταλλικό δοκάρι με απομειωμένες διατομές στα άκρα του, ενώ ένας σύνδεσμος του συστήματος πείρων σύζευξης FUSEIS αποτελείται από δύο δοκούς υποδοχείς στα άκρα και έναν πείρο στο κέντρο. Το πλάστιμο στοιχείο των δυο συστημάτων FUSEIS, είναι οι απομειωμένες διατομές των δοκών και ο πείρος αντίστοιχα.

Στο πρώτο κεφάλαιο γίνεται μία εισαγωγή στα αντισεισμικά συστήματα και στην συνέχεια μια σύντομη περιγραφή των συστημάτων FUSEIS που χρησιμοποιήθηκαν στα πλαίσια της παρούσας μεταπτυχιακής εργασίας.

Στο δεύτερο κεφάλαιο παρουσιάζεται η διαδικασία για τον σχεδιασμό ενός κτιρίου με συστήματα σύζευξης FUSEIS, καθώς και η επιβεβαίωση του μηχανισμού κατάρρευσης, όπως περιγράφονται στους Οδηγούς Σχεδιασμού [3], [5].

Στο τρίτο κεφάλαιο εξετάζονται δύο περιπτώσεις κτιρίων όπου στο πρώτο εφαρμόζεται το σύστημα δοκών σύζευξης FUSEIS, ενώ στο δεύτερο το σύστημα των πείρων. Γίνεται λεπτομερής σχεδιασμός των κτιρίων υπό κατακόρυφα και σεισμικά φορτία, επιβεβαίωση του μηχανισμού κατάρρευσης και της κατανομής των πλαστικών αρθρώσεων μέσω μη γραμμικής στατικής ανάλυσης (Pushover) και τελικά παρουσιάζονται κάποια συμπεράσματα και συγκρίσεις μεταξύ των δύο συστημάτων.

Στο τέταρτο κεφάλαιο, το σύστημα πείρων σύζευξης FUSEIS εφαρμόζεται, με δύο διαφορετικές διαμορφώσεις, σε ένα τετραώροφο μεταλλικό κτίριο. Στην πρώτη περίπτωση χρησιμοποιείται το κλασικό σύστημα πείρων σύζευξης FUSEIS, ενώ στην δεύτερη μια διαφορετική διαμόρφωση εξετάζεται, όπου οι δοκοί υποδοχείς αφαιρούνται. Από την μελέτη και σύγκριση των δύο περιπτώσεων, τελικά, παρουσιάζονται κάποια συμπεράσματα σχετικά με το αν οι δοκοί υποδοχείς αποτελούν ένα απαραίτητο στοιχείο του συστήματος.

Στο πέμπτο κεφάλαιο παρουσιάζονται κάποια αποτελέσματα από μη γραμμική ανάλυση χρονοϊστορίας στο κτίριο που περιγράφεται στο Κεφάλαιο 4. Συνολικά δέκα επιταχυνσιογραφήματα χρησιμοποιήθηκαν για την μελέτη της απόκρισης του κτιρίου σε δυναμικά φορτία. Γίνεται περιγραφή του μοντέλου που χρησιμοποιήθηκε στο οποίο πλέον εισάγεται κινηματικό μοντέλο υστέρησης μέσω μη γραμμικών ελατηρίων. Γίνεται έλεγχος σε παραμένουσες παραμορφώσεις και κρίνεται η δυνατότητα του συστήματος να επαναφέρει την κατασκευή στην αρχική της θέση, με πρακτικά μηδενικές παραμένουσες μετακινήσεις, ύστερα από έναν ισχυρό σεισμό. Τέλος, γίνεται χρήση του κριτηρίου Palmgren – Miner για τον έλεγχο των πείρων σε ολιγοκυκλική κόπωση.

Ευχαριστίες

Ολοκληρώνοντας τη μεταπτυχιακή μου εργασία, θα ήθελα να ευχαριστήσω όσους με βοήθησαν και με στήριξαν όλο αυτό το διάστημα.

Αρχικά θα ήθελα να ευχαριστήσω τον επιβλέποντά μου και καθηγητή Ε.Μ.Π. κ. Ιωάννη Βάγια για την ανάθεση του συγκεκριμένου θέματος, τη συνεχή καθοδήγησή του, το ενδιαφέρον του, τη βοήθειά του σε θέματα γνωστικού αντικειμένου, αλλά και για την εμπιστοσύνη που δείχνει στο πρόσωπό μου. Εύχομαι η αποδοτική μας σχέση να συνεχιστεί και τα επόμενα χρόνια στα πλαίσια της διδακτορικής μου διατριβής, την οποία έχω μόλις ξεκινήσει.

Ιδιαίτερες ευχαριστίες θα ήθελα να απευθύνω στον κ. Παύλο Θανόπουλο, Λέκτορα Ε.Μ.Π., για τις συμβουλές του και την άψογη συνεργασία που έχουμε. Οι γνώσεις του σε θέματα αντισεισμικής μηχανικής και στατικής, η μεταδοτικότητά του και η υπομονή του ήταν καθοριστικοί παράγοντες για την πρόοδο της συγκεκριμένης εργασίας.

Ακόμη, θα ήθελα ευχαριστήσω τη συνάδελφο και υποψήφια διδάκτορα Ε.Μ.Π Στέλλα Αυγερινού, για τη συμβολή της στην ολοκλήρωση της μεταπτυχιακής μου εργασίας, την καθοδήγησή της στα πρώτα μου βήματα ως μηχανικός αλλά και για την ψυχολογική στήριξη όταν το χρειαζόμουν.

Σε προσωπικό επίπεδο, θα ήθελα να ευχαριστήσω την οικογένειά μου και την Ευαγγελία για την αγάπη, τη βοήθεια και την υπομονή τους σε ό,τι κι αν αποφασίσω. Θέλω επίσης να ευχαριστήσω τον νονό μου Βασίλειο Μαραγκό για τη στήριξή του, υλική και μη, όλα τα χρόνια των σπουδών μου, αλλά και για την καθοδήγησή του στο να γίνομαι καλύτερος άνθρωπος.

1 Introduction

1.1 General

Composite construction is a generic term to describe any building construction involving multiple dissimilar materials. In structural engineering, composite construction exists when two different materials are bound together so strongly that they act together as a single unit. One common example involves steels beams supporting concrete or composite floor slabs.

Steel composite buildings are concerned as the most modern constructions, with the least economical and time effort to build (Figure 1.1). The percentage of steel building has been increased after World War II, when steel became more available. The range of application has been expanded with improved materials, products and design capabilities with the availability of computer aided design software.

Figure 1.1: Example of a steel composite building

The largest threat to composite buildings, as to all structural constructions, is earthquake. Seismic resistant systems are those who provide lateral stability and hence seismic safety to a structure. The most common anti-seismic systems are moment-resisting frames (MRF) and concentrically braced frames (CBF). MRFs provide resistance to lateral loads through rigid frame action, that is, by developing bending moment and shear in the members and the joints of the frame. CBFs are less ductile and stiffer than MRFs and they provide lateral stability by developing axial forces in the diagonals steel sections.

Despite being the most commonly used in the structural engineer section, these systems, have a lot of disadvantages. Under a strong earthquake, brittle kind of failures may occur, while the repair and substitution works are too difficult or too expensive to implement. The loss in terms of economy can be either direct, as large steel members need replacement, or indirect, related to temporary or permanent closure of the building.

(a) (b)

Figure 1.2: (a) Moment-resisting frames (b) Concentrically braced frames

Following the international needs, extensive research has been carried out, to improve the behaviour and response of a building under seismic loading. The main purpose was to present innovative anti-seismic systems, where the energy dissipation is restricted to small fuses and therefore, the repair works cost is considerably reduced.

1.2 Innovative seismic resistant systems

As mentioned, the most common seismic resistant systems in steel structures are currently moment resisting frames, concentric braced frames, eccentric braced frames and steel or composite vertical walls. Such systems, under severe earthquakes, may suffer significant structural damage or exhibit large residual drifts resulting loss of occupancy or high repair cost.

In the recent years, a number of innovative systems based on energy dissipation and damping have been invented as the result of national and European research projects, such as dissipative connections assign in braced steel frames (INERD) [7], replaceable thin-walled shear panel (SPSW) and dissipative links (FUSEIS) [4]. These innovative systems consist of small and dismountable dissipative parts where damage concentrates hence they have increased reparability while comparable stiffness and ductility to the conventional ones. In Figure 1.3 (a) and (b), FUSEIS and INERD systems are shown correspondingly.

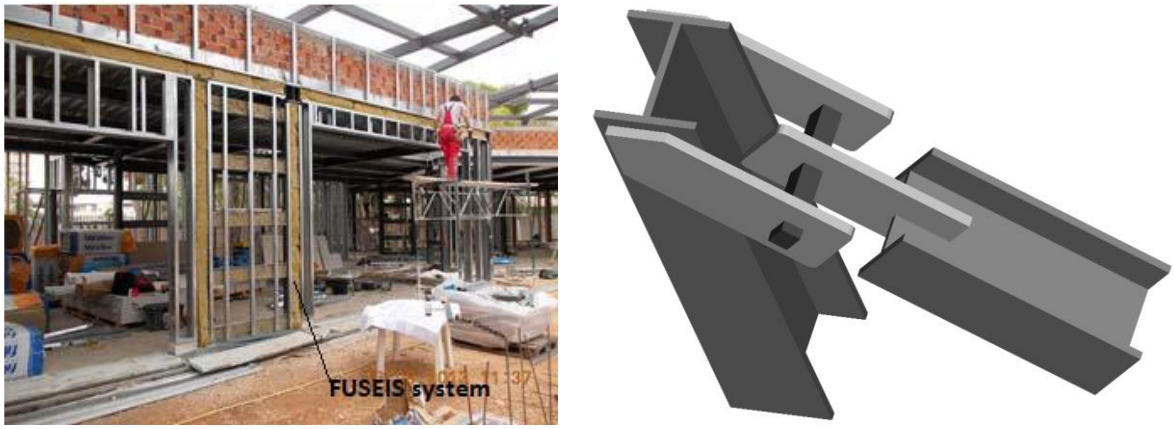

(a) (b)

Figure 1.3: (a) FUSEIS link system (b) INERD pin connection

1.3 FUSEIS beam/pin link system

In the frame of the European research program "Dissipative Devices for Seismic Resistant Steel Frames" (Acronym: FUSEIS), two innovative dissipative systems were introduced, named "FUSEIS beam/pin links" and "FUSEIS bolted/welded beam splices", depending on the geometry of the fuse.

1.3.1 Description of FUSEIS beam link system

The FUSEIS beam link system is composed of two, closely spaced, strong columns, rigidly connected by multiple horizontal beams. The section of the beams can be SHS, CHS or I-shaped (HEA or IPE) sections. The general layout of the system is given in Figure 1.4 (a). In order to protect the column and the beam-to-column connection against yielding, reduced beam section (RBS) are foreseen at the ends of the beam (Figure 1.6). After a strong earthquake, inelastic deformations will only occur in the RBS of the dissipative beam link elements, which can be easily replaced.

(a) (b)

Figure 1.4: (a) General layout of FUSEIS beam link system (b) Position of FUSEIS beam link system in a building

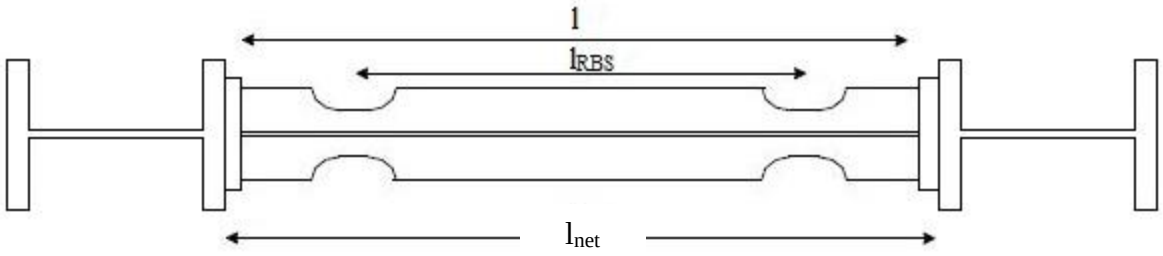

Figure 1.5: Typical section view and dimension of FUSEIS beam link system

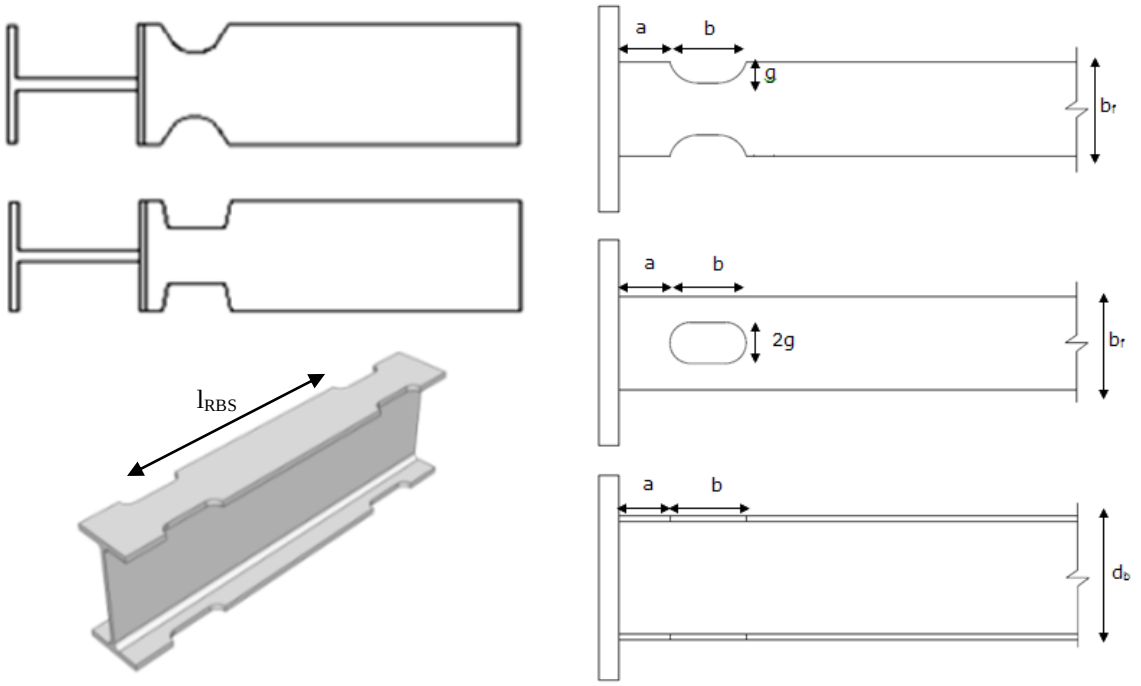

Figure 1.6: Geometry of reduced beam section

Table 1.1: Geometry of RBS according to codes

According to FEMA-350	According to EN1998-3
$a = (0.50 - 0.70)\ b_f$	$a = 0.60 b_f$
$b = (0.65 - 0.85)\ d_b$	$b = 0.75 d_b$
$c = g \leq 0.25 b_f$	$g \leq 0.25 b_f$
$r = (4c^2 + b^2) / 8c$	$r = (4g^2 + b^2) / 8g$

1.3.2 Description of FUSEIS pin link system

The FUSEIS pin link system consists of a pair of strong columns rigidly connected by multiple horizontal links (Figure 1.7). The horizontal links consist of two receptacle beams connected through a short steel pin. The receptacle beams can have an H or hollow section and they are welded to the column flanges. The joint between the receptacles and the pins, is formed through an end plate on which the threaded section of the pin is screwed (Figure 1.8). Pin section is reduced in the middle part of the pin to promote damage away from the connection area.

Under strong lateral forces, plastic hinges will form on the ends of the pins, thus dissipating a large amount of energy, while leaving the rest of the structure undamaged. The pin section is reduced in the middle part of the pin to ensure that plastification will take place away from the connection area. Repair works are easy, since they are restricted to the pins which are not generally subjected to vertical loads, as they are placed between floor levels.

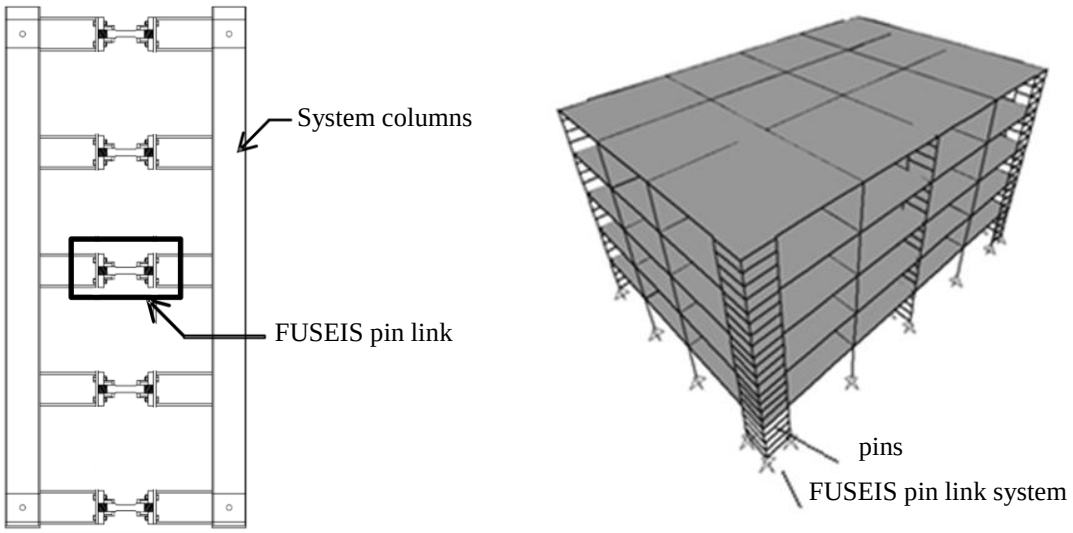

Figure 1.7: (a) FUSEIS pin link system configuration (b) Position of FUSEIS pin link system in a building

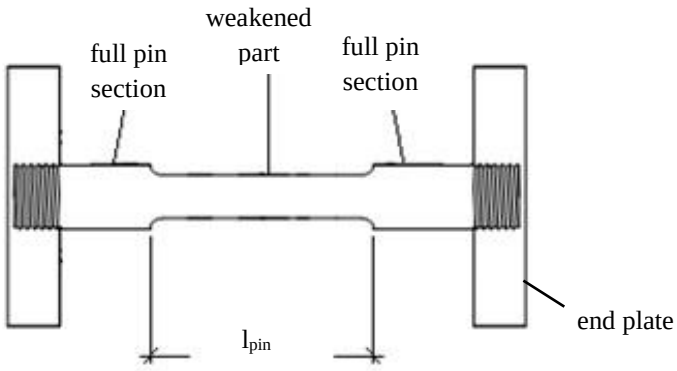

Figure 1.8: FUSEIS pin link

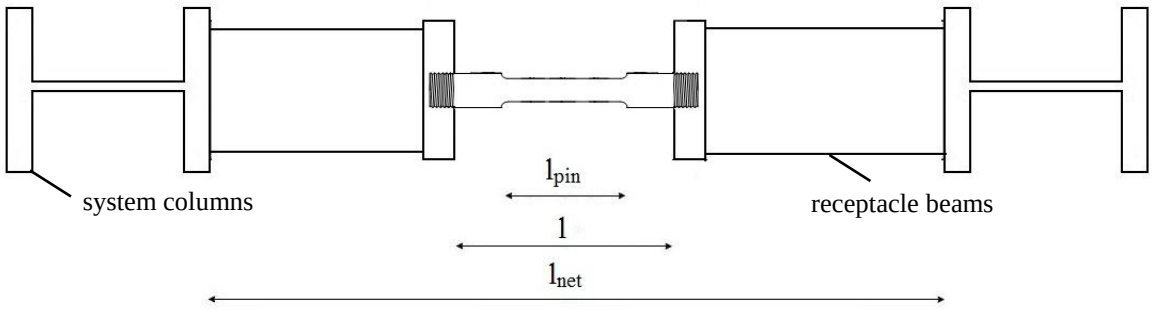

Figure 1.9: Typical plan view and dimensions of FUSEIS pin link system

1.3.3 Vierendeel beam

Experimental investigations ([1], [2]) showed that the FUSEIS systems (both beam and pin link) resist lateral loads as a vertical Vierendeel beam, where the main actions are bending and shear in the horizontal links and axial and bending in the columns, Figure 1.10. Con-

sidering hinges at the reduced section positions, the internal moments and forces for horizontal loading in the elastic state may be derived from statics.

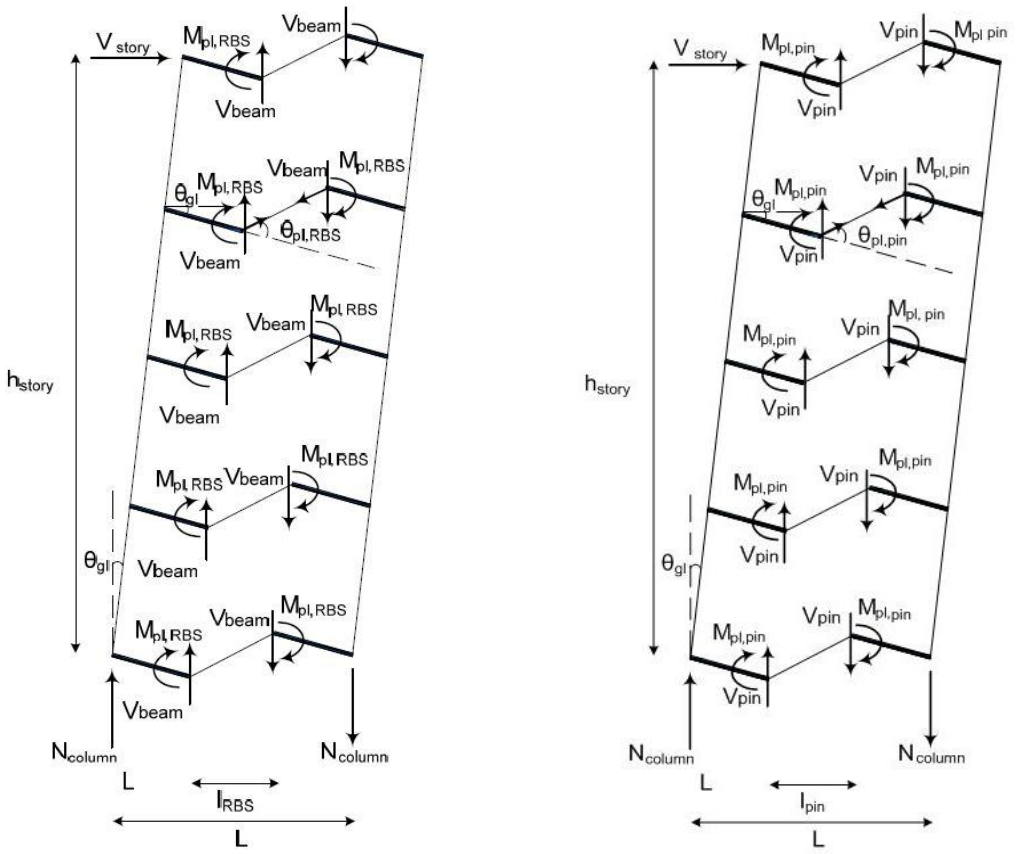

(a) (b)

Figure 1.10: Vierendeel behaviour (a) FUSEIS beam link system, (b) FUSEIS pin link system

Regarding the FUSEIS pin link system, the system's resistance is significantly increasing after the plastification of the pins, due to catenary action of the pins and strain hardening. Because of this, the system can develop large rotations and the bending moment of the pins transforms to tensile forces until they reach their plastic axial resistance.

2 Design Rules

The design methodology of steel building with FUSEIS beam/pin link systems, is based on the provisions of Eurocode 3 [9] and Eurocode 8 [8]. Additional rules, to those given by the normal Code provisions, are proposed by the design guides to cover the use of the FUSEIS systems. The rules given are intended to ensure that yielding will take place in the beam/pin links prior to any other member of the structure. Therefore, the design of buildings with FUSEIS link systems is based on the assumption that the seismic energy will be dissipated by plastic bending mechanisms formatted on the beams/pins.

2.1 Design for linear elastic analysis

1) Simulation

A building with FUSEIS systems may be simulated with a linear-elastic model consisted of beam elements. The simulation of the links is different for the beam and the pin link systems.

a) The horizontal beam FE-elements used to simulate the FUSEIS beam links are divided into five parts with different cross sections (Figure 2.1 (a)): representing the full sections (two at the ends and one in the middle) and the two RBS section (in the between).

b) The horizontal beam FE-elements used to simulate the FUSEIS pin links are divided into three parts with different cross sections (Figure 2.1 (b)): representing the receptacle beams at the ends and the weakened pin in the middle.

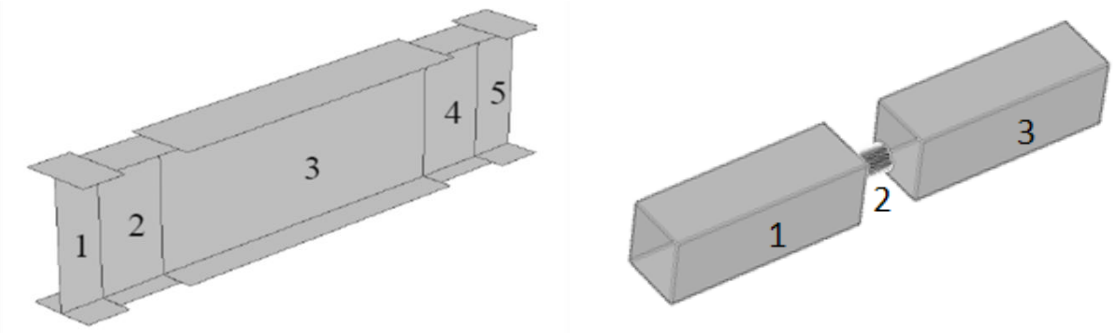

(a) (b)

Figure 2.1: Simulation of FUSEIS horizontal links (a) FUSEIS beam link system, division into five parts (b) FUSEIS pin link system, division into three parts

To enable the Vierendeel action, the joints between the system beams and the columns are simulated as rigid. Rigid zones are foreseen between the column centres and the columns faces, to consider in the analysis the clear length of the horizontal links and, therefore, the true flexibility and strength of the system.

The connections between the floor beams and the system columns are formed as simple to avoid additional forces being transferred to the system and to capacity design the system columns in respect to the system beams/pins only and not to the strong floor beams. On the

other hand, the joints between the floor beams and the columns of the main frame can be rigid, semi-rigid or hinged. In the first two cases, lateral stability is provided by the FUSEIS system in cooperation with the MRF while in the third case by system alone. In any case, the bases of all the columns of the building are pinned.

2) Analysis

Vertical loads are inserted in the model according to Eurocode 1 [14], linear elastic analysis is performed and internal forces of the main frame are exported. All members of the main frame are dimensioned and checked at ULS and SLS according to the provisions of Eurocode 3 [9].

The conventional method for calculating the seismic loads is by applying Multi - Modal Response Spectrum Analysis, according to Eurocode 8 [8]. In each direction, the number of modes taken into consideration is such, that the sum of the effective modal mass is greater than the 90% of the total mass. For the inelastic deformations to be considered, a behaviour factor must be introduced. The design guidelines propose a maximum value of the behaviour factor q equal to 5 for FUSEIS beam and 3 for FUSEIS pin system.

3) Limitation of inter-storey drift

The protection of non-structural elements of the building, the minimum required stiffness and the serviceability of the building after the earthquake occurs, is ensured through the limitation of inter-storey drift check. This check, along with the 2nd order effects, consists a basic criterion for the design and the dimensioning of the FUSEIS systems.

From the linear elastic analysis performed in the previous step, elastic deformations were calculated d_e. Inelastic displacements d_s can be calculated by multiplying the elastic deformations d_e with the behaviour factor q, as shown in Eq. (2.1):

$$d_s = q \times d_e \qquad \text{Eq. (2.1)}$$

It is very common that the capacity ratios of the dissipative elements (Ω) are low. In that case, the design inter-storey drifts d_r based on d_s are conservative, thus a reduction factor $q_\Omega = \frac{1}{\min\Omega}$ equal to the capacity ratio of the links may be inserted in Eq. (2.1), as follows:

$$d_s = q \times q_\Omega \times d_e \qquad \text{Eq. (2.2)}$$

The design inter-storey drift d_r is defined as the difference of the horizontal displacements d_s at the top and bottom of each storey. Depending on the type of the non-structural elements and the importance class of the building, the limit values of the design inter-storey drift d_r varies. According to EN1998-1 §4.4.3.2 [12], the following limits must be met:

a) For buildings with brittle non-structural elements connected with the main frame:

$$d_r v \leq 0.005h \qquad \text{Eq. (2.3)}$$

b) For buildings with ductile non-structural elements:

$$d_r v \leq 0.0075h \qquad \text{Eq. (2.4)}$$

c) For buildings with non-structural elements connected with the main frame in such way that they are not affected by the deformations of the structure or for buildings with no non-structural elements:

$$d_r v \leq 0.010h \qquad \text{Eq. (2.5)}$$

Where,

h is the height of the floor

v is a reduction factor that takes into account the shorter earthquake return period associated with the damage limitation requirement (proposed values v=0.4 for importance class III and IV, while v=0.5 for class I and II.

4) 2nd order effects.

The influence of 2nd order effects shall be controlled by the limitation of the inter-storey drift sensitivity coefficient θ within the values of the Code. Coefficient θ is calculated for each floor in both directions, through

$$\theta = \frac{P_{tot} \times d_r}{V_{tot} \times h_{storey}} \qquad \text{Eq. (2.6)}$$

where,

P_{tot} is the total gravity load, in the seismic design state, of the floor under consideration and the overlying floors.

V_{tot} is the total seismic storey shear

Alternative, the inter-storey drift coefficient θ may be calculated by a linear buckling analysis through the factor α_{cr}, the factor by which the design loading has to be increased to cause elastic instability in a global mode. The analysis is carried out under the constant vertical loads of the seismic combination $(1.0 \cdot G + 0.3 \cdot \varphi \cdot Q)$ and produces the buckling modes. The modes moving the building in a global sense at x and y directions are chosen and the corresponding α_{cr} factors are calculated as follows:

$$\alpha_{cr} = \frac{1}{\theta} = \frac{F_{cr}}{F_{Ed}} \qquad \text{Eq. (2.7)}$$

where,

F_{cr} is the elastic critical buckling load for global instability

F_{ed} is the design loading for the seismic combination

The factor α_{cr} shall be multiplied by the q behaviour factor, in order to take into consideration, the inelastic displacements of the building, as shown in Eq. (2.8).

$$\theta = \frac{q}{\alpha_{cr}} \quad \text{Eq. (2.8)}$$

According to EN1998-1 §4.4.2.2 [12], when the inter-storey drift sensitivity coefficient θ is limited to $\theta \leq 0.1$, 2nd order effects can be ignored. If $0.1 < \theta \leq 0.2$, 2nd order effects may approximately be taken into account by increasing the seismic action's effects, by a factor equal to 1/ (1 - θ). If $0.2 < \theta \leq 0.3$ a more accurate second order analysis must be performed. In any case, the value of coefficient θ shall not exceed 0.3.

Limitation of inter-storey drift and 2nd order effects, are the most critical while the configuration of the FUSEIS system is mainly depending on them. The factors that primarily affect the stiffness of the FUSEIS systems and therefore the satisfaction of these checks are the section of the system columns, their axial distance and the receptacle beams.

5) Dissipative elements verifications

The horizontal links of the system shall be verified to resist the internal forces of the most unfavourable seismic combination and fulfil the following conditions:

a) Axial forces

This check ensures that the plastic moment and shear forces resistance, are not decreased due to axial forces.

$$\frac{N_{Ed}}{N_{pl,RBS/pin,Rd}} \leq 0.15 \quad \text{Eq. (2.9)}$$

where,

N_{ed} is the design axial force

$N_{pl,RBS/pin,Rd}$ is the design axial force resistance of the weakened part of the pin or of the reduced beam section, depending on the system examined

b) Shear force resistance

The reduced beam sections at FUSEIS beam and the ends of the weakened part of the pins at FUSEIS pin system, shall be capacity designed in shear resistance, considering that plastic hinges have been developed at these positions. In order to ensure that $M_{pl,RBS/pin,Rd}$ will not be reduced due to the influence of shear, the ratio between acting shear and shear resistance should be verified in accordance to Eq. (2.10):

$$\frac{V_{CD,Ed}}{V_{pl,RBS/pin,Rd}} \leq 0.5 \qquad \text{Eq. (2.10)}$$

where,

$V_{CD,Ed} = \frac{2 \times M_{pl,RBS/pin,Rd}}{l_{RBS/pin}}$ is the capacity design shear force

$M_{pl,RBS/pin,Rd}$ is the design plastic moment resistance of the RBS section/weakened part of the pin

$V_{pl,RBS,pin,Rd}$ is the design shear resistance of the RBS section/ weakened part of the pin

$l_{RBS/pin}$ is the length between the RBS sections/ the length of the weakened part of the pin (Figure 1.5 and Figure 1.9)

Replacing $V_{CD,Ed}$ in Eq. (2.10) and solving by $l_{RBS/pin}$, is found that the length between the RBS sections l_{RBS} or the length of the weakened part of the pin l_{pin}, should be checked to be above the limit value calculated from Eq. (2.11).

$$l_{RBS/pin} \geq \frac{4 \times M_{pl,RBS/pin,Rd}}{V_{pl,RBS/pin,Rd}} = \frac{4 \times W_{pl,RBS/pin}}{A_v / \sqrt{3}} \qquad \text{Eq. (2.11)}$$

where,

$W_{pl,RBS/pin}$ is the plastic section modulus of the RBS/weakened part of the pin

c) Bending moment resistance

For the moment resistance check the Eq. (2.12) must be fulfilled:

$$\frac{M_{Ed}}{M_{pl,RBS/pin,Rd}} = \frac{1}{\Omega} \leq 1.0 \qquad \text{Eq. (2.12)}$$

where,

M_{ed} is the design bending moment

$M_{pl,RBS/pin,Rd}$ is the design plastic moment resistance of the RBS section/weakened part of the pin

Ω is the overstrength of the RBS section/weakened part of the pin

d) Global dissipative behaviour

To achieve, in a global sense, a uniform dissipative behaviour of the structure, it should be checked in each direction, that the maximum ratios Ω over the entire structure do not differ from the minimum more than 25%.

$$\frac{max\Omega}{min\Omega} \leq 1.25 \qquad \text{Eq. (2.13)}$$

e) Beams/Pins rotations

Considerably large big rotations develop in FUSEIS beams/pins links during seismic excitation as shown in Figure 1.10. Therefore, it is necessary to limit these rotations bellow the values that define the Ultimate Limit State (ULS). The rotations at the ULS have been calculated from a number of tests, that were conducted in the frame of the FUSEIS research program.

$$\theta_{RBS} = \frac{L}{l_{RBS}} \times \theta_{gl} \leq \theta_{ULS,RBS} \qquad \text{Eq. (2.14)}$$

$$\theta_{pin} = \frac{L}{l_{pin}} \times \theta_{gl} \leq \theta_{ULS,pin} \qquad \text{Eq. (2.15)}$$

Where,

$\theta_{ULS,pin}=14\%$, $\theta_{\underline{ULS},RBS}=5\%$

θ_{gl} is the global rotation of the FUSEIS system as shown in Figure 1.10

L is the axial distance of the system columns

6) Non-dissipative elements verifications

The non-dissipative elements of the system, the columns, the receptacle beams (if they exist), the full beam/pin section and their connections are capacity designed.

a) System columns

Concerning the FUSEIS beam link system the internal forces of the system columns emerged from the analyses with the most unfavourable seismic combination, are increased according to Eq. (2.16), Eq. (2.17) and Eq. (2.18), to ensure that failure will occur in the horizontal beams prior to the FUSEIS columns.

$$N_{CD,Ed} = N_{Ed,G} + 1.1 \times \gamma_{ov} \times \Omega \times N_{Ed,E} \qquad \text{Eq. (2.16)}$$

$$M_{CD,Ed} = M_{Ed,G} + 1.1 \times \gamma_{ov} \times \Omega \times M_{Ed,E} \qquad \text{Eq. (2.17)}$$

$$V_{CD,Ed} = V_{Ed,G} + 1.1 \times \gamma_{ov} \times \Omega \times V_{Ed,E} \qquad \text{Eq. (2.18)}$$

The internal forces of the system columns for the FUSEIS pin link system, are similarly increased according to Eq. (2.19), Eq. (2.20) and Eq. (2.21).

$$N_{CD,Ed} = N_{Ed,G} + 1.1 \times \alpha \times \gamma_{ov} \times \Omega \times N_{Ed,E} \quad \text{Eq. (2.19)}$$

$$M_{CD,Ed} = M_{Ed,G} + 1.1 \times \alpha \times \gamma_{ov} \times \Omega \times M_{Ed,E} \quad \text{Eq. (2.20)}$$

$$V_{CD,Ed} = V_{Ed,G} + 1.1 \times \alpha \times \gamma_{ov} \times \Omega \times V_{Ed,E} \quad \text{Eq. (2.21)}$$

where,

$N_{Ed,G}$, $M_{Ed,G}$, $V_{Ed,G}$ are the internal forces due to the non-seismic actions of the seismic combination

$N_{Ed,E}$, $M_{Ed,E}$, $V_{Ed,E}$ are the internal forces due to the seismic action

$\Omega = min\Omega_i = min\left\{\frac{M_{pl,RBS,pin,Rd,i}}{M_{Ed,i}}\right\}$ is the minimum overstrength factor

γ_{ov} is the material overstrength factor (suggested value 1.25)

$\alpha=1.5$ is an additional factor only used for the FUSEIS pin link system, to ensure that pin links will yield first

In any case, the increment factor ($1.1\times\gamma_{ov}\times\Omega$ or $1.1\times\alpha\times\gamma_{ov}\times\Omega$) shall not exceed the behaviour factor q.

b) Receptacle beams (only for FUSEIS pin system)

The receptacle beams shall be capacity designed, to ensure that they will not yield prior to the reduced diameter section pin, according to Eq. (2.23):

$$\frac{M_{CD,Ed}}{M_{pl,rec,Rd}} \leq 1.0 \quad \text{Eq. (2.22)}$$

$$M_{CD,Ed} = \frac{l_{net}}{l_{RBS/pin}} M_{pl,RBS/pin,Rd} \quad \text{Eq. (2.23)}$$

where,

$M_{CD,Ed}$ is the capacity design bending moment

l_{net} is the total length of the link between the column flanges (Figure 1.9)

$M_{pl,rec,Rd}$ is the design bending moment resistance of the receptacle beam

c) Full beam/pin section

To ensure that the full cross section of the beams/pins will not yield prior to the reduced sections, the moment resistance of the full cross section shall be verified to be greater than the capacity design moment $M_{CD,Ed}$, calculated as shown in Eq. (2.24).

$$\frac{M_{CD,Ed}}{M_{pl,Rd}} \leq 1.0 \qquad \text{Eq. (2.24)}$$

$$M_{CD,Ed} = \frac{l}{l_{RBS/pin}} M_{pl,RBS/pin,Rd} \qquad \text{Eq. (2.25)}$$

where,

l for FUSEIS beam link system is the length between the face plates of the columns and for FUSEIS pin links is the length between the face plates of the receptacles (Figure 1.5 and Figure 1.9)

$M_{pl,Rd}$ is the design bending moment resistance of the full beam/pin section

d) Connection between the FUSEIS links and the columns

The joints between the horizontal links and the system columns, are formed as fully welded. To ensure that these connections will have enough overstrength to yield after the plastification of the links, they are capacity designed according to Eq. (2.26) and Eq. (2.27).

$$M_{CD,con,Ed} = 1.1 \times \gamma_{ov} \frac{L_{net}}{l_{RBS,pin}} M_{pl,RBS,pin,Rd} \qquad \text{Eq. (2.26)}$$

$$V_{CD,con,Ed} = 1.1 \times \gamma_{ov} \frac{2 \times M_{pl,RBS,pin,Rd}}{l_{RBS,pin}} \qquad \text{Eq. (2.27)}$$

2.2 Design for non-linear static analysis (Pushover)

In general, when the structure is expected to remain elastic for the level of ground motion or when the design results in a nearly uniform non-linear response, linear procedures can be applied. However, as the performance of the building implies greater inelastic deformations and demands, the uncertainty with linear analysis increases to a point that requires a high level of conservatism in terms of demand assumptions and acceptability criteria. Therefore, inelastic analysis can be used to reduce these levels of uncertainty.

In order to verify the collapse mechanism and to check the behaviour factor used in the linear analysis, a non-linear static analysis (Pushover), must be performed. To perform this analysis, a pattern of forces is applied to a structural model that includes non-linear properties (such as steel yield), and the total force is plotted against a reference displacement to define a capacity curve. The elastic model must be upgraded to include the response of structural members beyond the elastic zone. Plastic hinges shall be inserted to all points of the structure that may be enter the plastic zone, according to the following:

- Bending moment type M3 plastic hinges at the ductile weakened parts of the FUSEIS links

- Bending moment type M3 plastic hinges at the full cross sections of the beam links and the receptacles
- Interaction between bending moment and axial forces type P-M3 plastic hinges at the columns
- Bending moment type M3 at the rigid or semi-rigid beam to column connections of the main frame

Plastification shall be represented by nonlinear moment-rotation curves. According to FEMA 356 [13], a generalized M-θ curve as shown in Figure 2.2 shall be used for components of steel moment frames. Point C shall be calculated considering a strain-hardening slope of 3% of the elastic slope.

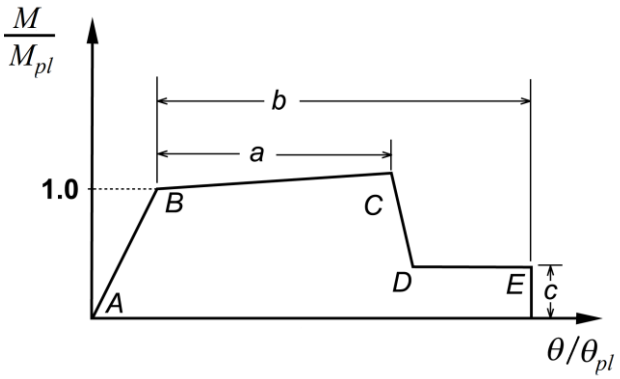

Figure 2.2: Generalized Moment-rotation curve for steel elements

Parameters a, b and c vary depending on the section class and whether the steel member is primary or secondary. The horizontal links of the FUSEIS systems shall be of section class 1, in order to have sufficient rotation capacity.

Considering the above mentioned, a generalized standard can be formed. In Table 2.1 the modelling parameters and acceptance criteria for the full beam section and the receptacle beams are shown.

Table 2.1: Plastic hinges parameters for full beam section and receptacle beams

Point	Modelling parameters		Acceptance criteria	
	M/M_{pl}	θ/θ_{pl}	Limit state	θ/θ_{pl}
A	0	0	IO	1
B	1	0	LS	6
C	α	9	CP	8
D	0.6	9	α factor: strain hardening slope 3% of elastic	
E	0.6	11		

The proposed characteristics and limit states of the plastic hinges of the weakened parts of the FUSEIS links were calculated from experimental results and were presented in the Design Guide [3]. Table 2.2 summarizes these parameters:

Table 2.2: Plastic hinges parameters for FUSEIS reduced section beams

Plastic hinge properties								
Point	I-shape sections		SHS		CHS		Reduced pin section	
	$M/M_{pl,\ RBS}$	$\theta/\theta_{pl,RBS}$	$M/M_{pl,\ RBS}$	$\theta/\theta_{pl,RBS}$	$M/M_{pl,\ RBS}$	$\theta/\theta_{pl,RBS}$	$M/M_{pl,pin}$	$\theta/\theta_{pl,pin}$
A	0	0	0	0	0	0	0	0
B	1	0	0.6	0	1	0	1	0
C	α	40	α	25	α	25	2	100
D	0.6	40	0.4	25	0.2	25	0.5	100
E	0.6	45	0.4	30	0.2	30	0.5	150
Acceptance criteria (θ/θ_{pl})								
IO	15		5		6		30	
LS	20		12		10		45	
CP	35		18		16		60	
factor α derives from a strain hardening slope equal to 3% of the elastic slope								

Parameters of plastic hinges assigned on the beam to column connections of the main frame, shall be calculated according to the relevant code, but in any case, the rotation capacity of the connection must exceed 40mrad, to ensure that they will not yield prior to the dissipative elements of the FUSEIS systems. According to composite joints, that were used for the case study described in Chapter 4, the relevant code suggests, that their strength and deformation acceptance criteria shall be based on approved rational analysis procedures and experimental evidence.

At this point, it is worth noting the need of a standard analytical procedure that will allow the designer to calculate the rotation capacity of a composite joint. Currently, this is a very unclear point, that depends on the engineer judgment and can lead to uncertainties and possible failures.

The design procedure of FUSEIS beam/pin link system for the linear analysis, is briefly illustrated in the following chart (Figure 2.3).

Preliminary design and geometry of FUSEIS system

Suggested distance between the centers of the columns L = 2.5m	
Geometry of RBS	
a = 0.60bf	$l_{RBS} \geq \frac{4 \times M_{pl,RBS,Rd}}{V_{pl,RBS,Rd}}$
b = 0.75db	
g ≤ 0.25bf	
r = (4g2 + b2) / 8g	

Suggested distance between the centers of the columns L = 1.5m
Geometry of reduced pin section
$l_{pin} \geq \frac{4 \times M_{pl,pin,Rd}}{V_{pl,pin,Rd}}$

Simulation of the building with linear elastic elements

Multi-Modal Response Spectrum Analysis
FUSEIS beam q=5
FUSEIS pin q=3

Limitation of inter-storey drift	2nd order effects
$d_r v \leq 0.0075h$	$\theta = \frac{P_{tot} \times d_r}{V_{tot} \times h_{storey}}$

Axial force	Shear force	Bending moment	Uniform global behavior
$\frac{N_{Ed}}{N_{pl,RBS,pin,Rd}} \leq 0.15$	$\frac{V_{CD,Ed}}{V_{pl,RBS,pin,Rd}} \leq 0.5$	$\frac{M_{Ed}}{M_{pl,RBS,pin,Rd}} \leq 1.0$	$\frac{max\Omega}{min\Omega} \leq 1.25$

Beam/pin rotation
$\theta_{RBS,pin} \leq \theta_{pl,RBS,pin}$

Beam link system columns capacity design
$N_{CD,Ed} = N_{Ed,G} + 1.1 \times \gamma_{ov} \times \Omega \times N_{Ed,E}$
$M_{CD,Ed} = M_{Ed,G} + 1.1 \times \gamma_{ov} \times \Omega \times M_{Ed,E}$
$V_{CD,Ed} = V_{Ed,G} + 1.1 \times \gamma_{ov} \times \Omega \times V_{Ed,E}$

Pin link system columns and receptacles beams capacity design	
$N_{CD,Ed} = N_{Ed,G} + 1.1 \times \alpha \times \gamma_{ov} \times \Omega \times N_{Ed,E}$	
$M_{CD,Ed} = M_{Ed,G} + 1.1 \times \alpha \times \gamma_{ov} \times \Omega \times M_{Ed,E}$	
$V_{CD,Ed} = V_{Ed,G} + 1.1 \times \alpha \times \gamma_{ov} \times \Omega \times V_{Ed,E}$	
$\frac{M_{CD,Ed}}{M_{pl,rec,Rd}} \leq 1.0$	$M_{CD,Ed} = \frac{l_{net}}{l_{RBS/pin}} M_{pl,RBS/pin,Rd}$

Full beam/pin section capacity design	System's connections capacity design
$\frac{M_{CD,Ed}}{M_{pl,Rd}} \leq 1.0$	$M_{CD,con,Ed} = 1.1 \times \gamma_{ov} \frac{l_{net}}{l_{RBS,pin}} M_{pl,RBS,pin,Rd}$
$M_{CD,Ed} = \frac{l}{l_{RBS/pin}} M_{pl,RBS/pin,Rd}$	$V_{CD,con,Ed} = 1.1 \times \gamma_{ov} \frac{2 \times M_{pl,RBS,pin,Rd}}{l_{RBS,pin}}$

Figure 2.3: Summarized design procedure of FUSEIS beam/pin link system

3 Seismic design of two-storey steel building

3.1 General

In this chapter, the detailed design of a 2-storey steel building incorporating the two FUSEIS link systems is presented. In the first case, the building is examined with FUSEIS beam link system and in the second with pin system. The geometry of the building, vertical and lateral loads, results, seismic checks and design are presented for both systems and afterwards the results from the Pushover analysis. Finally, a comparison is made between the two systems of how they react to seismic loads.

The design of the building was performed according to the provisions of the Eurocodes and the design guidelines, as it is described in Chapter 2 of current document.

3.2 Geometry and assumptions

The building is a 2-storey composite building, consisting of four frames with three 8m bays in each direction (Figure 3.1). All the connections of the frames are pinned and two FUSEIS beam/pin link systems are applied on each of the external frames in order to provide the required lateral resistance. The non-system columns are I shaped (HEB type), the main and the secondary floor beams composed of steel beams with IPE and HEA sections respectively, both acting compositely with the concrete slab.

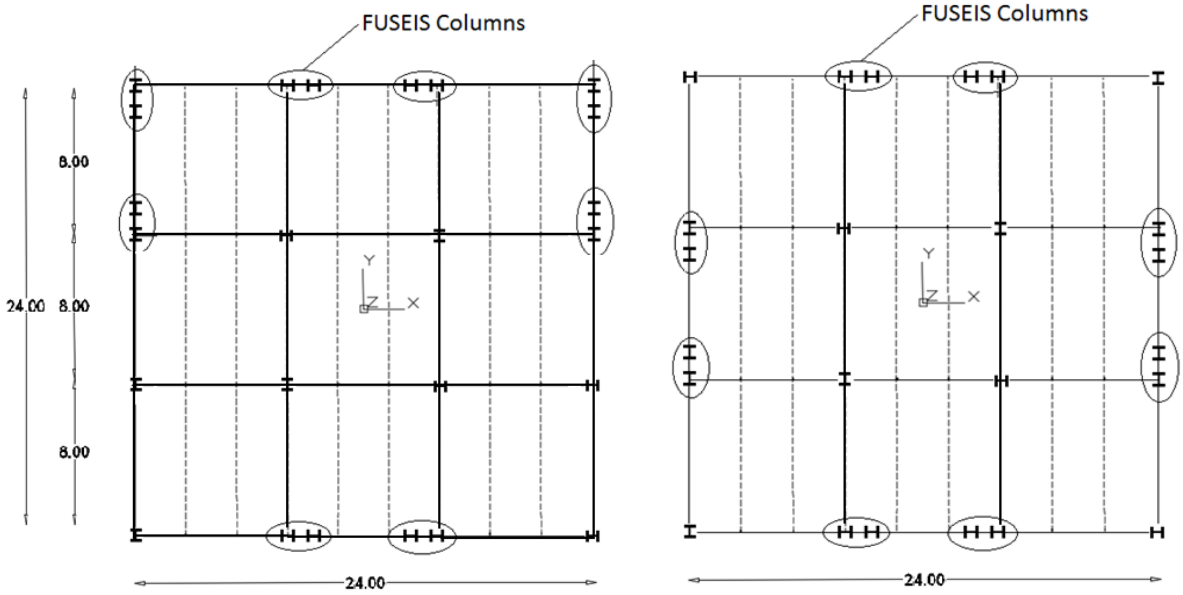

(a) FUSEIS beam system plan view (b) FUSEIS pin system plan view

Figure 3.1: Plan and side view of the building - FUSEIS systems position

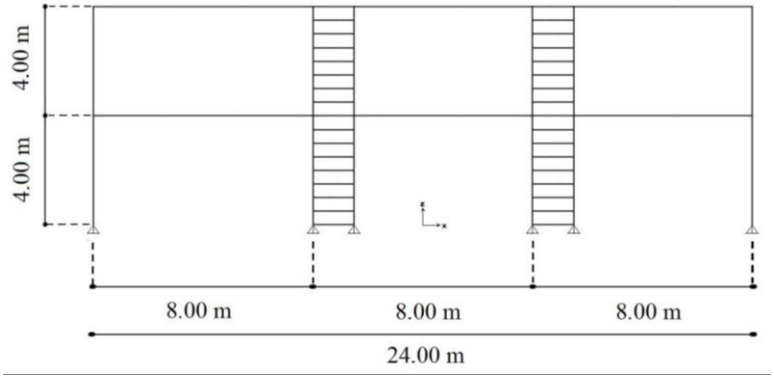

(c) Side view

Figure 3.1: Plan and side view of the building - FUSEIS systems position (continuation

Gravity and seismic loads are summarised in Table 3.1, according to EN 1991-1-1 [14]. The behaviour factors are equal to 5 and 3 as proposed by the design guidelines.

Table 3.1: Loading assumptions

Vertical loads	
dead loads (composite slab + steel sheeting)	2.75 kN/m²
superimposed loads for intermediate floors:	0.70 kN/m²
superimposed loads for top floor:	1.00 kN/m²
perimeter walls:	4.00 kN/m
total live load:	3.80 kN/m²:
Design spectrum characteristics	
Elastic response spectra	Type 1
Peak ground acceleration	0.30g
Importance class II	$\gamma_I = 1.0$
Ground type	C
Behaviour factor q (FUSEIS beam/pin system)	q=5 / q=3
Seismic combination coefficient for the quasi-permanent value of variable actions	ψ_2=0.30

3.3 Simulation, analysis and design

The modelling and design of the building, has been performed with the finite element software SAP2000v19 [10]. The structural model is a linear-elastic model with beam elements, while no-section area elements were used for the correct distribution of the loads. The beam elements representing the FUSEIS beam/pin links are divided into five/three parts with different cross sections in order to simulate the reduction of the flange and the receptacle beams (Figure 2.1).

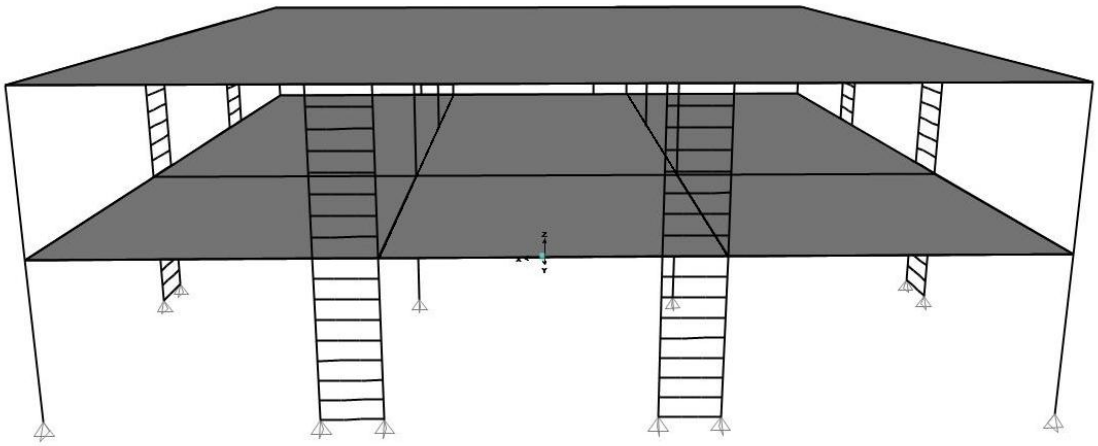

Figure 3.2: 3D view of the model in SAP2000

The columns and the beams of the main frame as well as the composite slabs, were designed both in the Ultimate Limit State (ULS) and the Serviceability Limit State (SLS) in accordance with the provisions of Eurocode 3 and 4.

The profiles of all non-system members have been selected so that all the Eurocodes requirements are satisfied. When the programme automatic calculations were inadequate, e.g. for the design of the composite beams, hand calculations were used instead. The resulting cross section for the main beams was IPE500, for the secondary beams HEA200 and for the columns varied between HEB200 and HEB220. For the design of the secondary beams, construction phases were critical, so temporary supports should be placed to reduce both bending deformation and section size.

The slabs are composite for all floors and were designed with the program SymDeck Designer [15], a software provided by the manufacturer, which takes into account construction phases both for the ultimate and serviceability limit states. The materials used are Fe320 for the steel sheet, C25/30 for concrete and B500C for reinforcing steel. The thickness of the steel sheet is 0.80mm and the longitudinal reinforcement is Ø8/100.

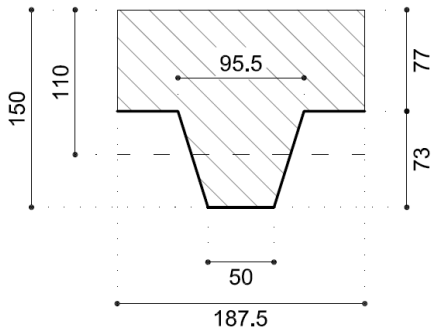

Figure 3.3: Composite slab section

Multi - Modal Response Spectrum Analysis was carried out, to calculate the lateral loads and deformations and to dimension the FUSEIS systems. The first 20 modes were used to

activate more than 90% of the mass. The first and the second modes were translational while the third was rotational for both cases, with their eigen periods given in Table 3.2.

Table 3.2: Eigen periods

Mode No	Eigen Period (s) (beam system)	Eigen Period (s) (pin system)
1	0.74	0.62
2	0.74	0.62
3	0.44	0.38

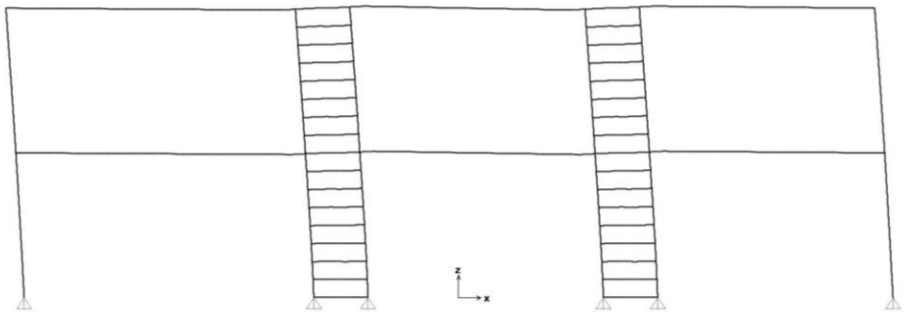

(a) 1st mode of vibration ($T_{1,1}$=0.74s, $T_{2,1}$=0.62s)

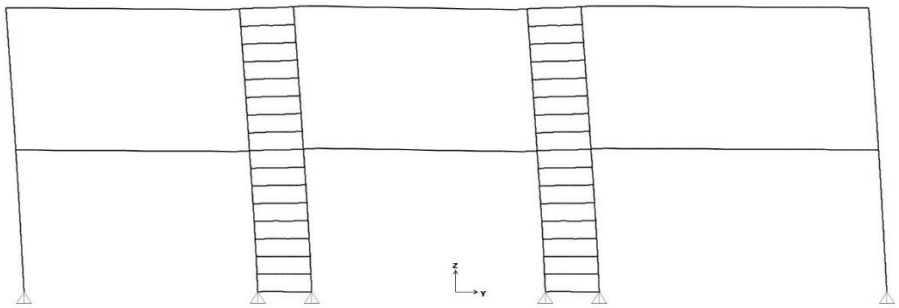

(b) 2nd mode of vibration ($T_{1,2}$=0.74s, $T_{2,2}$=0.62s)

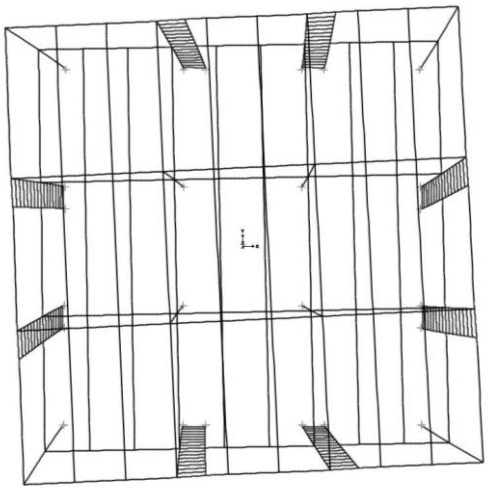

(c) 3rd mode of vibration ($T_{1,3}$=0.44s, $T_{2,3}$=0.38s)

Figure 3.4: 1st, 2nd and 3rd modes shapes

The sections and configuration of the system were chosen after an iterative process. The FUSEIS columns consisted of a pair of strong columns (HEB300) at a central distance of 2.00m and 1.50m for beam and pin system correspondingly, while nine horizontal links per storey were used in both cases, rigidly connected to the system columns. The dissipative elements of the links have steel grade S235, while the receptacle beams are S275, lower than the rest of the structural members (S355). Table 3.3, and Table 3.4 summarize the cross sections of the FUSEIS systems, starting from the foundation level.

Table 3.3: Cross sections of FUSEIS beam system (starting from foundation level)

Number of links	Full cross section	b_f / $b_{f,RBS}$	FUSEIS columns section
×9	HEA200	200 / 120	HEB300
×1	HEA180	180 / 110	HEB300
×7	HEA180	180 / 90	HEB300
b_f is the full flange width $b_{f,RBS}$ is the reduced flange width			

Table 3.4: Cross sections of FUSEIS pin system (starting from ground floor)

Number of links	Full diameter section	Reduced diameter section	FUSEIS receptacle beams	FUSEIS columns section
×2	Φ110	Φ90	HEA240	HEB300
×3	Φ100	Φ80	HEA240	HEB300
×4	Φ95	Φ75	HEA240	HEB300

In order to ensure the development of a bending mechanism at the RBS/RDS positions, the lengths l_{RBS} and l_{pin} were taken larger than the ones calculated from Eq. (2.11), i.e. 1300mm and 300mm respectively.

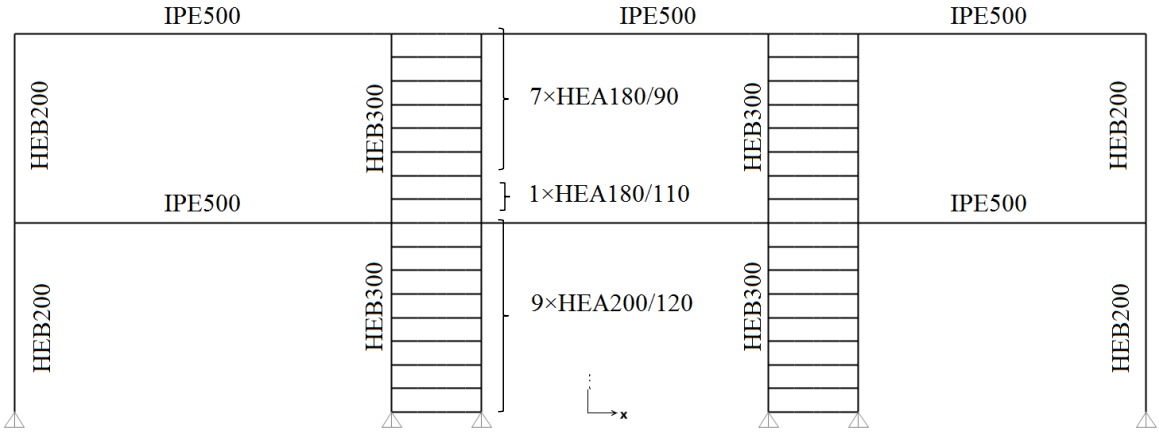

(a) External frame sections 1st case

Figure 3.5: Cross sections of the building

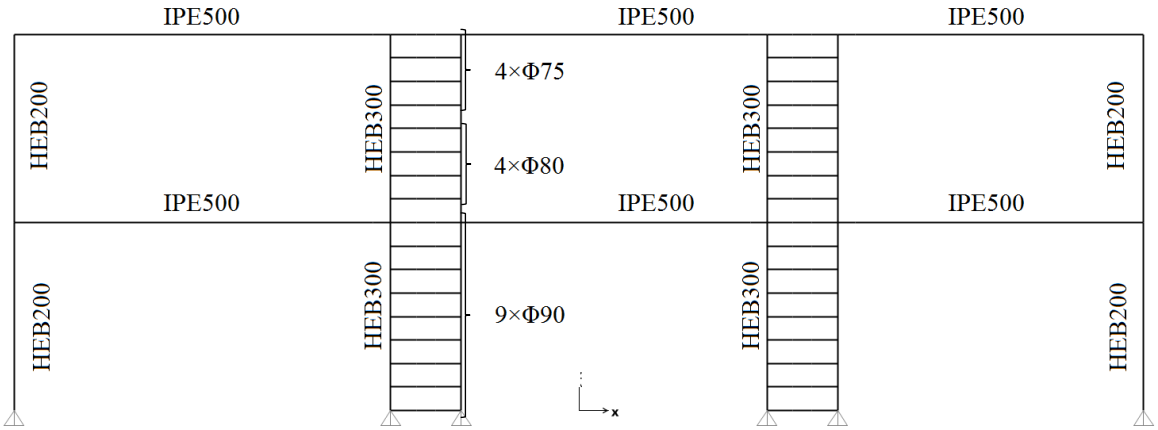

(b) External frame sections 2nd case

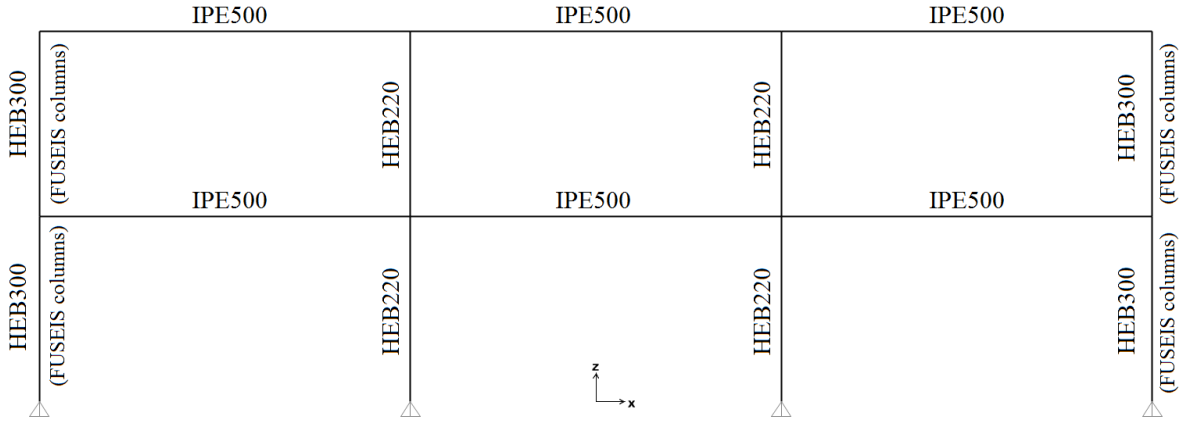

(c) Internal frame sections

Figure 3.5: Cross sections of the building (continuation)

3.4 Seismic design

In order to control the overall stability of the structure and the design of the ductile and non-ductile members under seismic loads, the conditions of §3.4.1-§3.4.4 should be fulfilled, according to the design procedure described in §2.1. Because the structure has similar stiffness and behaviour in both directions, only the results of x-direction are presented.

3.4.1 Limitation of inter-storey drift

Considering that the building has ductile non-structural members, Eq. (2.4) must be fulfilled. Table 3.5 shows the results of the analysis and in both cases the check is verified in all storeys.

Table 3.5: Limitation of inter-storey drift

Case	Storey	u_x (mm)	d_{ex} (mm)	$q*d_{ex}$ (mm)	$v*d_{rx}$ (mm)	Check	0.0075h
1st	1st	11.8	11.8	59.1	29.6	≤	30
	2nd	23.8	12.0	60.0	30.0	≤	30

Table 3.5: Limitation of inter-storey drift (continuation)

Case	Storey	u_x (mm)	d_{ex} (mm)	$q*d_{ex}$ (mm)	$v*d_{rx}$ (mm)	Check	0.0075h
2nd	1st	16.4	16.4	49.2	24.6	≤	30
	2nd	35.0	18.6	55.7	27.8	≤	30

3.4.2 Magnitude of 2nd order effects

This check indicates whether the deformations of the structure are too big to ignore 2nd order effects. As proposed, a linear buckling analysis was performed and the critical buckling factor α_{cr}, coefficient θ and checks derived from this analysis are presented in Table 3.6.

Table 3.6: Magnitude of 2nd order effects

Case	α_{cr}	$\theta = q / \alpha_{cr}$	Check	limit	Seismic load multiplier
1st	51	0.098	≤	0.1	1.00
2nd	70	0.043	≤	0.1	1.00

3.4.3 Dissipative elements verifications

The FUSEIS systems were designed based on the results of the most unfavourable seismic combination 1.0G+0.3Q+E. In order to ensure a uniform dissipative behaviour, the overstrength values Ω of the reduced sections were checked to differ less 25%. A factor maxΩ/minΩ=1.24 and 1.18 was calculated for each case.

Table 3.7 to Table 3.9 summarize the results of all dissipative element verifications described in §2.1. As shown, the bending moment check was the most critical, with maximum utilization factors equal to 94.6% and 92.4% for each case. Additionally, it was derived from the shear check, that no reduction of bending moment resistance was needed due to high shear force.

Table 3.7: Check of axial forces

Reduced beam flange b_f (mm)	N_{Ed} (kN)	$N_{pl,RBS,Rd}$ (kN)	$\frac{N_{Ed}}{N_{pl,RBS,Rd}} \le 0.15$
120	3.50	889.01	0.004
110	3.50	750.83	0.004
90	3.00	661.53	0.005
Reduced diameter pins Φ(mm)	N_{Ed} (kN)	$N_{pl,pin,Rd}$ (kN)	$\frac{N_{Ed}}{N_{pl,pin,Rd}} \le 0.15$
90	10.58	1495.01	0.007
80	18.12	1181.24	0.015
75	5.00	1038.20	0.005

Table 3.8: Check of shear forces

Reduced beam flange b_f (mm)	$V_{CD,Ed}$ (kN)	$V_{pl,RBS,Rd}$ (kN)	$\frac{V_{CD,Ed}}{V_{pl,RBS/pin,Rd}} \leq 0.5$
120	103.04	245.30	0.42
110	78.64	196.33	0.40
90	67.54	196.33	0.34
Reduced diameter pins Φ(mm)	$V_{CD,Ed}$ (kN)	$V_{pl,pin,Rd}$ (kN)	$\frac{V_{CD,Ed}}{V_{pl,RBS/pin,Rd}} \leq 0.5$
90	188.00	863.14	0.22
80	133.17	682.00	0.20
75	109.67	599.40	0.18

Table 3.9: Check of bending moments

Reduced beam flange b_f (mm)	M_{Ed} (kNm)	$M_{pl,RBS,Rd}$ (kNm)	$\frac{M_{Ed}}{M_{pl,RBS,Rd}} \leq 1.00$
120	59.25	66.98	0.88
110	48.37	51.11	0.94
90	37.86	43.90	0.86
Reduced diameter pins Φ(mm)	M_{Ed} (kNm)	$M_{pl,pin,Rd}$ (kNm)	$\frac{M_{Ed}}{M_{pl,pin,Rd}} \leq 1.00$
90	25.14	28.20	0.89
80	18.14	19.98	0.91
75	15.19	16.45	0.92

It was also checked that the RBS/pin chord rotations were below the limit suggested by the design guides, according to Eq. (2.14) and Eq. (2.15). The results in Table 3.10 show that all rotations are well below the limit.

Table 3.10: Check of chord rotation

1st case			
Storey number	θ_{RBS} (mrad)	check	$\theta_{pl,RBS}$ (mrad)
1	22.73	≤	50
2	23.08	≤	50
2nd case			
Storey number	θ_{pin} (mrad)	check	$\theta_{pl,pin}$ (mrad)
1	12.31	≤	140
2	13.92	≤	140

3.4.4 Non-dissipative elements verifications

The non-dissipative elements i.e. the system columns, the receptacle beams, the full section beams/pins and their connections were capacity designed for increased internal forces, as suggested in Eq. (2.16) to Eq. (2.27). The utilization factors of the system columns were calculated according to the provisions of EN1993-1-1 [9] and the highest were 91% and 100% for the 1st and 2nd case respectively.

The moment resistance of the full beams/pins sections was verified at the contact area with the face plates and the results are shown in Table 3.11.

Table 3.11: Capacity design check of the full beam/pin sections and receptacles

Reduced beam flange b_f (mm)	$M_{CD,Ed}$ (kNm)	$M_{pl,Rd}$ (kNm)	$\frac{M_{CD,Ed}}{M_{pl,Rd}} \leq 1.00$
120	87.58	100.82	0.87
110	66.84	76.35	0.88
90	57.41	76.35	0.75
Reduced diameter pins Φ(mm)	$M_{CD,Ed}$ (kNm)	$M_{pl,Rd}$ (kNm)	$\frac{M_{CD,Ed}}{M_{pl,Rd}} \leq 1.00$
90	37.60	51.70	0.73
80	26.63	38.78	0.69
75	21.93	33.37	0.66
Receptacles	107.16	204.77	0.52

3.5 Non-linear static analysis (Pushover)

In order to verify the collapse mechanism, the plastic hinges distribution and to check the behaviour factor q used in linear analysis, a non-linear static analysis (Pushover) was performed. Analysis was done in x and y directions, in both Modal and Uniform shapes, including P-Delta effects and a target displacement equal to 1m. In the following paragraphs, only the results for the fundamental mode of vibration in x direction are presented, due to the similar behaviour of the structure in each direction and loading shape. Afterwards, an evaluation of the q factor is presented, based on the results of the Pushover analysis.

3.5.1 Evaluation of the non-linear behaviour of the building

In order to perform the Pushover analysis, non-linear plastic hinges were inserted in critical points of the structure i.e. the weakened parts, the receptacles, the full beam section and the system columns.

The characteristics of some typical plastic hinges assigned on the full section and the weakened parts of the links, are shown in Table 3.12 and Table 3.13 and were calculated according to §2.2.

Table 3.12: Example of plastic hinge of an I-section beam

Section	M (kNm)	θ (mrad)	M / M_{pl}	θ / θ_{pl}
HEA200	0	0	0	0
	205	0	1	0
	260.05	6.97	1.27	9.00
	122.86	6.97	0.60	9.00
	122.86	8.52	0.60	11.00

Table 3.13: Example of plastic hinge of pin

Section	M (kNm)	θ (mrad)	M / M_{pl}	θ / θ_{pl}
Ø80	0	0	0	0
	20	0	1	0
	40	240	2	100
	10	240	0.50	100
	10	360	0.50	150

The Pushover analysis continued until roof displacement 0.8m, whereupon the structure lost its overall stability and the method failed to converge. The plastic hinge distribution at first yield, at performance point and at ULS are given in Figure 3.6 and Figure 3.7, for both cases. It is observed that the columns remained elastic and that plastic hinges formed only at the horizontal links of the FUSEIS systems.

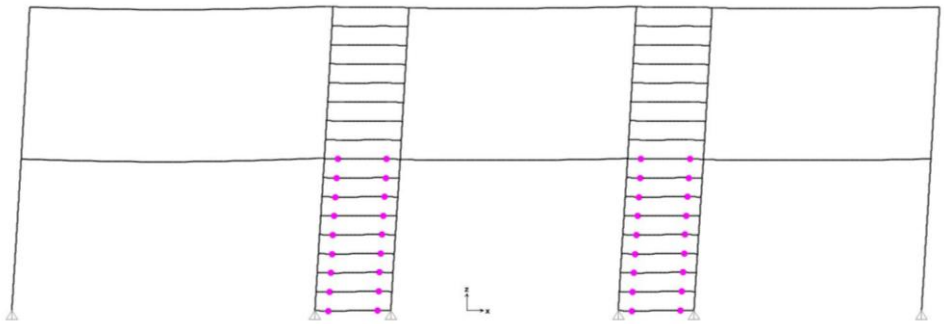

(a) First yield, θ_{gl} = 0.74%

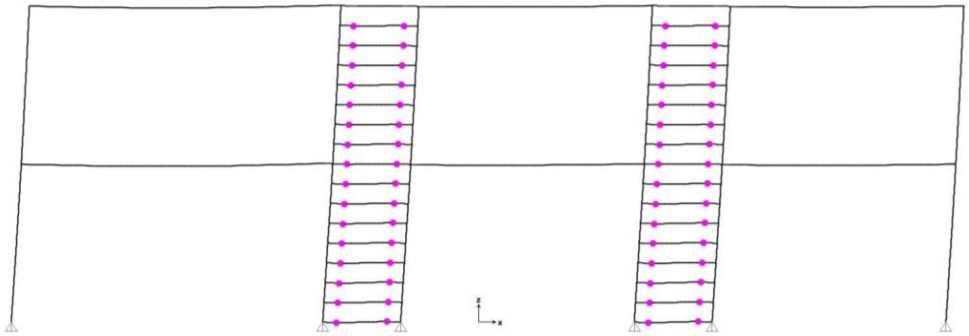

(b) Performance Point, θ_{gl} = 0.96%

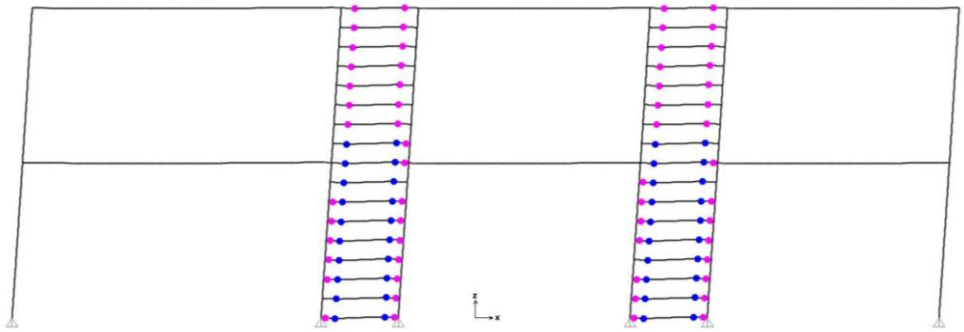

(c) ULS, θ_{gl} = 3.25 %

Figure 3.6: Deformed frame and plastic hinge formation of 1st case study

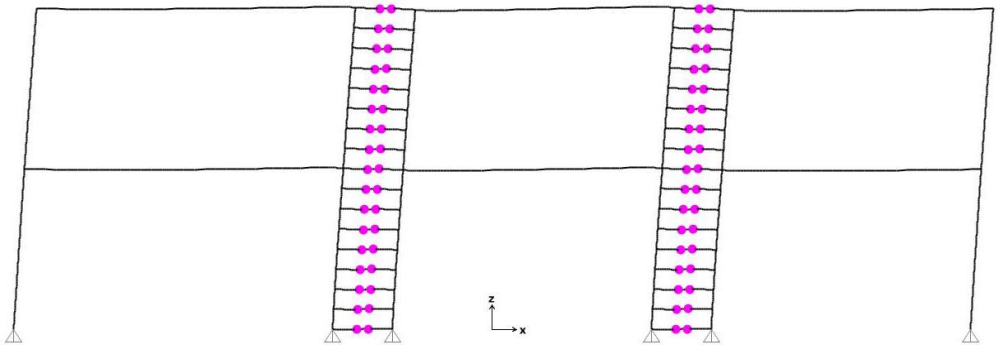

(a) First yield, θ_{gl} = 0.63%

Figure 3.7: Deformed frame and plastic hinge formation of 2nd case study

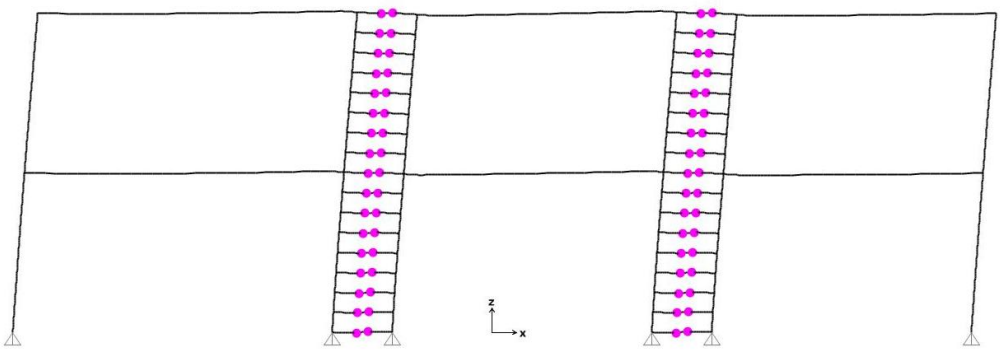

(b) Performance Point, θ_{gl} = 0.78%

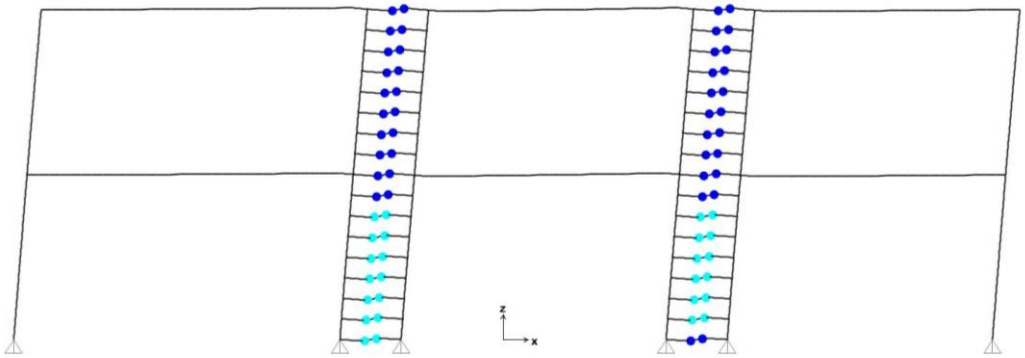

(c) ULS, θ_{gl} = 2.80%

Figure 3.7: Deformed frame and plastic hinge formation of 2nd case study (continuation)

The capacity curves of the two case studies are shown in Figure 3.8, where the performance point, the limit states Immediate Occupancy (IO), Life Safety (LS) and Collapse Prevention (CP) are defined. It is observed that in both cases the Performance Point is below the limit state IO and that the overall behaviour of the structure is not affected by the plastification of one hinge, but of many. In Table 3.14 are given important states of the analysis as well the respectively roof displacement and global drift.

Table 3.14: Important States of Pushover Analysis

Case		First Yield	Perf. Point	(IO)	(ULS)	(LS)	(CP)
1st	δ_{roof} (mm)	59.20	76.82	193.75	259.08	349.53	580.69
	θ_{gl} (%)	0.74%	0.96%	2.42%	3.24%	4.37%	7.26%
2nd	δ_{roof} (mm)	50.53	62.37	167.89	223.17	223.17	283.47
	θ_{gl} (%)	0.63%	0.78%	2.10%	2.79%	2.79%	3.54%

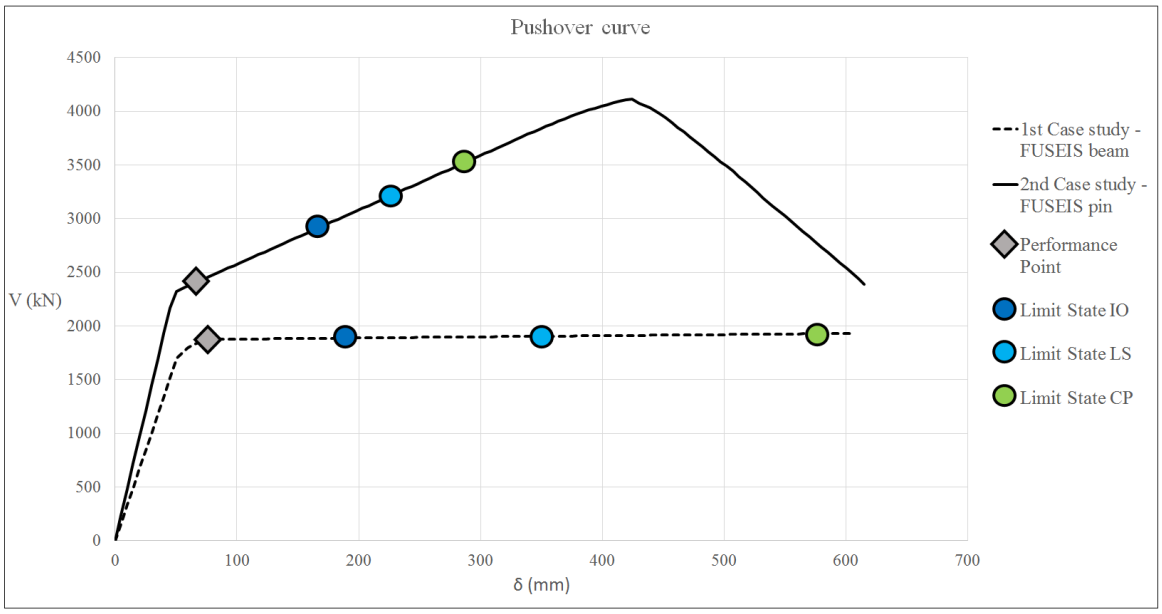

Figure 3.8: Pushover Curves of both Case studies

3.5.2 Evaluation of the behaviour factor q

For the calculation of the behaviour factor the procedure described in the design guides was followed. This procedure suggests the evaluation of the q-factor through the multiplication of the ductility (q_μ) and the overstrength (Ω).

$$q = q_\mu \times \Omega \qquad \text{Eq. (3.1)}$$

Considering that the eigen-periods of the buildings are above T_c=0.60s, the "rule of equal displacement" can be performed. Therefore, ductility factor q_μ is determined as the ratio between $\delta_{LS,\,ULS}$ to δ_{el} as shown in Eq. (3.2). The first coefficient $\delta_{LS,\,ULS}$ is the actual roof displacement of the building when the rotation of the ductile members of the FUSEIS reach either the Life Safety (LS) performance level or the ULS, whichever occurs first. The second coefficient δ_{el} is the displacement of the equivalent elastic model.

$$q_\mu = \frac{\delta_{LS,ULS}}{\delta_{el}} \qquad \text{Eq. (3.2)}$$

Overstrength Ω is the ratio between $V_{LS,\,ULS}$ to V_y as shown in Eq. (3.3). Where $V_{LS,\,ULS}$ is the base shear of the building relevant to $\delta_{LS,\,ULS}$ and V_y is the yield force of the structure.

$$\Omega = \frac{V_{LS,ULS}}{V_y} \qquad \text{Eq. (3.3)}$$

To make the procedure more comprehensible, a typical capacity curve and the parameters mentioned above are given in Figure 3.9.

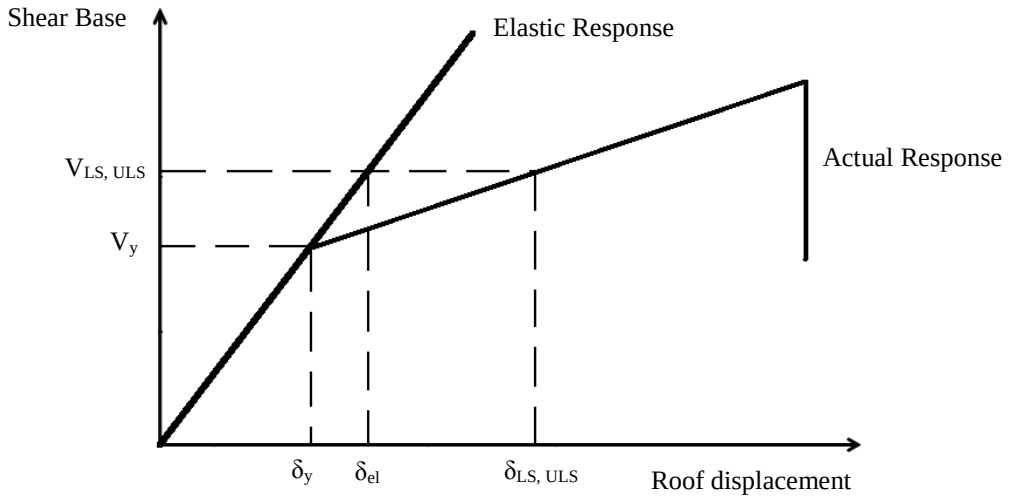

Figure 3.9: Evaluation of behaviour factor q from capacity curve

The calculated ductility, overstrength and behaviour factors for both cases, are given in Table 3.15. As shown, the calculated behaviour factors are slightly higher than the values proposed by design guides.

Table 3.15: Evaluated behaviour factor

Case	$\delta_{LS, ULS}$ (mm)	δ_{el} (mm)	q_μ	$V_{LS, ULS}$ (kN)	V_y (kN)	Ω	q
1st	259.08	56.45	4.59	1895.31	1690	1.12	5.15
2nd	223.17	69.58	3.21	3198.16	2322.61	1.38	4.42

3.6 Comparison between the two systems

To conclude a comparison between the two FUSEIS systems is made:

- In both cases the stiffness of the building was mostly affected by the section of the system columns and the receptacle beams.
- For the FUSEIS beam system a larger central distance of the columns can be used in contrast with the pin system were this distance is limited by the length of the pin.
- Because of the smaller distance between the system columns, strong sections were used for the receptacle beams (comparing to the beam used in first case) in order to increase the stiffness and fulfil the deformations checks.
- The larger beams used in the pin system led to a heavier structure. In the first case, the steel weight was calculated equal to 65.20kg/m^2, while in the second 71.11kg/m^2.
- After the design earthquake only the pins entered the plastic zone while the receptacles remained elastic. Therefore, the replaceable element in the FUSEIS pin link system is only the pin (with length equal to 400), while in the beam system is the whole beam link (with length equal to 1640mm).

- From the Pushover curves, it can be observed that after the yield of the structure, the pin system has a significant load-bearing capacity due to hardening.

4 Seismic design of four-storey steel building

4.1 General

In this chapter, the detailed design of a 4-storey steel building incorporating the FUSEIS pin link system. Two case studies are presented. In the first case, the classic FUSEIS pin link configuration, as described in chapter 1.3.2, is designed, while in the second an alternative set-up of the system is tested, where no receptacle beams are used. In the latter, the horizontal links are consisted only by the pins which are directly connected to the column flange through a face plate. The geometry of the building, vertical and lateral loads, results, seismic checks and design are presented for both cases and afterwards the results from the Pushover analysis. Finally, a comparison is made between the two approaches of the FUSEIS pin link system and how they react to seismic loads.

The design of the building was performed according to the provisions of the Eurocodes and the design guidelines, as it is described in Chapter 2 of current document.

4.2 Geometry and assumptions

The building is a 4-storey composite building with the same plan view as the 2-storey. Two FUSEIS pin link systems are applied on each of the external frames. The connections between the main beams and the non-system columns are semi-rigid, so lateral stability is provided by the FUSEIS systems and the semi-rigid frames.

The assumptions for gravity and seismic loads are the same as in the 2-storey building (Table 3.1). In Figure 4.1, the plan and the side view are shown, while in Figure 4.2 the configuration of the two cases is presented.

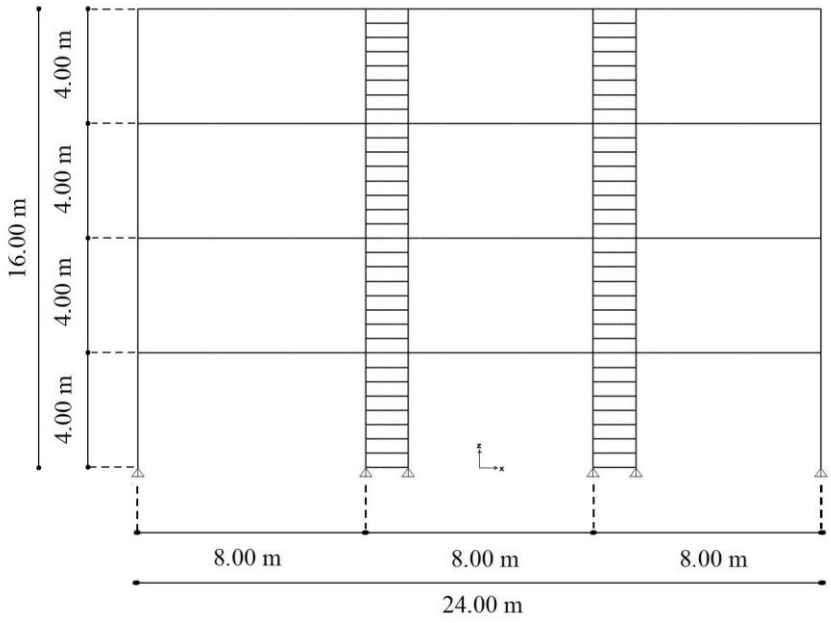

(a)

Figure 4.1: (a) Side view (b) Plan view of the 4-storey building

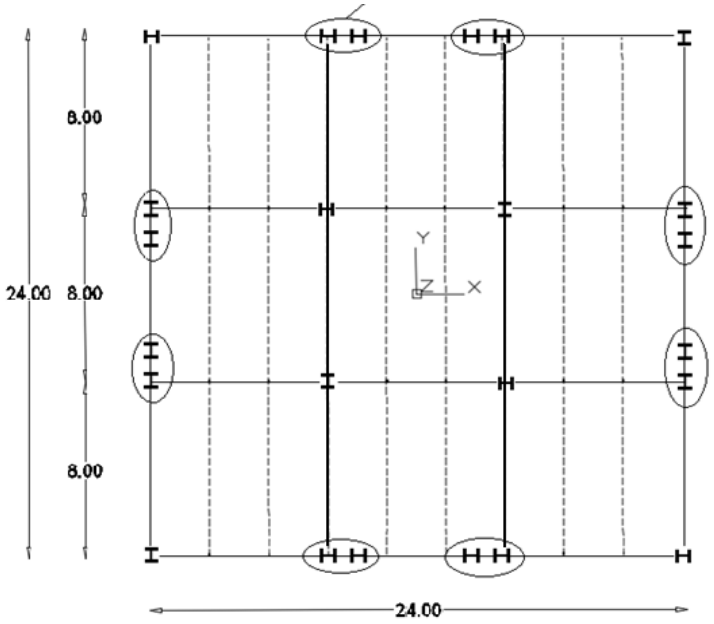

(b)

Figure 4.1: (a) Side view (b) Plan view of the 4-storey building (continuation)

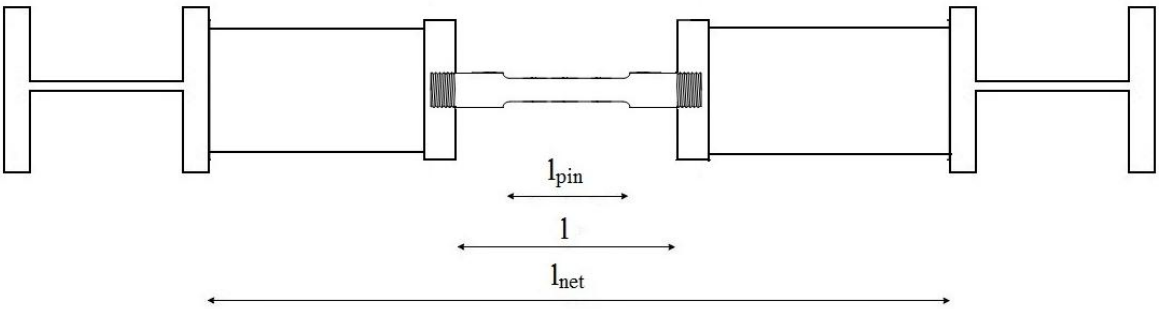

(a)

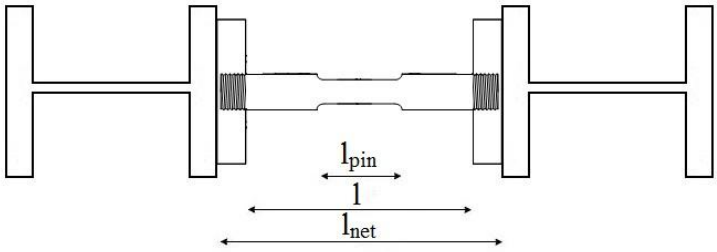

(b)

Figure 4.2: (a) Classic FUSEIS pin link configuration (b) Alternative FUSEIS pin link without receptacles

4.3 Simulation, analysis and design

The modelling and design of the building have also been performed with the software SAP2000v19. In the first case, the horizontal links were simulated according to the design guides (Chapter 2.1), while in the second case the beam elements representing the links were divided into 3 parts; two parts for the full diameter section and one for the reduced diameter in the middle.

The structural model is similar to the one used for the low-rise building, i.e. a linear-elastic model with beam elements and no-section area elements for the correct distribution of the loads

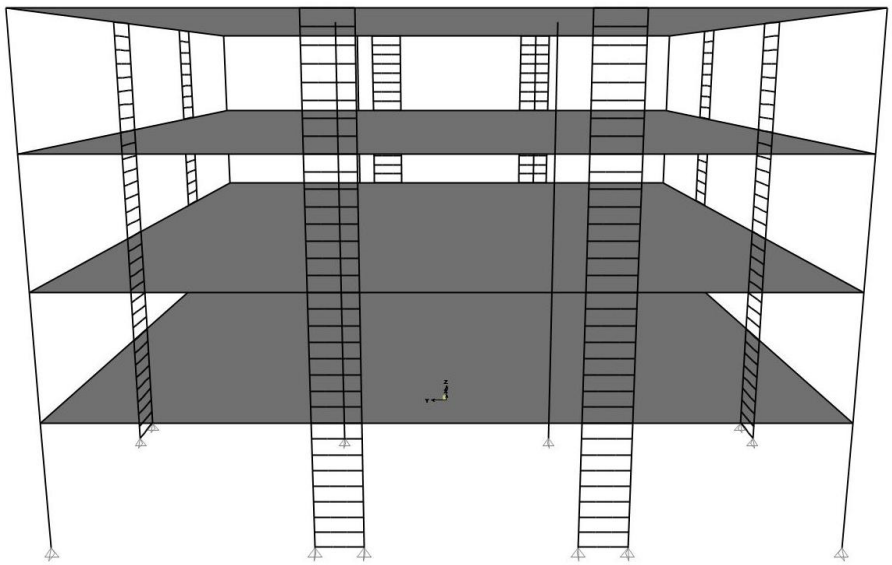

Figure 4.3: 3D view of the model in SAP2000

The difference from the previous model is that linear elastic springs were inserted at the ends of the main beams, to take into consideration the semi-rigid connection between the main beam and the columns. Each constituent part of the composite joint was analysed, according to EN1994-1-1 [11], EN 1993-1-8 [9], and EN1998-1 [8], and then, with the composition of them, the stiffness and the moment resistance of the whole joint was determined. The resulted stiffness of the springs varied between 19000kNm and 27000kNm, depending on the floor and whether the joint was internal or external.

The columns and the beams of the main frame as well as the composite slabs, were designed both in the Ultimate Limit State (ULS) and the Serviceability Limit State (SLS). Considering that the vertical loads and the length of each span was the same, the resulting cross section for these members was the same. In Table 4.1, the sections selected for the columns are given, varying from HEB200 to HEB280

Table 4.1: Loading assumptions

Floor	Centre	Perimeter
1, 2	HEB280	HEB220
3, 4	HEB220	HEB200

Multi - Modal Response Spectrum Analysis was performed to calculate the seismic load. The first 5 modes were used to activate more than 90% of the mass. The first and the second modes were translational, while the third was rotational, with their eigen periods given in Table 4.2.

Table 4.2: Eigen periods

Mode No	Eigen Period (s) (classic pin system)	Eigen Period (s) (alternative pin system)
1	1.07	1.14
2	1.07	1.14
3	0.69	0.73

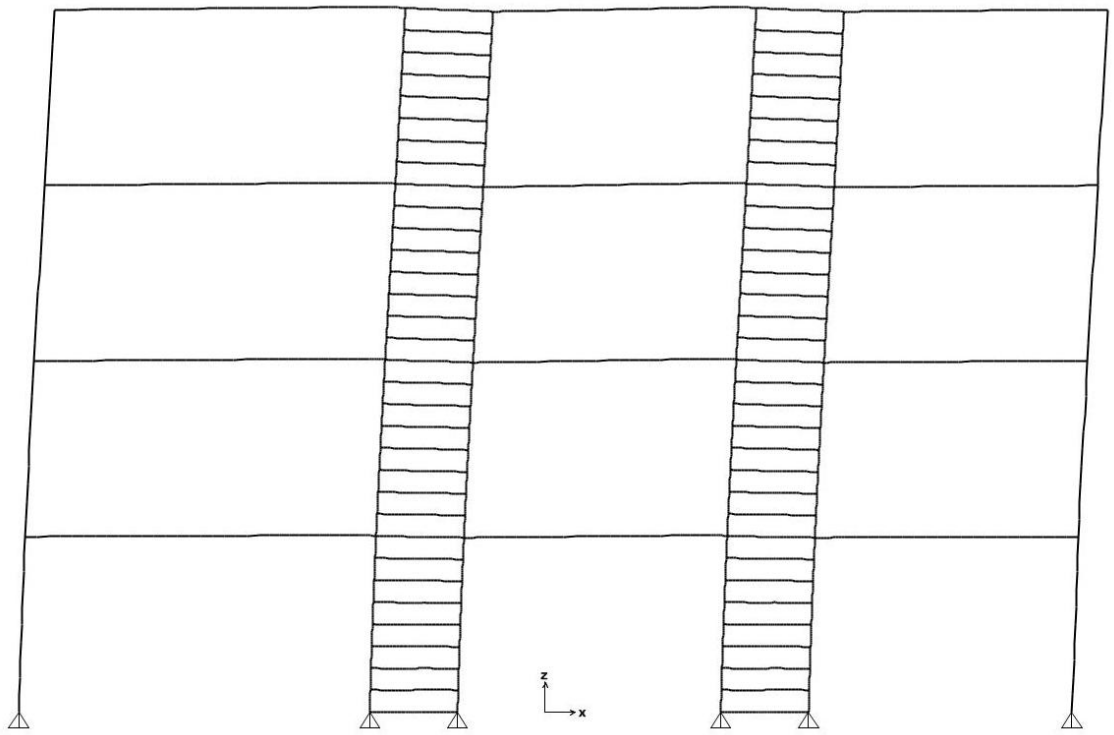

(a) 1st mode of vibration ($T_{1,1}$=1.07s, $T_{2,1}$=1.14s)

Figure 4.4: 1st, 2nd and 3rd modes shapes

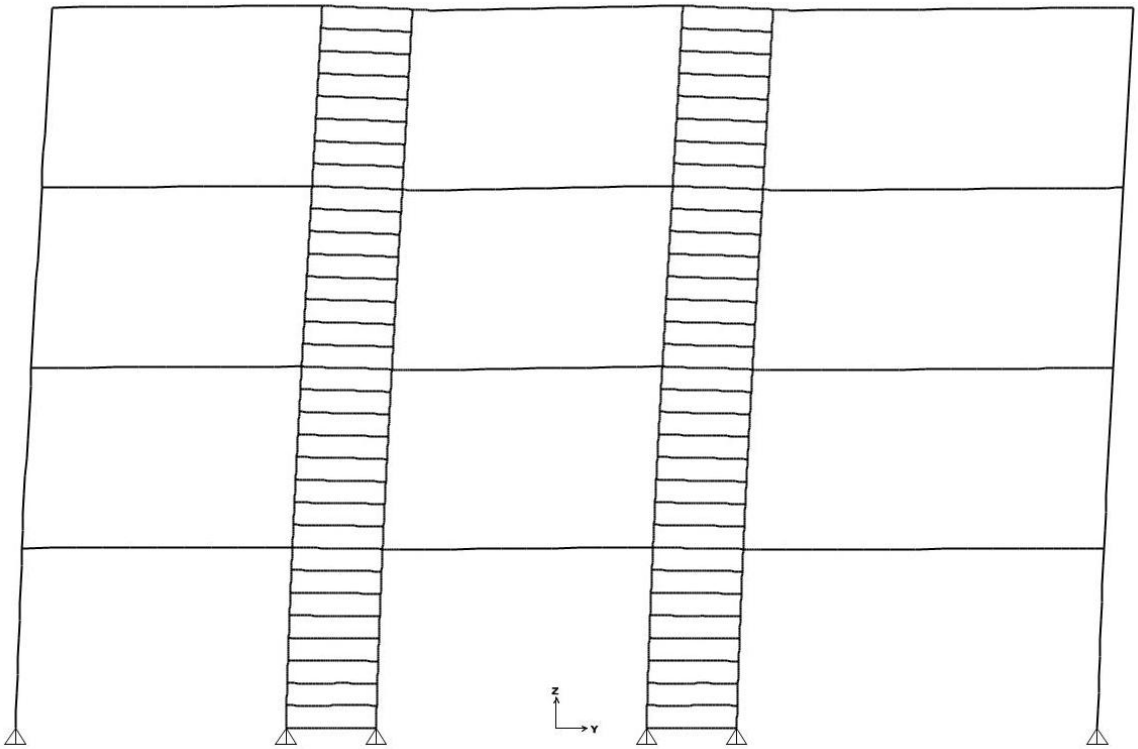

(b) 2nd mode of vibration ($T_{1,2}$=1.07s, $T_{2,2}$=1.14s)

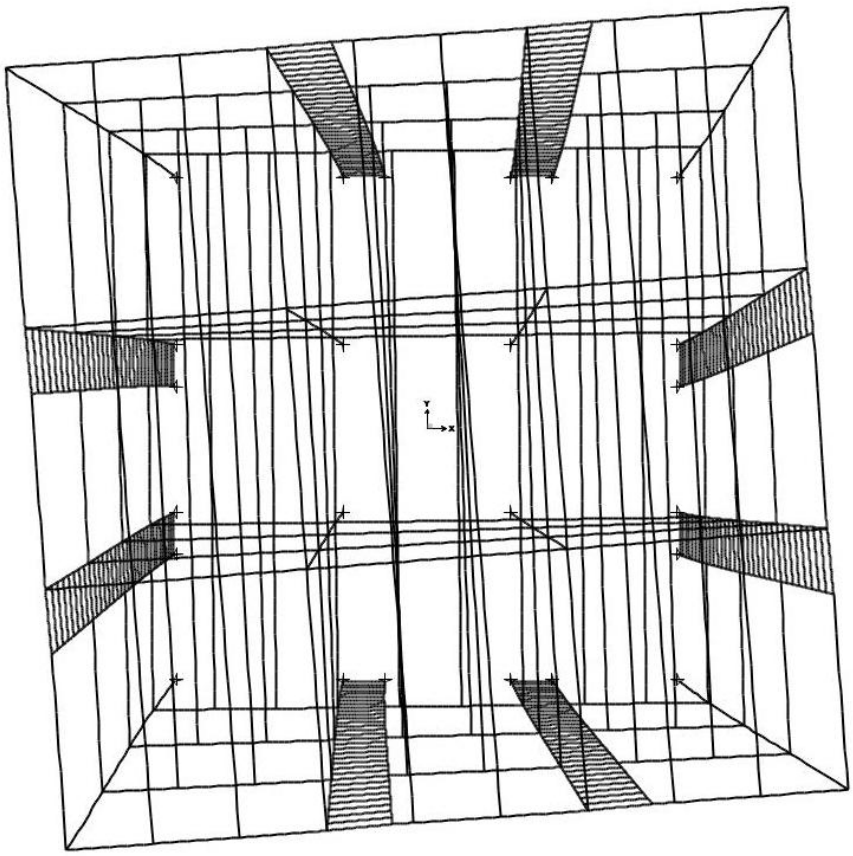

(c) 3rd mode of vibration ($T_{1,3}$=0.69s, $T_{2,3}$=0.73s)

Figure 4.4: 1st, 2nd and 3rd modes shapes (continuation)

The sections and configuration of the system were chosen after an iterative procedure. In the first case, the FUSEIS systems consisted of a pair of two strong columns (HEB450) at a central distance of 2.00m, while nine links per storey were used in both cases, rigidly connected to the system columns. The dissipative elements of the links have steel grade S235, while the receptacle beams are S275, which is lower than the rest of the structural members (S355). Table 4.3 summarizes the cross sections of the FUSEIS systems, starting from the foundation level.

Table 4.3: Cross sections of classic FUSEIS pin link system (starting from foundation level)

Number of links	Full diameter section	Reduced diameter section	FUSEIS columns section	FUSEIS receptacle beams
×9	Ø105	Ø90	HEB450	HEA260
×8	Ø95	Ø80	HEB450	HEA260
×8	Ø90	Ø75	HEB450	HEA260
×8	Ø80	Ø65	HEB450	HEA260

In order to ensure the development of a bending mechanism at the RDS positions, the length of the weakened part of the pin l_{pin} was equal to 300mm, larger than the one calculated from Eq. (2.11).

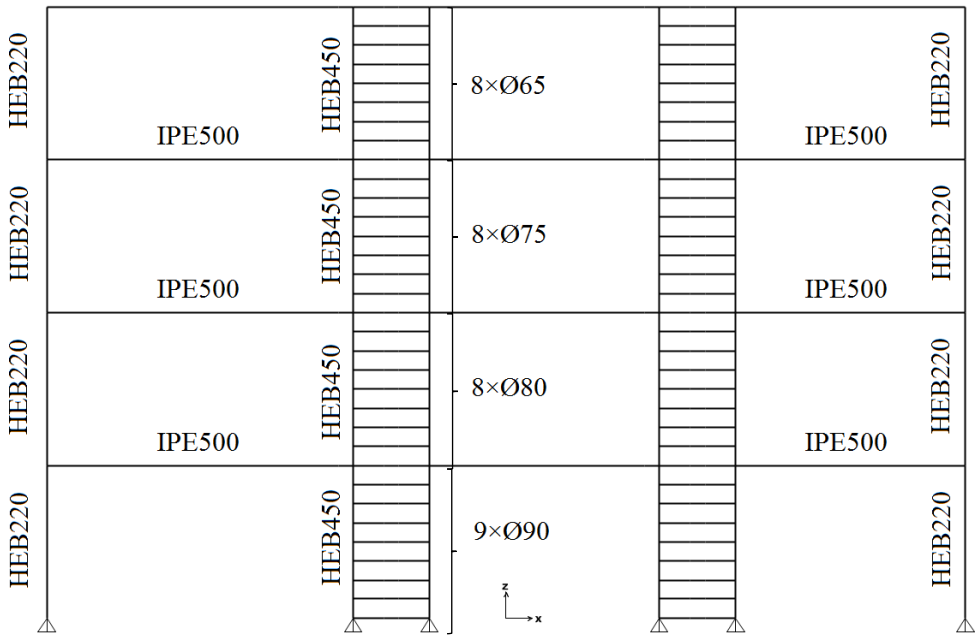

(a) External frame sections 2nd case

Figure 4.5: Cross sections of the building

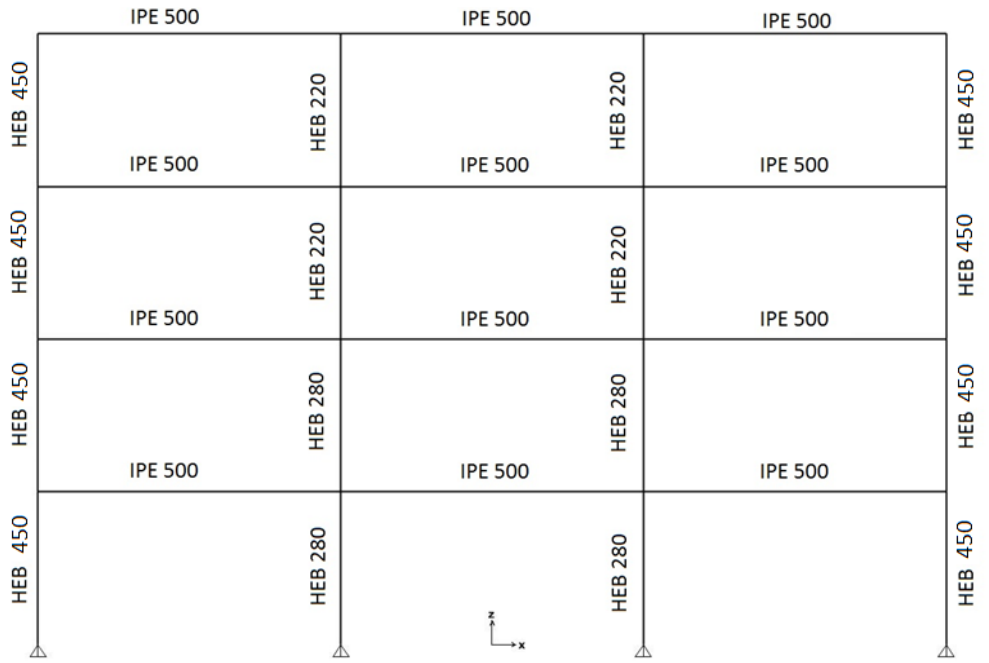

(b) Internal frame sections

Figure 4.5: Cross sections of the building (continuation)

Regarding the second case where the alternative FUSEIS system was tested, the absence of receptacle beams led to many restrictions in terms of geometry and seismic deformation. Provided that the FUSEIS links consisted only of the dissipative pins, the stiffness of the structure was significantly reduced. After many tests, it was observed that (similarly to the classic FUSEIS pin link system) the stiffness of the building was mainly affected by the section of the system columns. Moreover, the axial distance of the columns could not be higher than 1.50m, because then the length of the pin would be too large. Therefore, it was essential to choose a large section for the columns in order to reduce the length of the pin, to increase the stiffness of the model and to limit the seismic deformations. It was chosen HEB700 for the system columns with a central distance equal to 1.5m. The dissipative pins had steel grade S235, while the rest of the members S355. In Table 4.4 the cross sections of the alternative FUSEIS system used in the second case study are summarized, starting from the foundation level.

Table 4.4: Cross sections of alternative FUSEIS pin link system (starting from foundation level)

Number of links	Full diameter section	Reduced diameter section	FUSEIS columns section
×2	Ø160	Ø120	HEB700
×3	Ø150	Ø110	HEB700
×4	Ø140	Ø105	HEB700
×4	Ø130	Ø100	HEB700

Table 4.4: Cross sections of alternative FUSEIS pin link system (starting from foundation level) (continuation)

Number of links	Full diameter section	Reduced diameter section	FUSEIS columns section
×4	Ø130	Ø95	HEB700
×4	Ø130	Ø90	HEB700
×4	Ø130	Ø85	HEB700
×4	Ø130	Ø75	HEB700
×4	Ø120	Ø70	HEB700

In order to ensure the development of a bending mechanism at the RDS positions and to achieve a uniform dissipative behaviour, the length of the weakened part of the pin l_{pin} varied between 500mm and 600mm, but in any case, larger than the one calculated from Eq. (2.11).

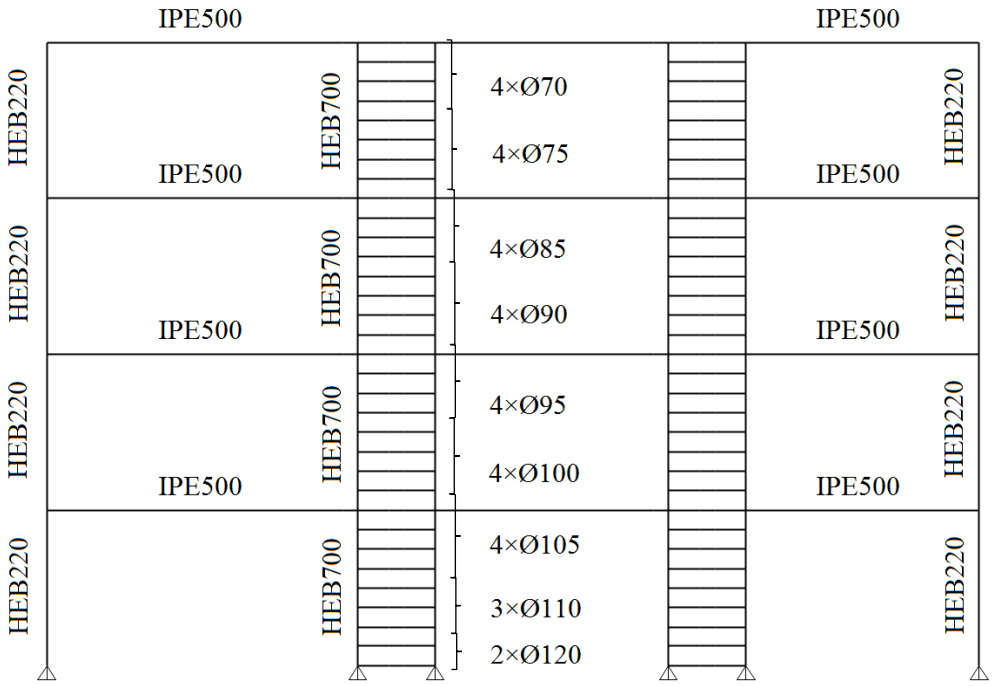

(a) External frame sections 1st case

Figure 4.6: Cross sections of the building

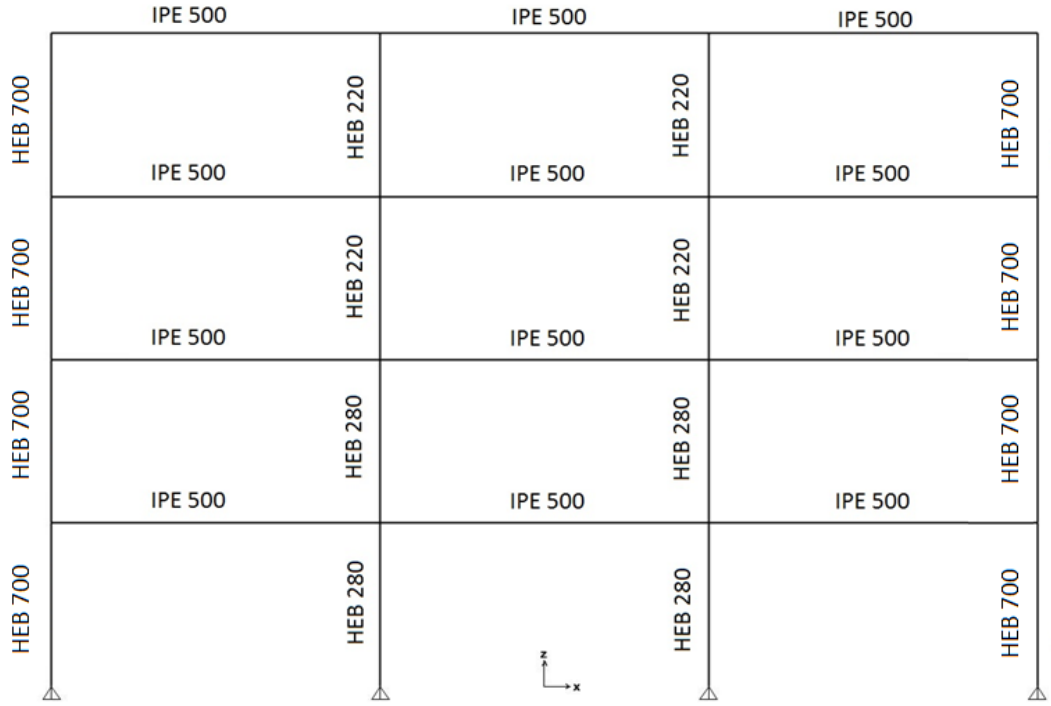

(b) Internal frame sections

Figure 4.6: Cross sections of the building (continuation)

4.4 Seismic design

In order to control the overall stability of the structure and the design of the ductile and non-ductile members under seismic loads, the conditions of §4.4.1-4.4.4 should be fulfilled, according to the design procedure described in §2.1. Because the structure has similar stiffness and behaviour in both directions, only the results of x-direction are presented.

4.4.1 Limitation of inter-storey drift

Considering that the building has ductile non-structural members, Eq. (2.4) must be fulfilled. Table 4.5 shows the results of the analysis and in both cases the check is verified in all storeys.

Table 4.5: Limitation of inter-storey drift

Case	Storey	u_x (mm)	d_{ex} (mm)	$q*d_{ex}$ (mm)	$v*d_{rx}$ (mm)	Check	0.0075h
1st	1st	11.9	11.9	35.6	17.8	≤	30
	2nd	28.3	16.4	49.2	24.6	≤	30
	3rd	46.8	18.5	55.5	27.7	≤	30
	4th	65.0	18.2	54.7	27.4	≤	30
2nd	1st	11.8	11.8	35.4	17.7	≤	30

Table 4.5: Limitation of inter-storey drift (continuation)

Case	Storey	u_x (mm)	d_{ex} (mm)	$q*d_{ex}$ (mm)	$v*d_{rx}$ (mm)	Check	0.0075h
2nd	2nd	28.0	16.2	48.6	24.3	≤	30
	3rd	46.8	18.8	56.3	28.1	≤	30
	4th	65.7	19.0	56.9	28.4	≤	30

4.4.2 Magnitude of 2nd order effects

This check indicates whether the deformations of the structure are too big to ignore 2nd order effects. As proposed, a linear buckling analysis was performed and the critical buckling factor α_{cr}, coefficient θ and checks derived from this analysis are presented in Table 4.6.

Table 4.6: Magnitude of 2nd order effects

Case	α_{cr}	$\theta = q / \alpha_{cr}$	Check	limit	Seismic load multiplier
1st	46	0.065	≤	0.1	1.00
2nd	37	0.081	≤	0.1	1.00

4.4.3 Dissipative elements verifications

The FUSEIS systems were designed based on the results of the most unfavourable seismic combination 1.0G+0.3Q+E. In order to ensure a uniform dissipative behaviour, the overstrength values Ω of the reduced sections were checked to differ less than 25%. It was calculated maxΩ/minΩ=1.23 and 1.24 for each case.

Table 4.7 to Table 4.9 summarize the results of all dissipative element verifications described in §2.1. As shown, the bending moment check was the most critical, with maximum utilization factors equal to 90% and 89% for each case. Additionally, it was derived from the shear check, that no reduction of bending moment resistance was needed due to high shear force.

Table 4.7: Check of axial forces

1st Case, reduced diameter pins (mm)	N_{Ed} (kN)	$N_{pl,pin,Rd}$ (kN)	$\frac{N_{Ed}}{N_{pl,pin,Rd}} \le 0.15$
Ø90	0.52	1495.00	0.000
Ø80	0.58	1181.24	0.000
Ø75	4.43	1038.20	0.004
Ø65	4.16	779.82	0.005

Table 4.7: Check of axial forces (continuation)

2st Case, reduced diameter pins (mm)	N_{Ed} (kN)	$N_{pl,pin,Rd}$ (kN)	$\frac{N_{Ed}}{N_{pl,pin,Rd}} \leq 0.15$
Ø120	1.04	2657.79	0.000
Ø110	1.26	2233.28	0.001
Ø105	4.50	2034.87	0.002
Ø100	4.29	1845.69	0.002
Ø95	4.32	1665.73	0.003
Ø90	4.18	1495.01	0.003
Ø85	4.15	1333.51	0.003
Ø75	7.60	1038.20	0.007
Ø70	7.58	904.39	0.008

Table 4.8: Check of shear forces

1st Case, reduced diameter pins (mm)	$V_{CD,Ed}$ (kN)	$V_{pl,pin,Rd}$ (kN)	$\frac{V_{CD,Ed}}{V_{pl,RBS/pin,Rd}} \leq 0.5$
Ø90	188.00	863.14	0.22
Ø80	133.17	681.98	0.20
Ø75	109.67	599.40	0.18
Ø65	70.50	450.21	0.16
2st Case, reduced diameter pins (mm)	$V_{CD,Ed}$ (kN)	$V_{pl,pin,Rd}$ (kN)	$\frac{V_{CD,Ed}}{V_{pl,RBS/pin,Rd}} \leq 0.5$
Ø120	267.90	1534.47	0.17
Ø110	206.80	1289.38	0.16
Ø105	160.30	1174.83	0.14
Ø100	129.25	1065.61	0.12
Ø95	119.18	961.71	0.12
Ø90	94.00	863.14	0.11
Ø85	84.77	769.90	0.11
Ø75	54.83	599.40	0.09
Ø70	47.84	522.15	0.09

Table 4.9: Check of bending moments

1st Case, reduced diameter pins (mm)	M_{Ed} (kNm)	$M_{pl,pin,Rd}$ (kNm)	$\frac{M_{Ed}}{M_{pl,pin,Rd}} \leq 1.00$
Ø90	24.44	28.20	0.87
Ø80	17.93	19.98	0.90
Ø75	14.52	16.45	0.88
Ø65	9.17	10.58	0.87
2st Case, reduced diameter pins (mm)	M_{Ed} (kNm)	$M_{pl,pin,Rd}$ (kNm)	$\frac{M_{Ed}}{M_{pl,pin,Rd}} \leq 1.00$
Ø120	58.38	66.98	0.87
Ø110	46.11	51.70	0.89
Ø105	34.39	44.89	0.77
Ø100	29.19	38.78	0.75
Ø95	26.34	33.37	0.79
Ø90	22.00	28.20	0.78
Ø85	19.75	23.74	0.83
Ø75	12.17	16.45	0.74
Ø70	10.20	13.40	0.76

It was also checked that the pin chord rotations were below the limit suggested by the design guides, according to Eq. (2.14) and Eq. (2.15). The results are shown in Table 4.10 and all rotations are well below the limit value.

Table 4.10: Check of chord rotation

1st case			
Storey number	θ_{pin} (mrad)	check	$\theta_{pl,pin}$ (mrad)
1st	59.38	≤	140
2nd	81.96	≤	140
3rd	92.45	≤	140
4th	91.21	≤	140

Table 4.10: Check of chord rotation (continuation)

2nd case			
Storey number	θ_{pin} (mrad)	check	$\theta_{pl,pin}$ (mrad)
1st	26.56	≤	140
	26.56	≤	140
	23.72	≤	140
2nd	30.37	≤	140
	32.54	≤	140
3rd	35.18	≤	140
	37.69	≤	140
4th	35.53	≤	140
	38.07	≤	140

4.4.4 Non-dissipative elements verifications

The non-dissipative elements i.e. the system columns, the receptacle beams, the full section pins and their connections were capacity designed for increased internal forces, as suggested in Eq. (2.16) to Eq. (2.27). The utilization factors of the system columns were calculated according to the provisions of EN1993-1-1 and were as high as 100% for both cases.

The moment resistance of the full pins sections was verified at the contact area with the face plates and the results are shown in Table 4.11.

Table 4.11: Capacity design check of the full pin sections and receptacles

1st Case, reduced diameter pins (mm)	$M_{CD,Ed}$ (kNm)	$M_{pl,Rd}$ (kNm)	$\frac{M_{CD,Ed}}{M_{pl,Rd}} \leq 1.00$
Ø105	37.60	44.91	0.84
Ø95	26.63	33.37	0.80
Ø90	21.93	28.20	0.78
Ø80	14.10	19.98	0.71
Receptacles	145.70	252.95	0.58
2st Case, reduced diameter pins (mm)	$M_{CD,Ed}$ (kNm)	$M_{pl,Rd}$ (kNm)	$\frac{M_{CD,Ed}}{M_{pl,Rd}} \leq 1.00$
Ø160	99.12	158.86	0.62
Ø150	76.52	130.90	0.58

Table 4.11: Capacity design check of the full pin sections and receptacles (continuation)

2st Case, reduced diameter pins (mm)	$M_{CD,Ed}$ (kNm)	$M_{pl,Rd}$ (kNm)	$\frac{M_{CD,Ed}}{M_{pl,Rd}} \leq 1.00$
Ø140	59.31	85.31	0.70
Ø130	47.82	85.31	0.56
Ø130	44.10	85.31	0.52
Ø130	34.78	85.31	0.41
Ø130	31.36	85.31	0.37
Ø130	20.29	85.31	0.24
Ø120	17.70	66.98	0.26

4.5 Non-linear static analysis (Pushover)

In order to verify the collapse mechanism, the plastic hinges distribution and to check the behaviour factor q used in linear analysis, a non-linear static analysis (Pushover) was performed. Analysis was done in x and y directions, in both Modal and Uniform shapes, including P-Delta effects and a target displacement equal to 1m. In the following paragraphs, only the results for the fundamental mode of vibration in x direction are presented, due to the similar behaviour of the structure in each direction and loading shape. Afterwards, an evaluation of the q factor is presented, based on the results of the Pushover analysis.

4.5.1 Evaluation of the non-linear behaviour of the building

In order to perform the Pushover analysis, non-linear plastic hinges were inserted in critical points of the structure i.e. the weakened parts, the receptacles, the full pin section and the system columns.

The characteristics of some typical plastic hinges assigned on the pin and the receptacle beams, are shown in Table 4.12 to Table 4.14 and were calculated according to §2.2.

Table 4.12: Typical plastic hinge of pin (1st case study)

Section	M (kNm)	θ (mrad)	M / M_{pl}	θ / θ_{pl}
Ø90	0	0	0	0
	28.2	0	1	0
	56.4	211.5	2	100
	14.1	211.5	0.50	100
	14.1	317.25	0.50	150

Table 4.13: Typical plastic hinge of receptacle beam (1st case study)

Section	M (kNm)	θ (mrad)	M / M_{pl}	θ / θ_{pl}
HEA260	0	0	0	0
	253	0	1	0
	321.31	9.9	1.27	9
	151.80	9.9	0.60	9
	151.80	12.1	0.60	11

Table 4.14: Typical plastic hinge of pin (2nd case study)

Section	M (kNm)	θ (mrad)	M / M_{pl}	θ / θ_{pl}
Ø120	0	0	0	0
	66.98	0	1	0
	133.96	270	1	100
	33.49	270	0.50	100
	33.49	405	0.50	150

The Pushover analysis continued until roof displacement 0.8m, whereupon the structure lost its overall stability and the method failed to converge. The plastic hinge distribution at first yield, at performance point and at ULS are given in Figure 4.7 and Figure 4.8, for both cases. It is observed that the columns remained elastic and that plastic hinges formed only at the horizontal links of the FUSEIS systems.

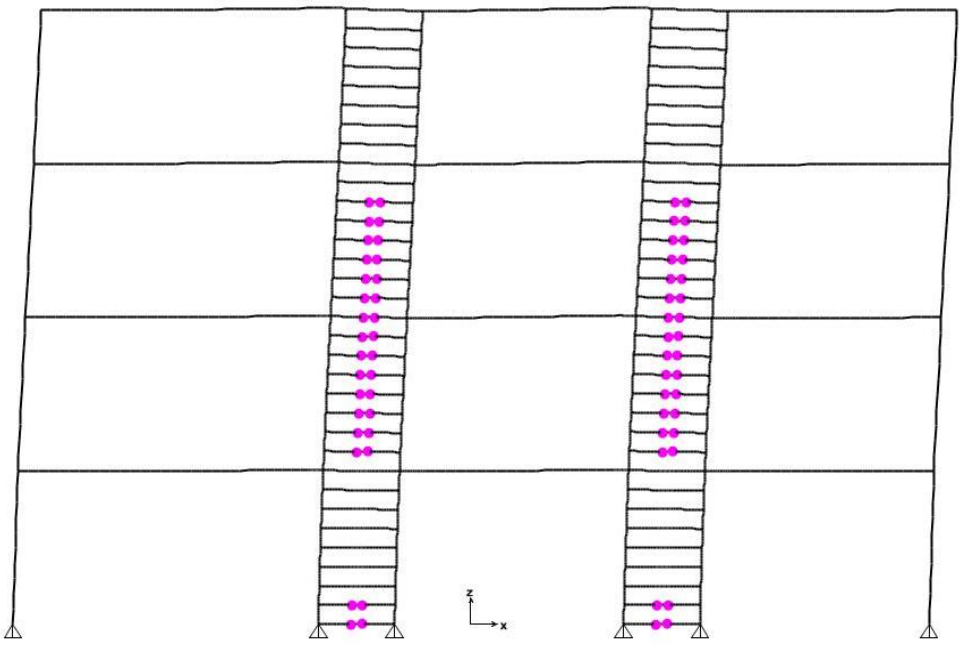

(a) First yield, θ_{gl} = 0.66%

Figure 4.7: Deformed frame and plastic hinge formation of 1st case study

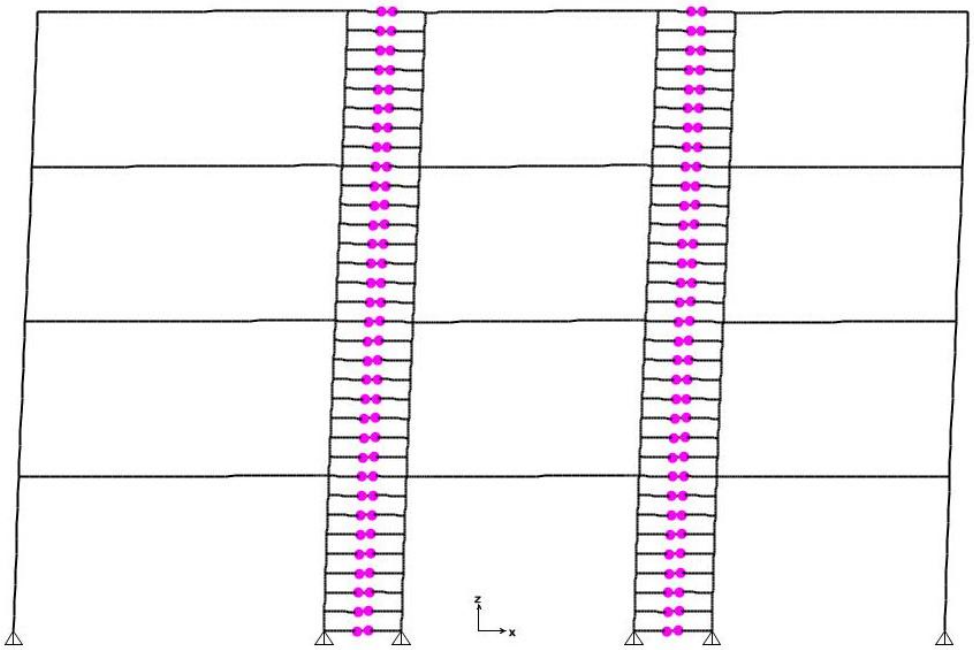

(b) Performance Point, θ_{gl} = 0.91%

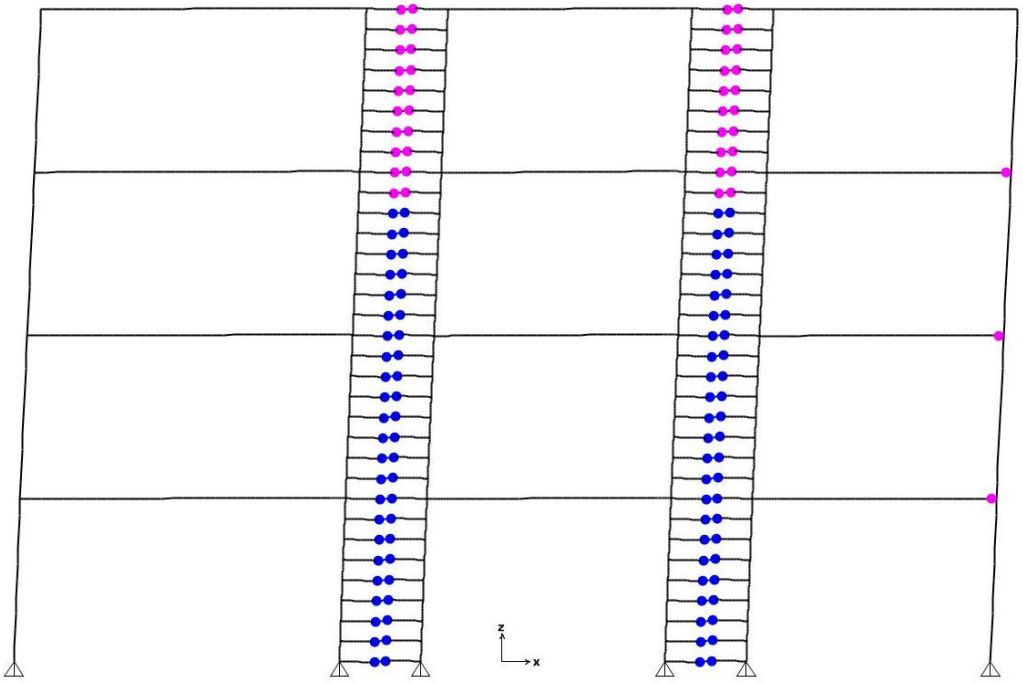

(c) ULS, θ_{gl} = 2.08 %

Figure 4.7: Deformed frame and plastic hinge formation of 1st case study (continuation)

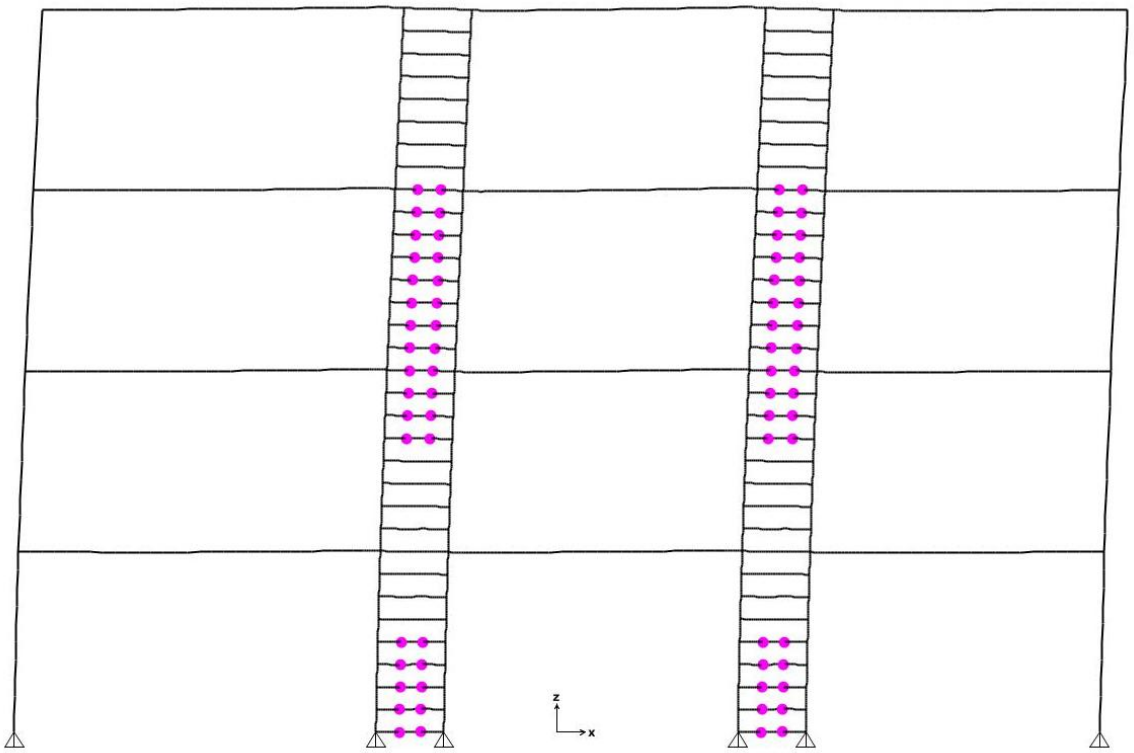

(a) First yield, θ_{gl} = 0.55%

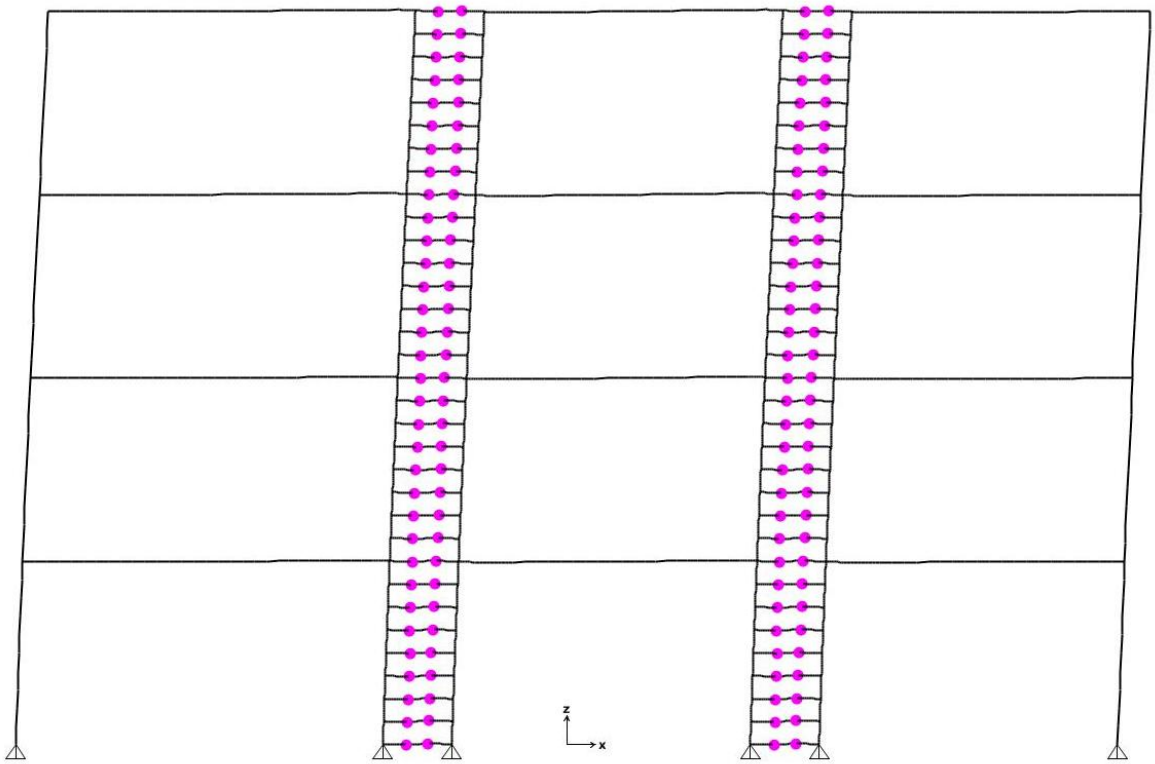

(b) Performance Point, θ_{gl} = 0.77%

Figure 4.8: Deformed frame and plastic hinge formation of 2nd case study

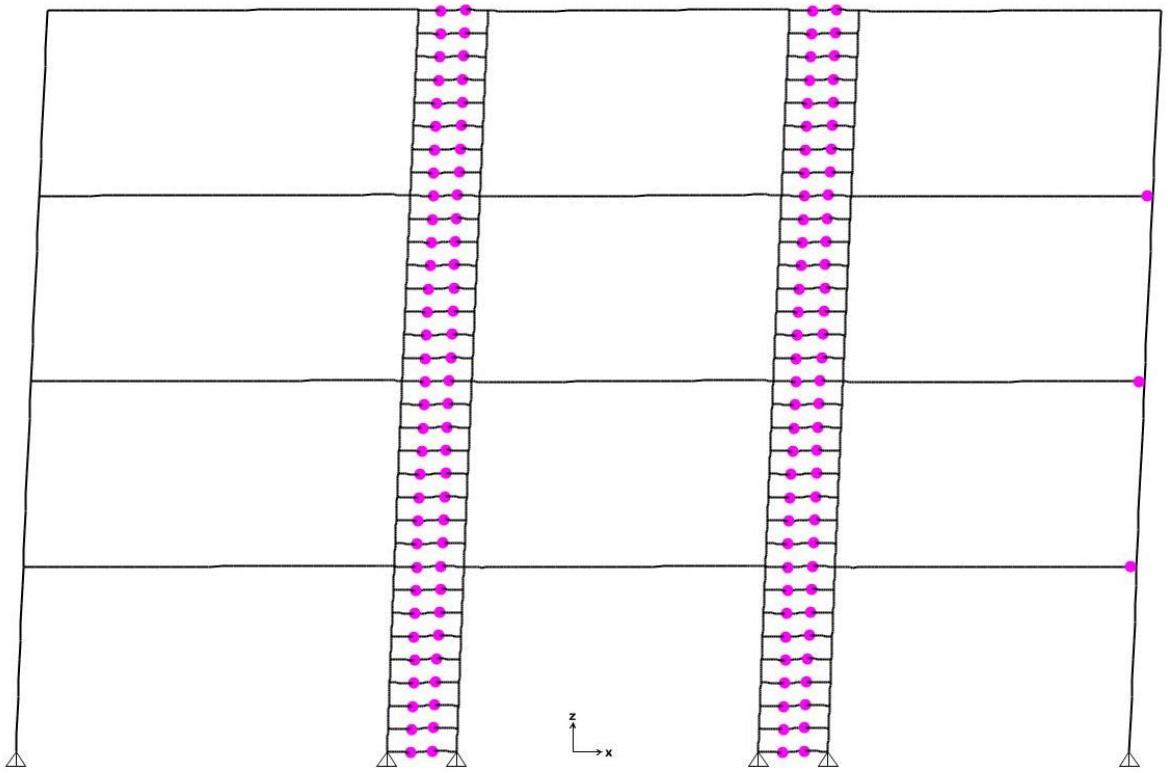

(c) ULS, θ_{gl} = 4.60%

Figure 4.8: Deformed frame and plastic hinge formation of 2nd case study (continuation)

The capacity curves of the two case studies are shown in Figure 4.9, where the performance point, the limit states Immediate Occupancy (IO), Life Safety (LS) and Collapse Prevention (CP) are defined. It is observed that in both cases the Performance Point is below the limit state IO and that the overall behaviour of the structure is not affected by the plastification of one hinge, but of many. In Table 4.15 are given important states of the analysis as well the respectively roof displacement and global drift.

Table 4.15: Important States of Pushover Analysis

Case		First Yield	Perf. Point	(IO)	(ULS)	(LS)	(CP)
1st	δ_{roof} (mm)	105.08	154.16	282.99	333.49	373.39	469.64
	θ_{gl} (%)	0.66%	0.96%	1.77%	2.07%	2.34%	2.94%
2nd	δ_{roof} (mm)	88.43	123.46	526.53	738.65	748.75	970.09
	θ_{gl} (%)	0.55%	0.77%	3.29%	4.62%	4.68%	6.07%

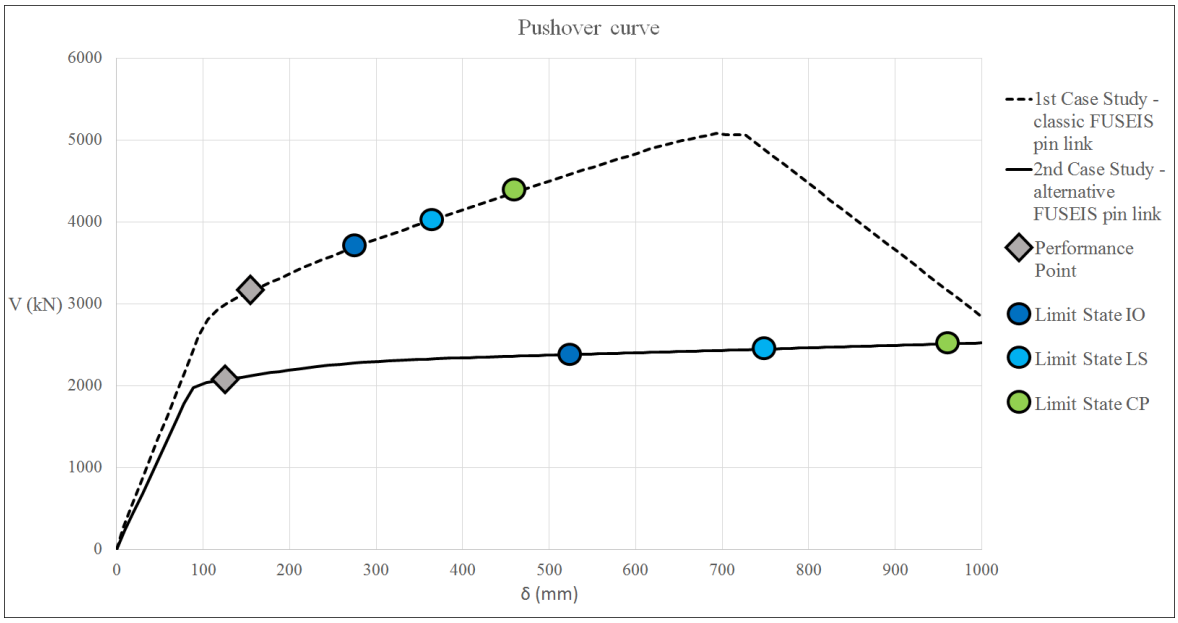

Figure 4.9: Pushover Curves of both Case studies

4.5.2 Evaluation of the behaviour factor q

For the calculation of the behaviour factor the same procedure described in §3.5.2 was used, where the evaluation of the q-factor is performed through the multiplication of the ductility (q_μ) and the overstrength (Ω).

Considering that the eigen-periods of the buildings are above T_c=0.60s, the "rule of equal displacement" can be performed. In both cases ULS occurs prior to the Life Safety (LS) performance level, therefore the ductility factor q_μ is determined as the ratio between δ_{ULS} to δ_{el}. The overstrength factor Ω is the ratio between V_{ULS} to V_y.

The results for both cases are given in Table 4.16 and Table 3.15. As shown, the calculated behaviour factors are higher than the values proposed by design guides.

Table 4.16: Evaluated behaviour factor

Case	δ_{ULS} (mm)	δ_{el} (mm)	q_μ	V_{ULS} (kN)	V_y (kN)	Ω	q
1st	333.50	146.24	2.28	3908.72	2808.69	1.39	3.17
2nd	738.65	109.11	6.77	2440.29	1977.70	1.23	8.35

4.6 Comparison between the two systems

- Because of the absence of the receptacle beams, the stiffness of the alternative FUSEIS system was almost entirely provided by the system columns.
- In order to increase the stiffness of the alternative system but also to keep within reasonable limits the length of the pin, a large section was chosen for the system columns (HEB700).

- The pins of the alternative system were also large in compare with the ones used for the classic system
- The large sections in the second case resulted a heavier structure, with steel weight equal to 92.17kg/m^2, while in the first case the steel weight was 81.24kg/m^2.
- After the earthquake occurred, the replaceable element in the first case was only the pin with length 400mm, while in the second case was a large pin with length 720mm.

From the analysis and comparison of these two, different configurations of the FUSEIS pin link system, it was clear that the second case clearly disadvantages in relation to the first. From the results of this study mentioned above, it can be safely concluded that the receptacle beam is an essential element of the FUSEIS pin link system, that contribute effectively to the total stiffness of the system but also improves its behaviour and response to lateral loads.

5 Non-linear Dynamic Analyses (Time History)

5.1 General

Non-linear dynamic analysis utilizes the combination of ground motion records with a detailed structural model, therefore is capable of producing results with relatively low uncertainty. In non-linear dynamic analysis, the detailed structural model subjected to a ground-motion record produces estimates of component deformation for each degree of freedom in the model [16].

In non-linear dynamic analysis the calculated response of the building is time dependent and can be very sensitive to the characteristics of the individual ground motion used as seismic input; therefore, several analyses are required using different ground motion records to achieve a reliable estimation of the probabilistic distribution of structural response.

5.2 Design for non-linear dynamic analysis

Non-linear dynamic analysis provides the time dependent response of steel buildings. Through this analysis the designer can check the distribution of damage after a realistic seismic event and whether or not the FUSEIS link system works as a self- centring system, with practically zero residual deformations. In the case FUSEIS pin link system, plastic rotations are considerably big. Results from non-linear time history analyses can also be used to determine the damage index for variable amplitude cycles according to Palmgren-Miner law of damage accumulation.

According to the Design Guides, in order to obtain a realistic response of the building, the model must be updated to include the non-linear properties of the FUSEIS systems. Regarding the FUSEIS beam system, the beam elements representing the RBSs shall be replaced with multi-linear plastic link elements, while for the pin system these link elements shall be inserted at the ends of the pins with length equal to 25% of the pin. The behaviour of the non-linear link is defined only for the rotational degree of freedom, while the rest are modelled as linear. The non-linear properties to be used for these links are shown in Table 5.1 and the hysteresis type should be according to the Multi-linear plastic kinematic model.

Table 5.1: Multi-linear force-rotation definition

Point	I-shape sections		SHS		CHS		Reduced pin	
	$M/M_{pl,\ RBS}$	$\theta/\theta_{pl,RBS}$	$M/M_{pl,\ RBS}$	$\theta/\theta_{pl,RBS}$	$M/M_{pl,\ RBS}$	$\theta/\theta_{pl,RBS}$	$M/M_{pl,pin}$	$\theta/\theta_{pl,pin}$
A	-α	-40	-α	-25	-α	-25	-2	-100
B	-1	-2.5	-0.6	-1.5	-1	-2.5	-1	-20
C	0	0	0	0	0	0	0	0
D	1	2.5	0.6	1.5	1	2.5	1	20
E	α	40	α	25	α	25	2	100
factor α derives from a strain hardening slope equal to 3% of the elastic slope								

5.3 Non-linear dynamic analysis on 3D building frame

The case study used for the non-linear time history analysis was the four-storey steel building with FUSEIS pin link system presented in Chapter 4. The analysis was performed with the software SAP2000 [10] which offers various options that determine the type of time history analysis to be performed. For example:

- Linear vs Non-linear time history analysis
- Transient vs Periodic. Transient analysis considers the applied load as a one-time event while periodic analysis considers it to repeat indefinitely.
- Modal vs Direct-integration. These are two different solution methods, each with advantages and disadvantages.
- Material non-linearity can be simulated by using non-linear link elements, tension or compression limits and hinges in beam elements.

The analysis was, as the title of current Chapter suggests, non-linear and 10 different accelerograms of real seismic events were introduced, Table 5.2. The model can be updated to include material non-linearity by inserting non-linear plastic link elements (§5.2), nevertheless, in this study an alternative approach is also being tested. In the latest versions of SAP2000, there is a variety of hysteresis models to be specified for single degree of freedom hinges, such as kinematic, degrading, Takeda, pivot, concrete, BRB hardening and isotopic. Therefore, in addition to the model with NL link elements, another with plastic hinges is being tested and compared. The motive for this, was the significantly easier simulation, the better supervision of the limit states and the fact that after the Pushover analysis there is already enough information regarding the hinges' properties, that only needs minor changes to match with the properties given in Table 5.1.

Dynamic equilibrium equations can be solved using either modal or direct-integration methods. The first, non-linear modal time history analysis, also known as Fast Non-linear Analysis (FNA), is based on the evaluation and superimposition of free-vibration mode shapes. In the second method, direct-integration time history analysis, the equilibrium equations of motion are fully integrated as the structure is subjected to dynamic loading and requires small enough time steps to accurately characterize dynamic behaviour. Two factors determined the choice of solution method, as described in the following.

Both hinges and links may be used to model localized non-linear behaviour. Either one may be more suitable depending on analysis goals. A summary of the primary advantages and disadvantages of each is available in SAP2000 manuals, but only one difference was crucial for current study. Direct-integration time history can consider both types of non-linearity, while FNA can only consider NL links. In order to make a comparison between the two types of non-linearity simulation, direct-integration method was chosen. This choice was strengthened since initial conditions in direct-integration method can be specified through a non-linear static load case, while FNA analyses can only continue from another FNA cases.

Table 5.2: Seismic records (from Seismomatch [17])

No	Year	Horizontal records	Station	Max PGA (g)
1	1999	Chi-Chi, Taiwan	TCU045	0.36
2	1976	Friuli, Italy	Tolmezzo	0.35
3	1961	Hollister, USA	USGS 1028	0.19
4	1979	Imperial Valley, USA	USGS 5115	0.32
5	1995	Kobe, Japan	Kakogawa	0.34
6	1999	Kocaeli, Turkey	Yarimca	0.35
7	1992	Landers, USA	000 SCE 24	0.78
8	1989	Loma Prieta, USA	090 CDMG 47381	0.37
9	1994	Northridge, USA	090 CDMG 24278	0.57
10	1983	Trinidad, USA	090 CDMG 1498	0.19

5.4 Residual roof drifts

The dynamic response of the building under real seismic events was initially evaluated through top displacement time histories. [_] shows the roof displacement time histories for each of the selected accelerograms, while a comparison is made between the results given by hinges and NL links. It is obvious that at the end of the seismic excitation the structure returned to its initial position, proving that the FUSEIS pin link system can work as a self-centring system. It is also observed that the difference between the two methods is insignificant and therefore the material non-linearity and hysteretic behaviour was successfully simulated with the hinge elements. Residual global drifts are summarized in [_]

Table 5.3: Residual global drifts

No	Horizontal records	Non-linear links (%)	Hinges (%)
1	Chi-Chi, Taiwan	0.028	0.031
2	Friuli, Italy	0.019	0.023
3	Hollister, USA	0.020	0.021
4	Imperial Valley, USA	0.011	0.021
5	Kobe, Japan	0.058	0.067
6	Kocaeli, Turkey	0.159	0.020
7	Landers, USA	0.016	0.015
8	Loma Prieta, USA	0.066	0.078
9	Northridge, USA	0.009	0.004
10	Trinidad, USA	0.018	0.020

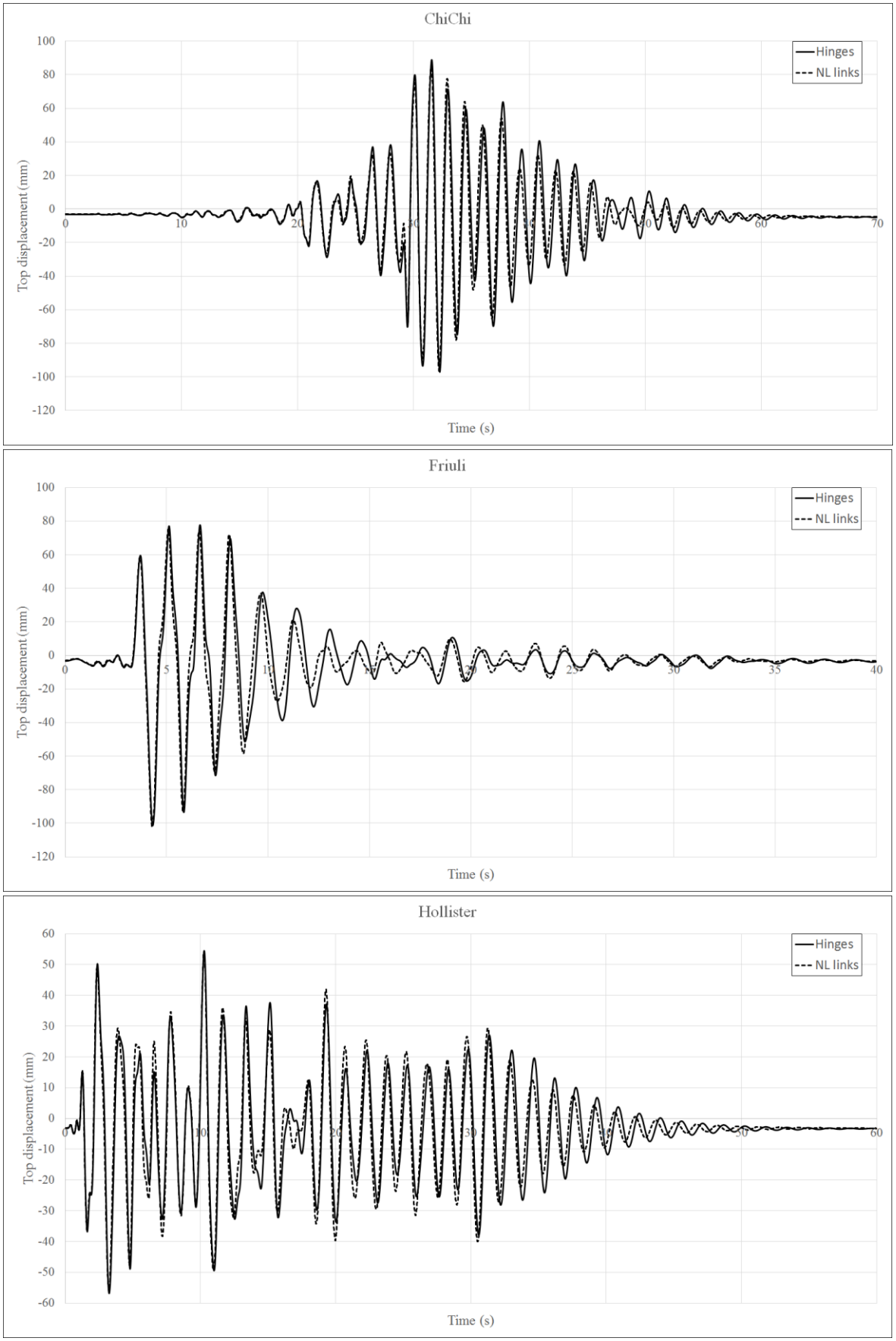

Figure 5.1: Top displacements time histories

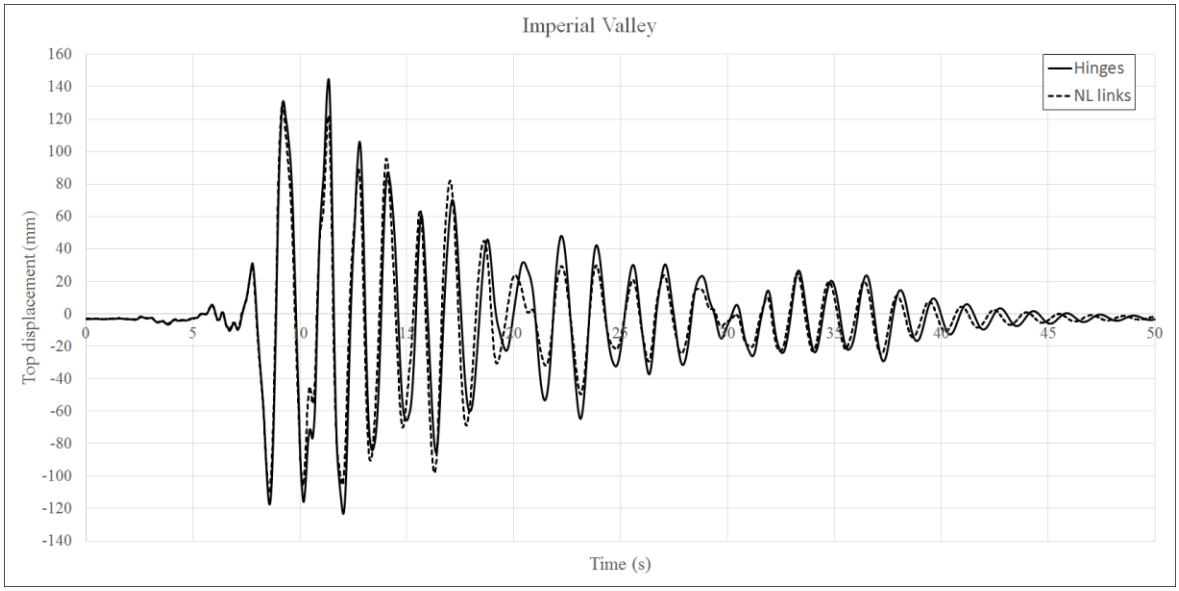

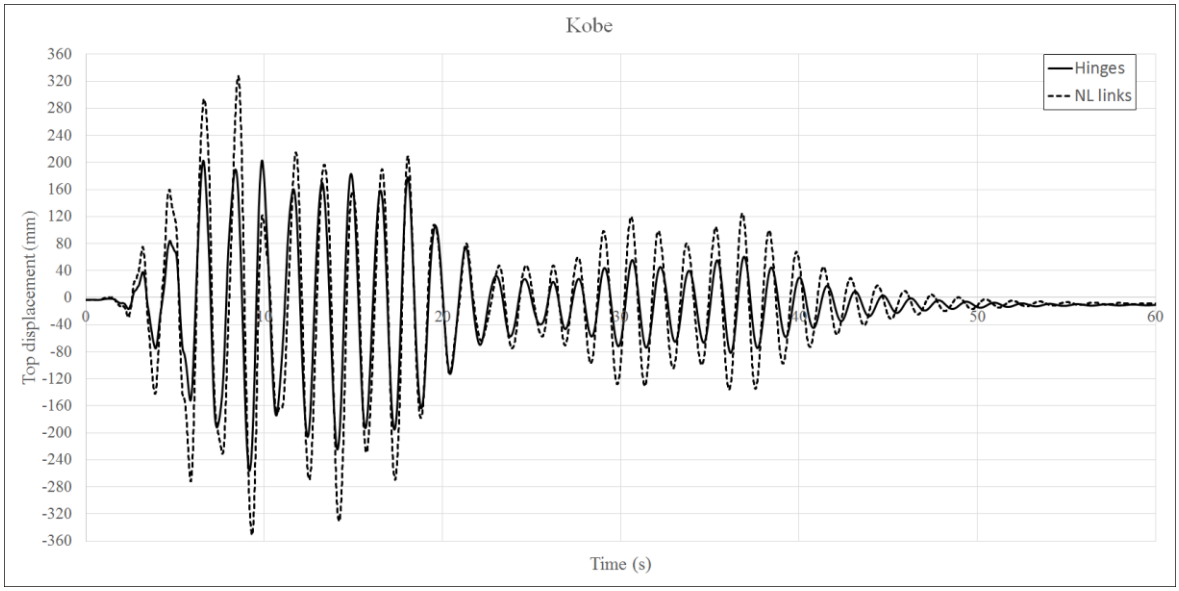

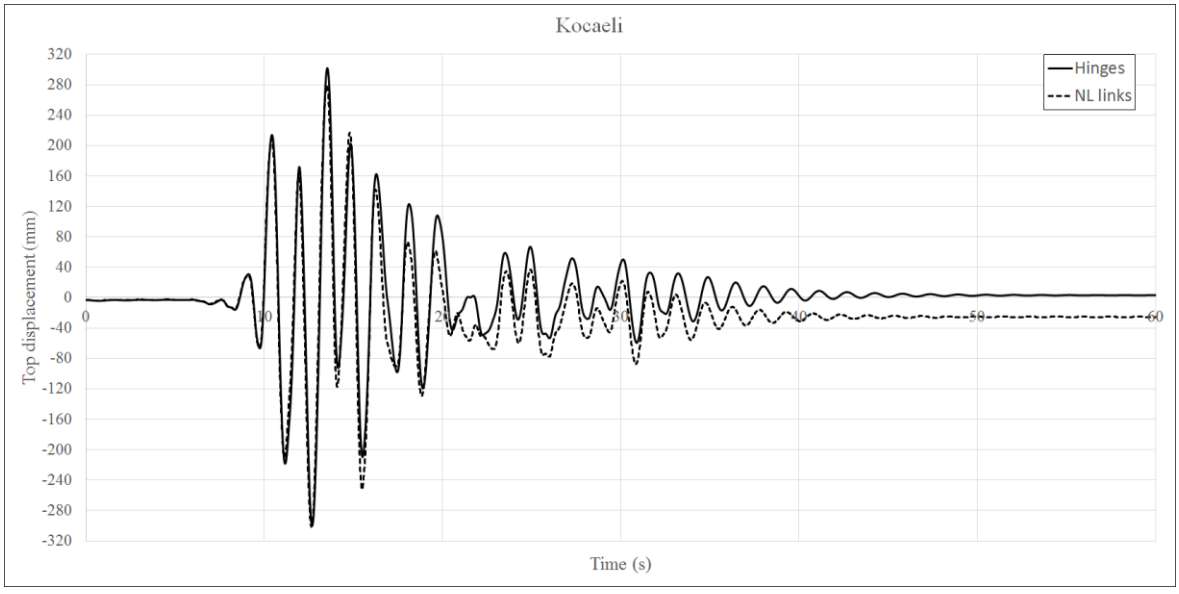

Figure 5.1: Top displacements time histories (continuation)

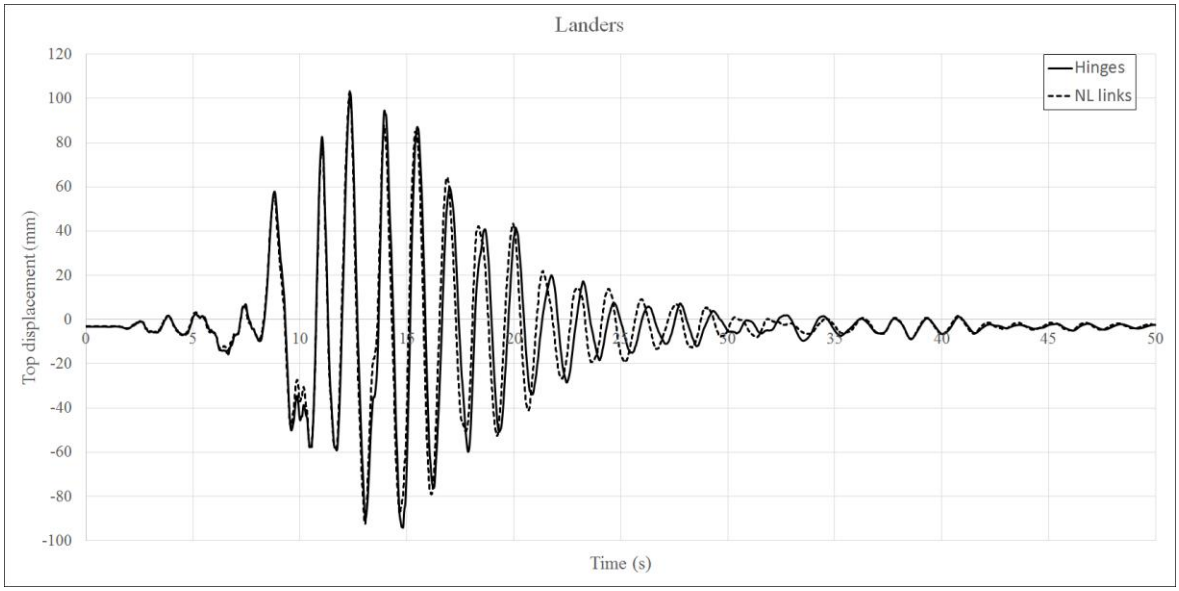

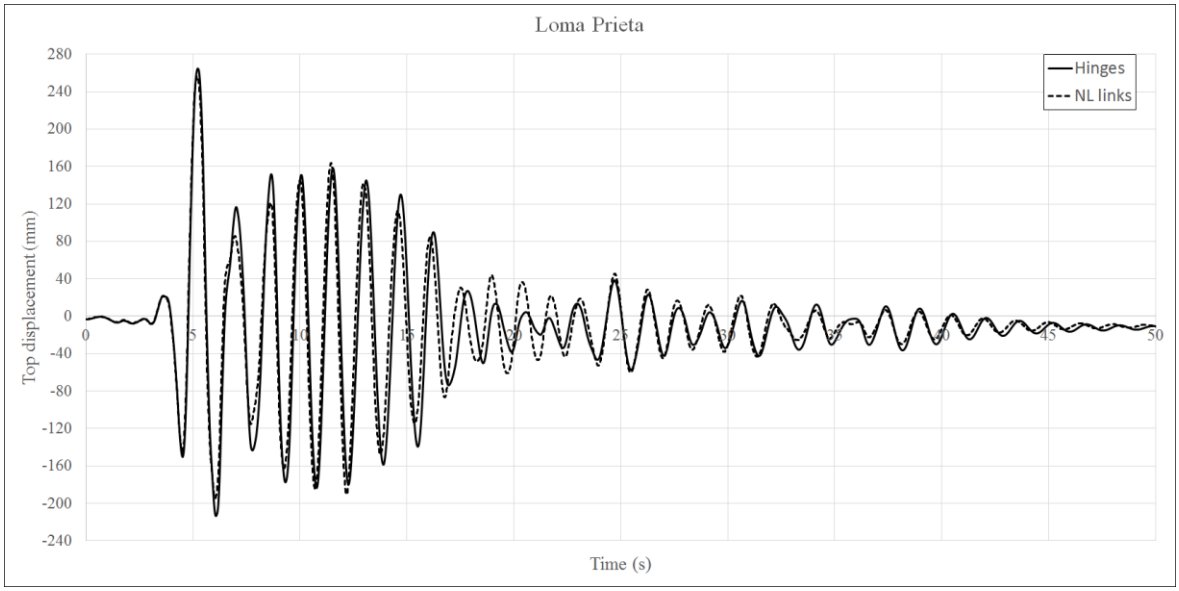

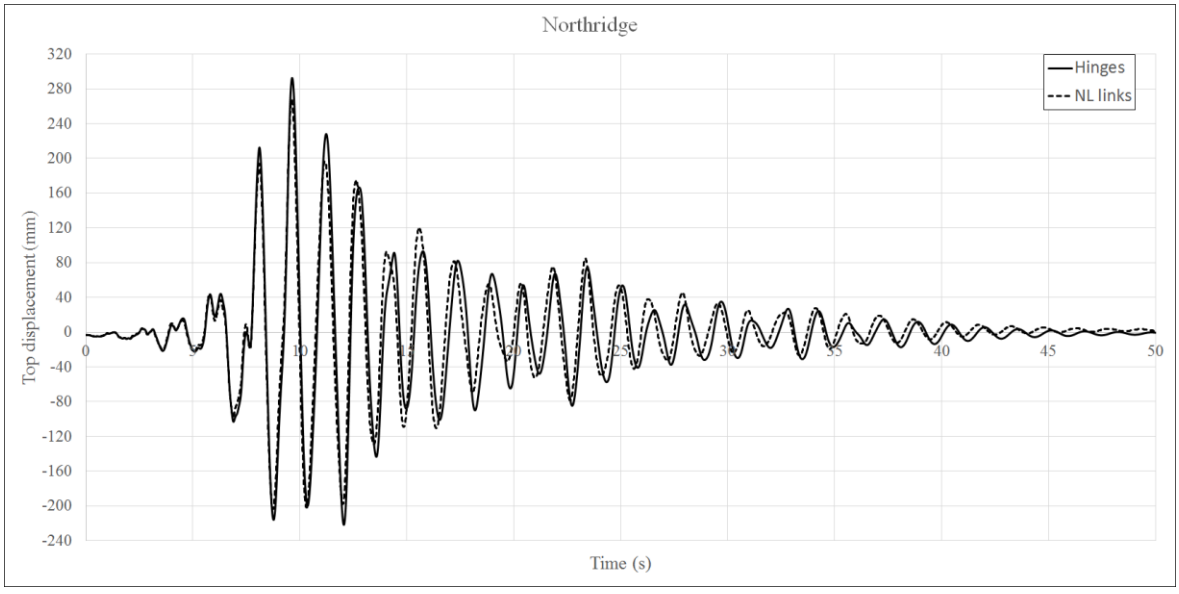

Figure 5.1: Top displacements time histories (continuation)

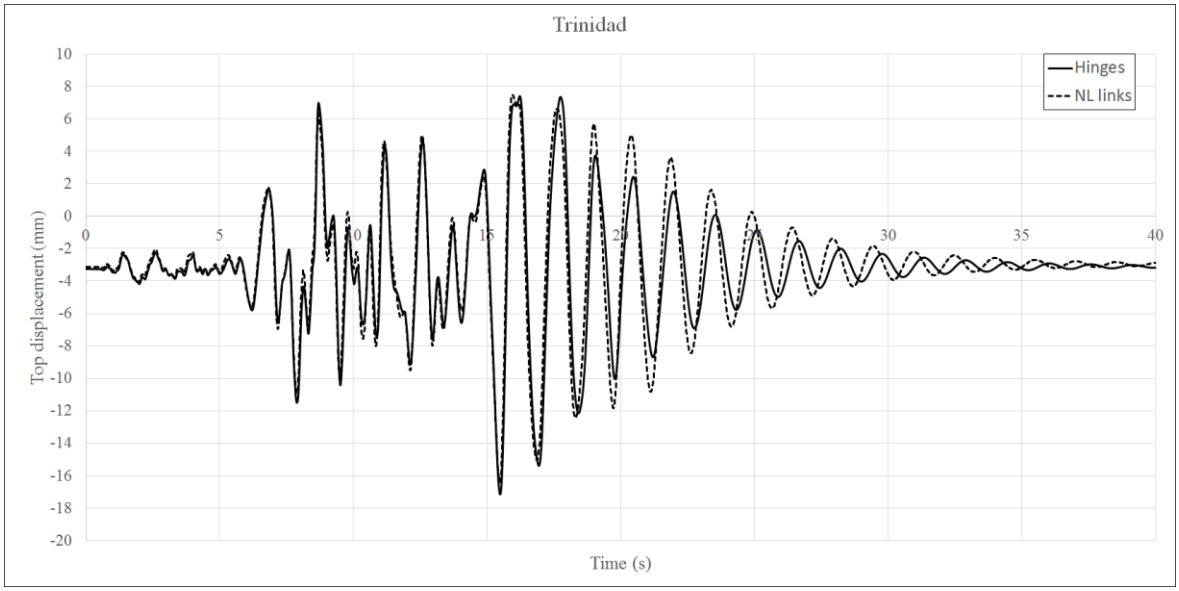

Figure 5.1: Top displacements time histories (continuation)

5.5 Low cycle fatigue

The number of cycles that the system can undergo is dictated by low-cycle fatigue considerations. Low-cycle fatigue deals with deformation and strain histories rather than stress histories (high-cycle fatigue). According to the design guides [3], [5] the number of the cycles N can be calculated by applying the drift ranges (Δφ) at the experimental fatigue curve, given in Eq. (5.1):

$$logN = -0.90 - 3log\Delta\varphi \qquad \text{Eq. (5.1)}$$

The damage index may be calculated with the Palmgren-Miner law, according to which, after a certain number of various amplitudes cycles fatigue occurs when:

$$D = \frac{n_1}{N_{f1}} + \frac{n_2}{N_{f2}} + ... \frac{n_i}{N_{fi}} \geq 1 \qquad \text{Eq. (5.2)}$$

Where,

n_i is the number of cycles carried out at the same range (for time histories $n_i = 1$)

N_{fi} is the number of cycles at which failure occurs in case of constant amplitude

Time history analyses allowed the determination of damage index of the pins, as described in the design guides. Table 5.4 summarizes the results for the analysis with non-linear links and as shown the Palmgren-Miner's law is fulfilled in all cases.

Table 5.4: Damage index

No	Horizontal records	Damage index (D ≤ 1)
1	Chi-Chi, Taiwan	0.02
2	Friuli, Italy	0.02
3	Hollister, USA	0.00
4	Imperial Valley, USA	0.05
5	Kobe, Japan	0.98
6	Kocaeli, Turkey	0.42
7	Landers, USA	0.02
8	Loma Prieta, USA	0.26
9	Northridge, USA	0.32
10	Trinidad, USA	0.00

6 References

1. Dimakogianni D., “Innovative seismic resistant systems FUSEIS with ductile pins”, PhD Thesis 2016
2. Dougka G., “Development of seismic resistant systems for multi-story buildings”, PhD Thesis 2016
3. Vayas, I., Karydakis, Ph., Dimakogianni, D., Dougka, G., Castiglioni, C. A., Kanyilmaz, A. et al. Dissipative devices for seismic resistant steel frames - The FUSEIS Project, Design Guide. Research Programme of the Research Fund for Coal and Steel 2012.
4. Vayas I., Karydakis Ph., Dimakogianni D., Dougka G., Castiglioni C.A., Kanyilmaz A. et al., “Dissipative devices for seismic-resistant steel frames (FUSEIS)”, Research Fund for Coal and Steel, European Commission, EU 25901 EN 2013.
5. Vayas, I., Thanopoulos P., Tsarpalis P., Dimakogianni, D., Innovative anti-seismic devices and systems - The INNOSEIS Project, Design Guides. Research Programme of the Research Fund for Coal and Steel 2016.
6. Vayas, I., Thanopoulos P., Tsarpalis P., Dimakogianni, D., Innovative anti-seismic devices and systems - The INNOSEIS Project, Information Brochures. Research Programme of the Research Fund for Coal and Steel 2016
7. Plumier, A., Doneux, C., Castiglioni, C., Brescianini, J., Crespi, A., Dell'Anna, S., Lazzarotto, L., Calado, L., Ferreira, J., Feligioni, S., Bursi, O., Ferrario, F., Sommavilla, M., Vayas, I., Thanopoulos, P. and Demarco, T. (2004). "Two Innovations for Earthquake Resistant Design - The INERD Project, Final Report". Research Programme of the Research Fund for Coal and Steel.
8. EN1998-1, Eurocode 8: Design of structures for earthquake resistance
9. EN1993-1, Eurocode 3: Design of steel structures
10. SAP2000, CSI, Computers and Structures Inc., www.csiberkeley.com.
11. EN1994-1: Eurocode 4: Design of composite steel and concrete structures.
12. EN1998-1-4, Eurocode 8: Design of structures for earthquake resistance, Part 1-4 Design of buildings
13. FEMA–356, “Prestandard and Commentary for the seismic rehabilitation of Buildings“, Federal Emergency Management Agency, Washington, 2000
14. EN1991-1: Eurocode 1: Actions on structures
15. SymDeck Designer, The ELASTRON Group, http://www.elastron.gr/gr/en/home/
16. https://en.wikipedia.org/wiki/Seismic_analysis#Nonlinear_dynamic_analysis
17. Seismomatch, Seismosoft, www.seismosoft.com

Annex A. Structural detailing of 2-storey building

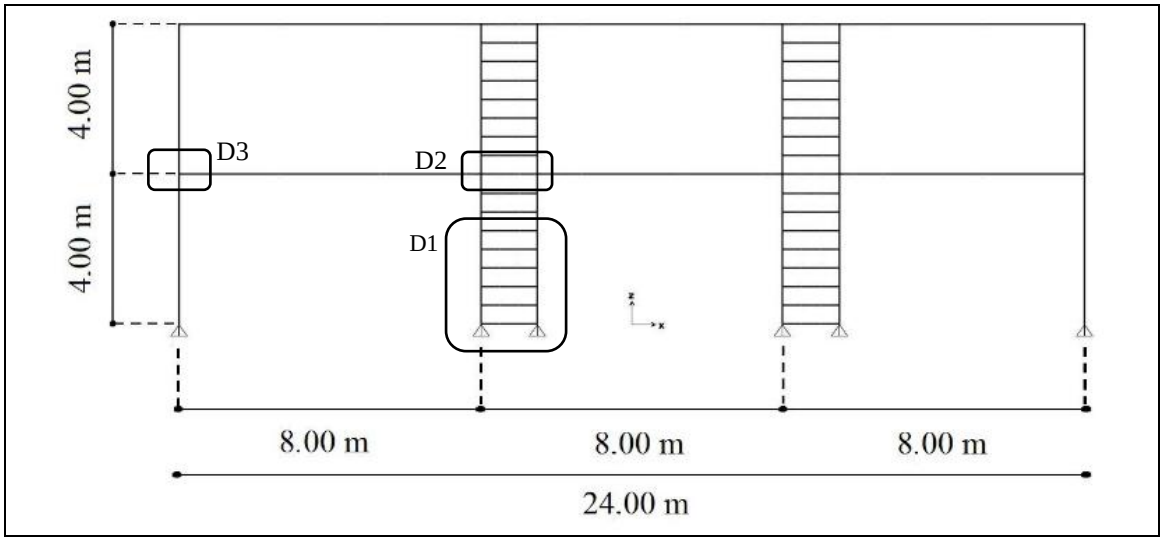

Figure A.1: Side view of building.

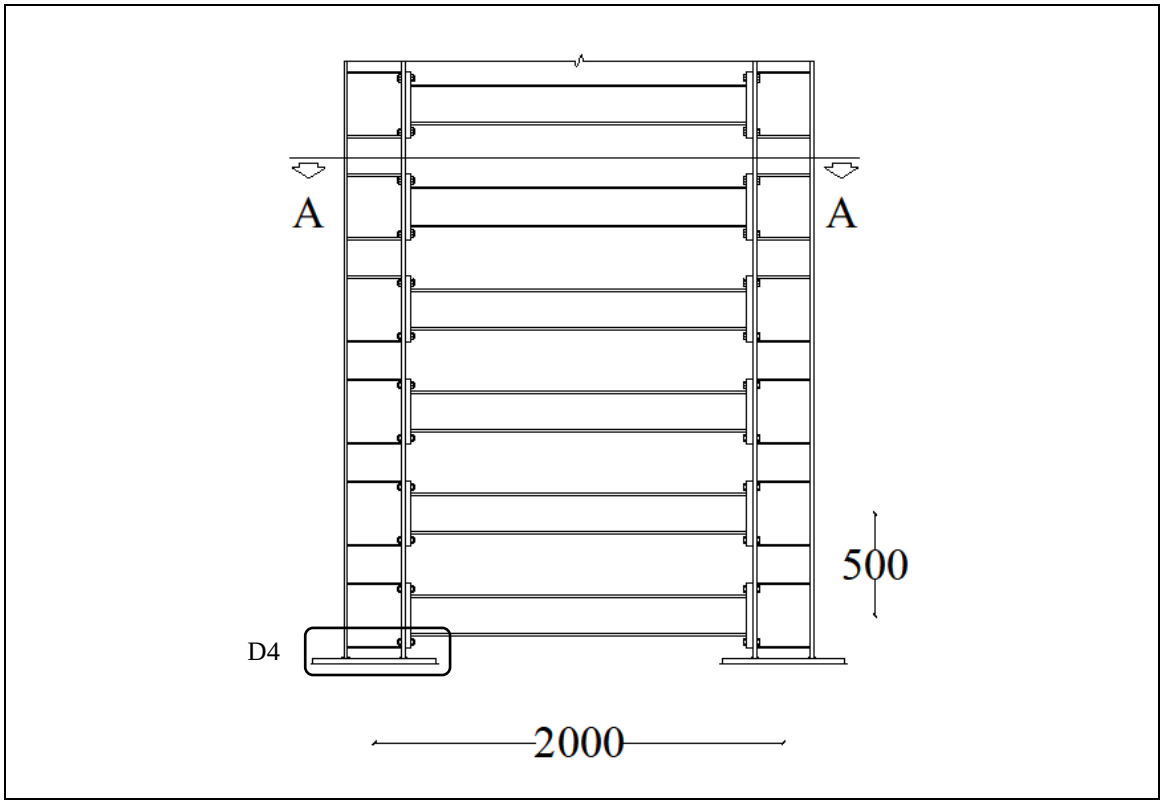

Figure A.2: Detail D1 of FUSEIS beam link system.

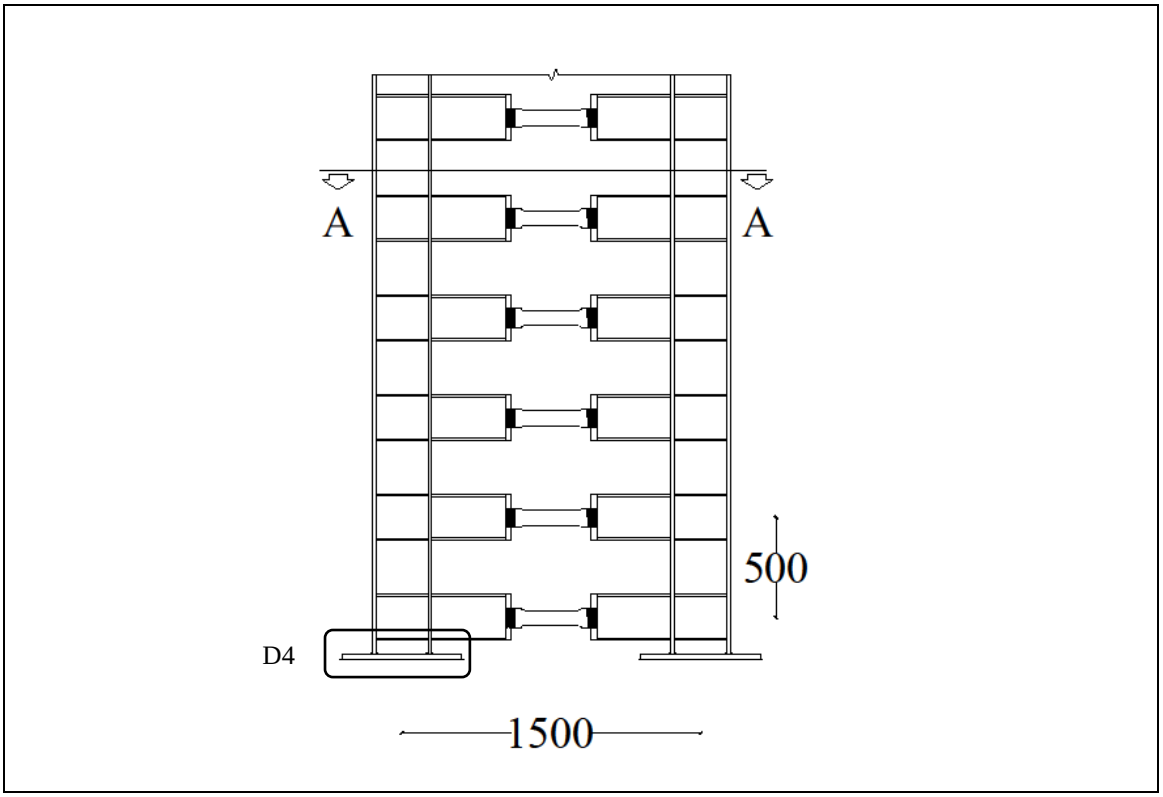

Figure A.3: Detail D1 of FUSEIS pin link system.

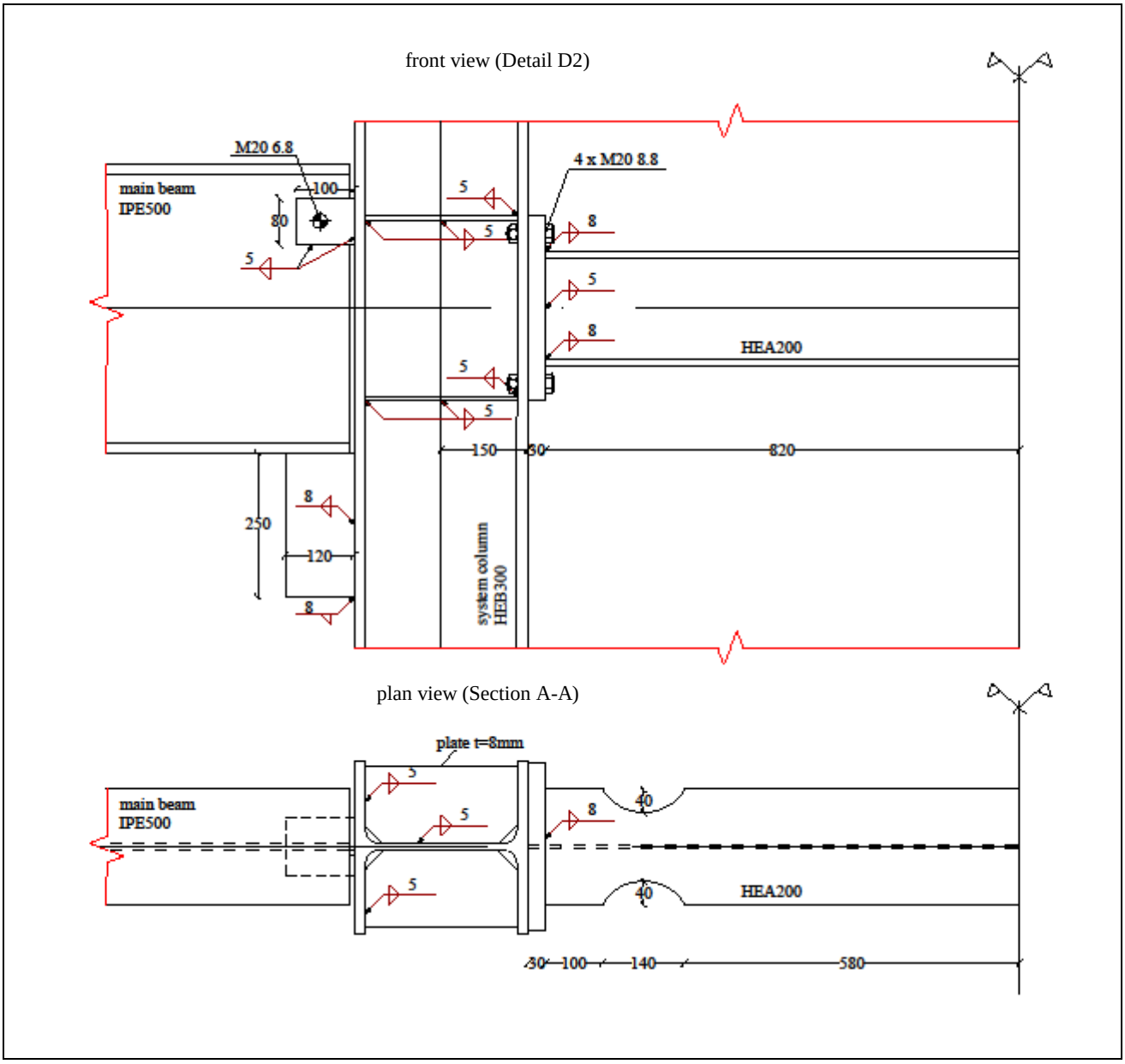

Figure A.4: Side view and plan view of a typical FUSEIS beam link

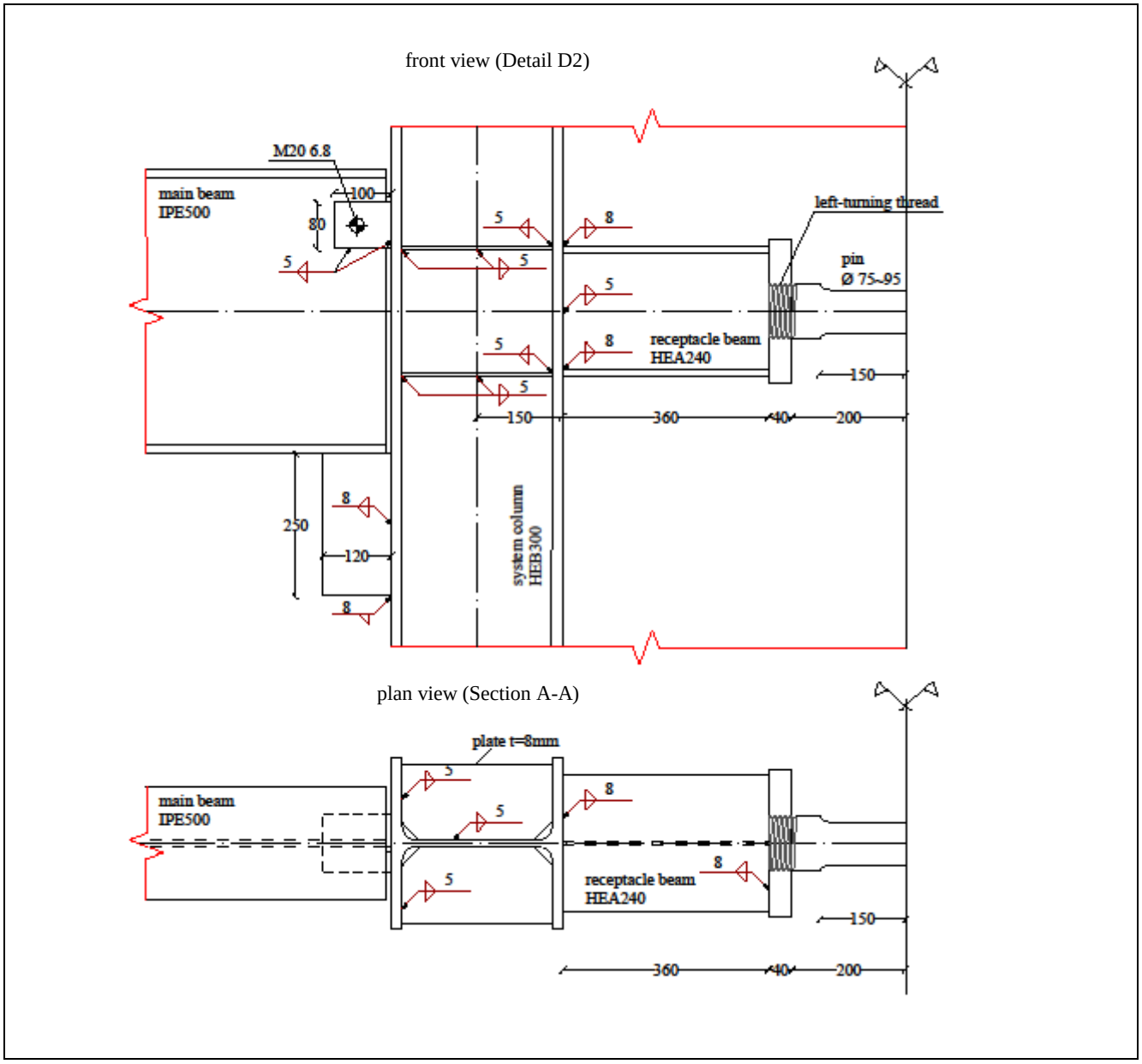

Figure A.5: Side view and plan view of a typical FUSEIS pin link

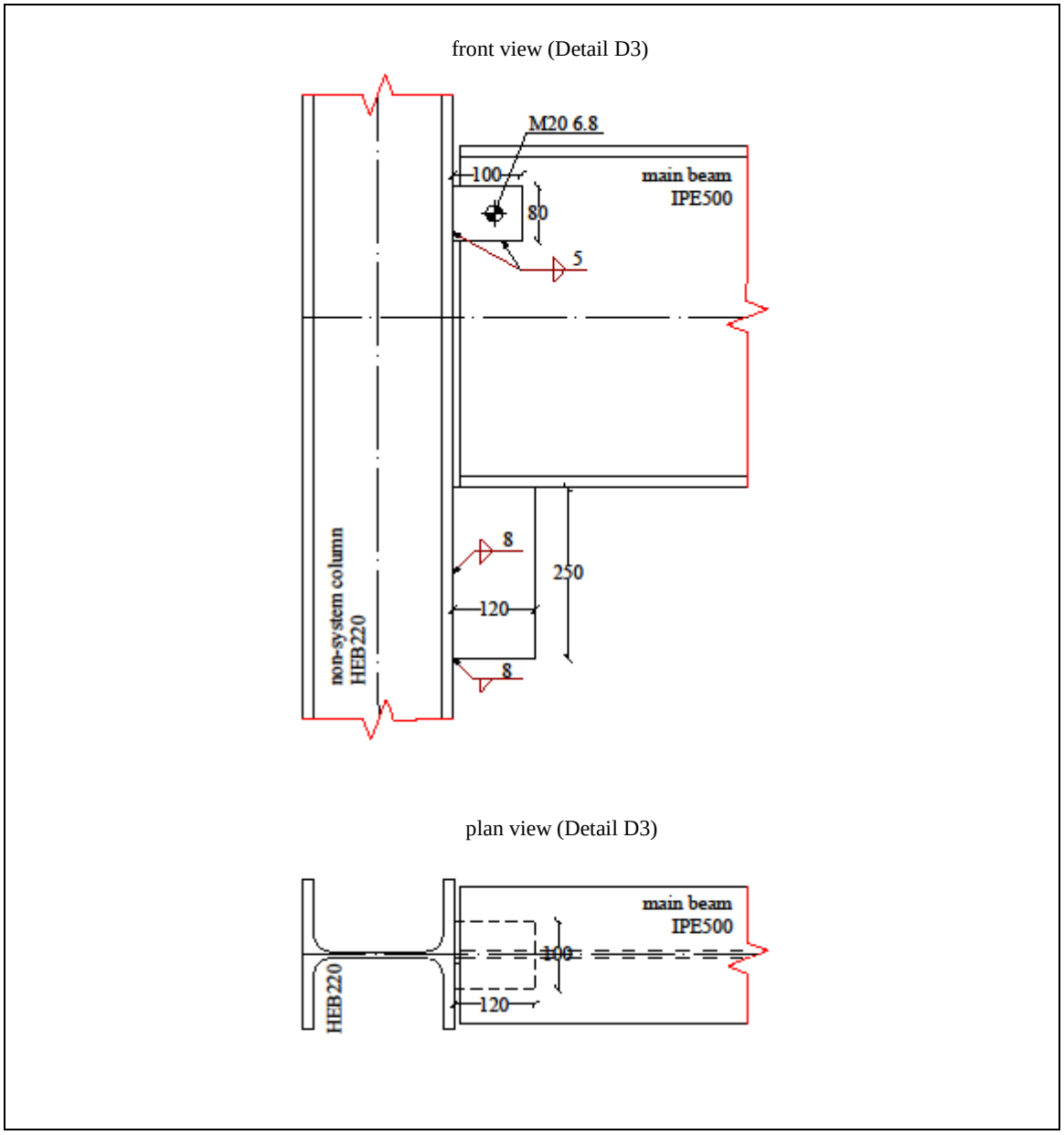

Figure A.6: Beam to column connection of the main frame

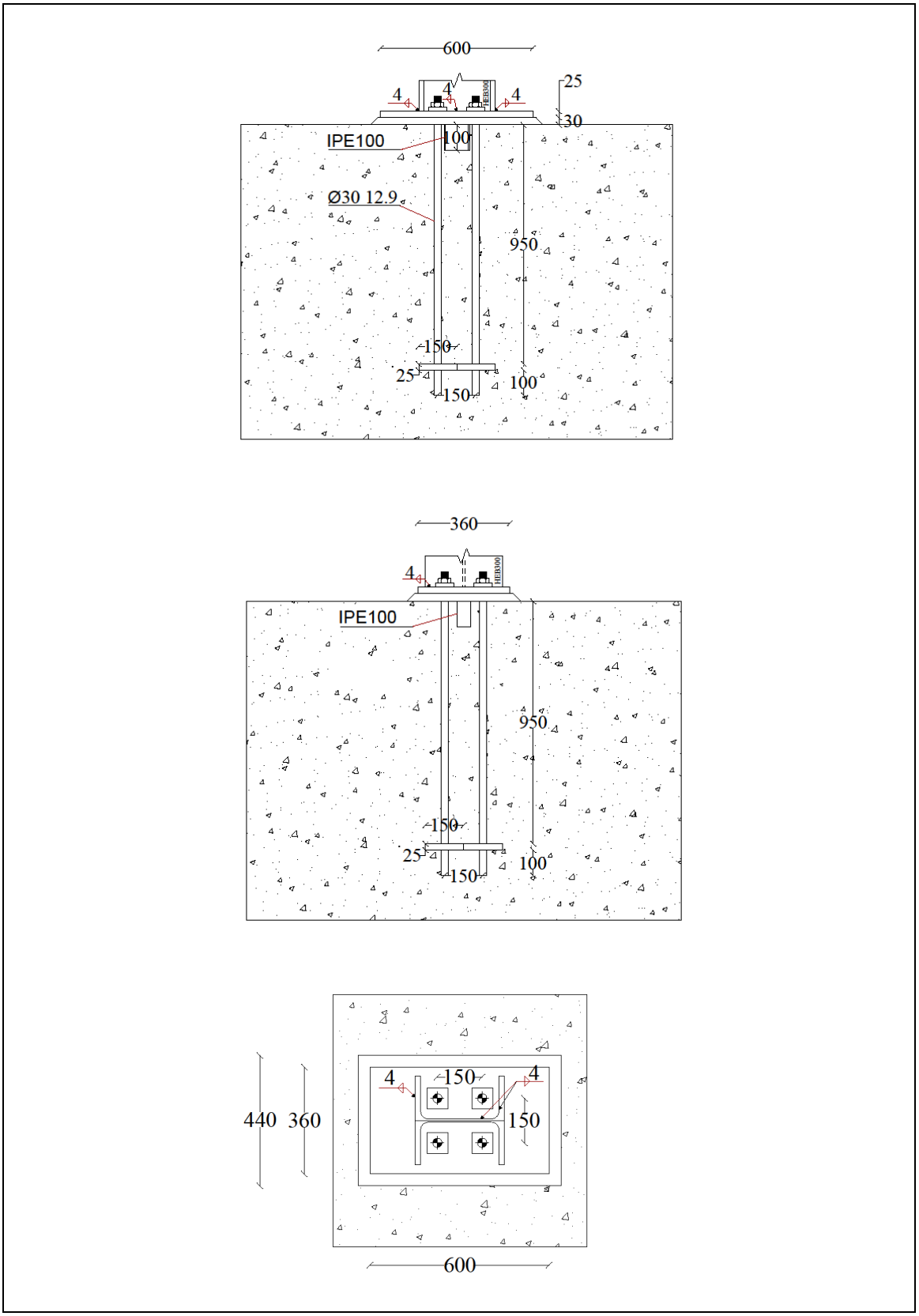

Figure A.7: Detail D4 of foundation connection

Annex B. Structural detailing of 4-storey building

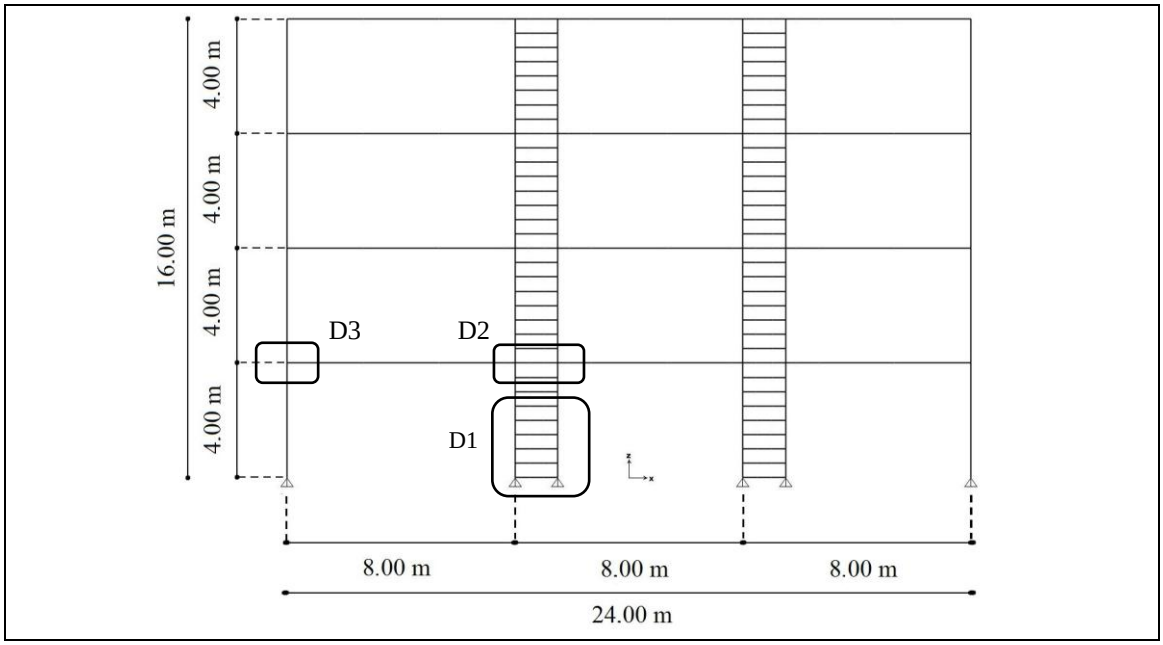

Figure B.1: Side view of building.

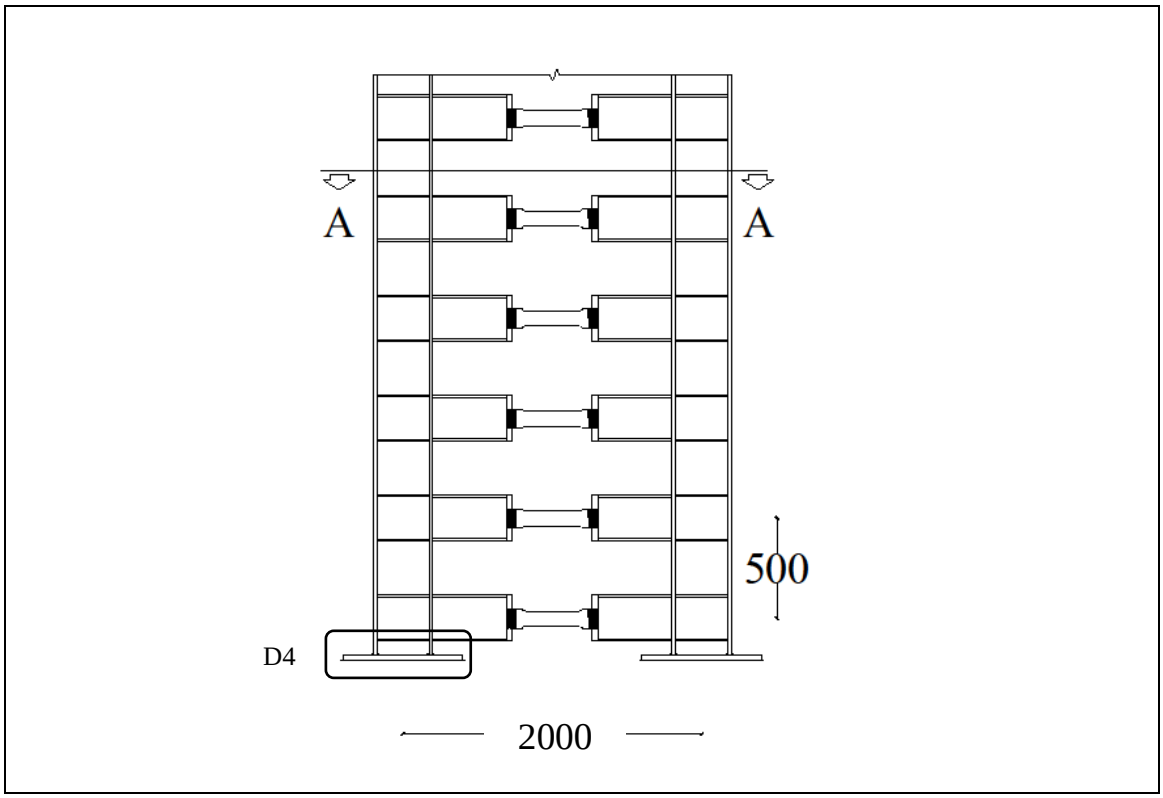

Figure B.2: Detail D1.

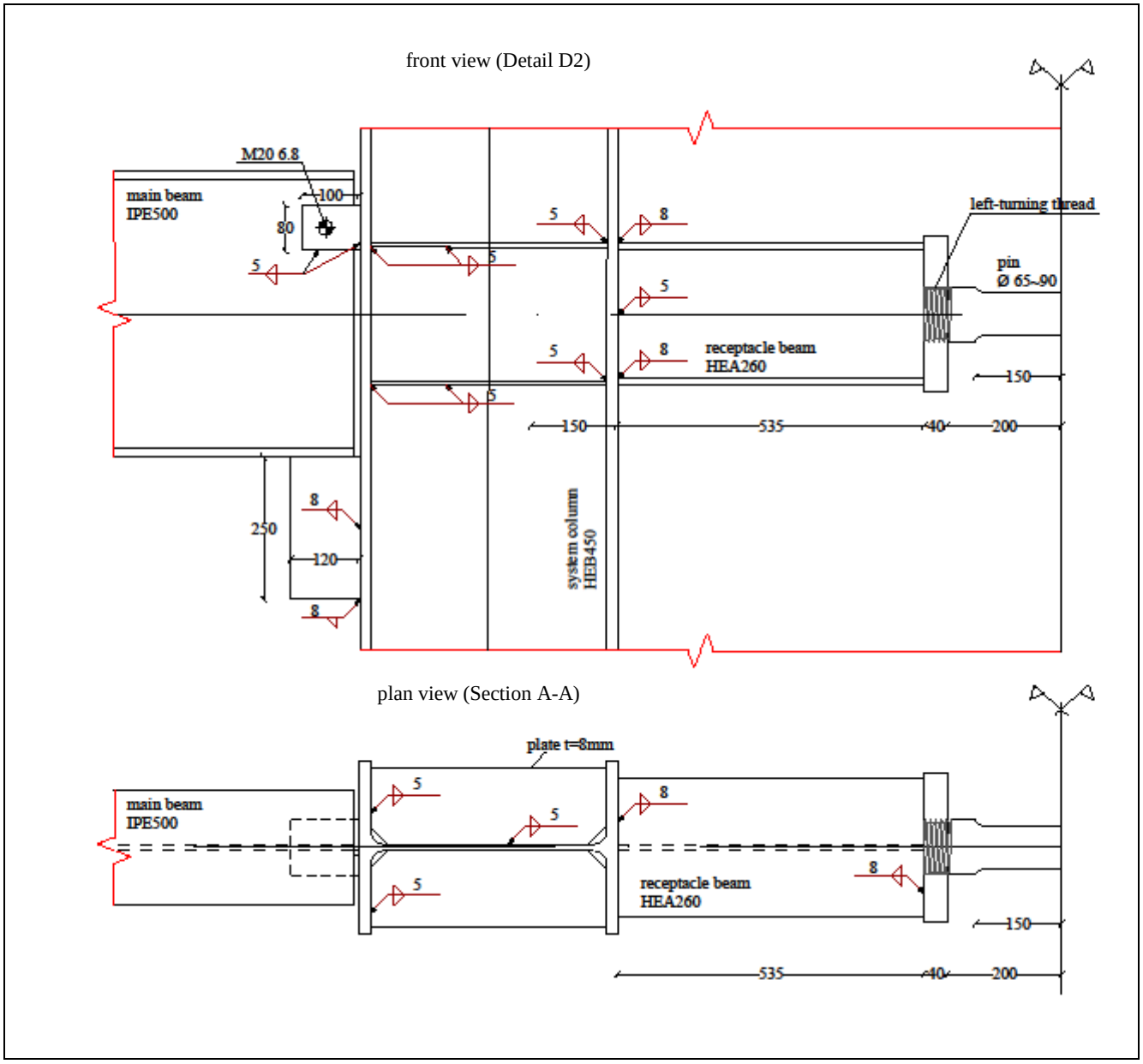

Figure B.3: Side view and plan view of a typical FUSEIS beam link

front view (Detail D3)

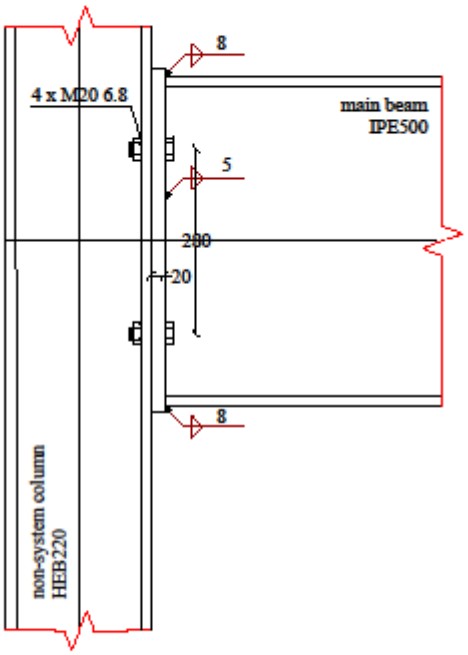

plan view (Detail D3)

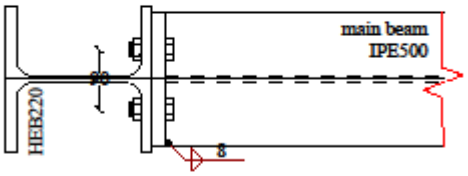

Figure B.4: Beam to column connection of the main frame